

MEASUREMENT OF ABSORPTION COEFFICIENT OF ROAD SURFACES USING
IMPEDANCE TUBE METHOD

Except where reference is made to the work of other, the work described in this thesis is my own or was done in collaboration with my advisory committee. This thesis does not include proprietary or classified information.

Krishnasudha Vissamraju

Certificate of Approval:

Winfred A. Foster Jr.
Professor
Aerospace Engineering

Malcolm J. Crocker, Chair
Distinguished University Professor
Mechanical Engineering

Greg Harris
Associate Professor
Mathematics and Statistics

Stephen L. McFarland
Dean
Graduate School

MEASUREMENT OF ABSORPTION COEFFICIENT OF ROAD SURFACES USING
IMPEDANCE TUBE METHOD

Krishnasudha Vissamraju

A Thesis
Submitted to
the Graduate Faculty of
Auburn University
in Partial Fulfillment of the
Requirements for the
Degree of
Master of Science

Auburn, Alabama
August 8, 2005

MEASUREMENT OF ABSORPTION COEFFICIENT OF ROAD SURFACES USING
IMPEDANCE TUBE METHOD

Krishnasudha Vissamraju

Permission is granted to Auburn University to make copies of this thesis at its discretion,
upon request of individuals and at their expense. The author reserves all
publication rights.

Signature of Author

8th August 2005

Date

VITA

Krishnasudha Vissamraju, daughter of Swathantra Rao and Prabhavathi Devi, was born on July 15, 1979, in Nellore, India. She graduated from Osmania University with a bachelor of engineering degree (mechanical) in May 2000. She worked as a research assistant under Dr. Malcolm Crocker in the Mechanical Engineering Department and also as a teaching assistant in the Mechanical Engineering Department from August 2000 to May 2003.

THESIS ABSTRACT

MEASUREMENT OF ABSORPTION COEFFICIENT OF ROAD SURFACES USING
IMPEDANCE TUBE METHOD

Krishnasudha Vissamraju
Master of Science, August 8, 2005
(Bachelor of Engineering, Mechanical Engineering,
Osmania University,
Hyderabad, India. May 2000)

135 Typed Pages

Directed by Dr. Malcolm J. Crocker

The absorption coefficient of dense and porous road surfaces has been measured using core samples with 4 and 6-inch diameter impedance tubes. The 6-inch tube allows the absorption of a large core sample surface to be determined, but only up to a frequency of about 1250 Hz. The 4-inch tube allows the absorption coefficient to be determined up to a frequency of about 1950 Hz. The two different diameter impedance tubes were also mounted vertically on road surfaces of the same pavement types and the absorption coefficient of these surfaces was measured in situ. The peak sound absorption coefficient of the fine and coarse mix aggregate porous surfaces shows that it is only slightly

different for the two types of porous surface. The fine mix aggregate porous surface is smoother and its acoustical performance is also preferable. It is also preferable since its use also results in less tire tread impact noise and thus lower overall tire-road noise than a coarse aggregate surface.

ACKNOWLEDGEMENTS

The author would like to thank Dr. Malcolm J. Crocker for all his help during the research and development of this project and thesis work. Thanks are due to Rajeev Dyamannavar, John Li and other colleagues for their assistance during the experimentation. The author would also like to thank all the family members for their support during the course of this investigation. Special thanks are due to Mr. Doug Hanson for his help at NCAT.

TABLE OF CONTENTS

1.0	INTRODUCTION.....	1
2.0	LITERATURE REVIEW.....	6
2.1	IMPEDANCE TUBE.....	8
3.0	MOTIVATION AND SCOPE.....	11
3.1	SPEED INFLUENCE.....	12
4.0	IMPEDANCE TUBE METHOD.....	16
4.1	INTRODUCTION.....	16
4.2	LABORATORY METHODS OF MEASUREMENT TECHNIQUES.....	17
4.2.1	REVERBERANT FIELD METHOD.....	17
4.2.2	FREE FIELD METHOD.....	18
4.2.3	IMPEDANCE TUBE METHOD (KUNDT'S TUBE).....	19
4.3	IMPEDANCE TUBE THEORY.....	20
4.4	EXPERIMENTAL PROCEDURE.....	25
4.5	EXPERIMENTAL SETUP.....	27
4.6	CONSTRUCTION OF THE TUBE.....	28
4.6.1	WORKING FREQUENCY RANGE.....	29
4.6.2	UPPER FREQUENCY RANGE.....	30
4.6.3	LOWER FREQUENCY RANGE.....	30
4.6.4	LENGTH OF IMPEDANCE TUBE.....	32
4.6.5	SOUND SOURCE.....	32

4.6.6	MICROPHONES.....	33
4.6.7	MICROPHONE TYPE.....	33
4.6.8	POSITION OF MICROPHONE.....	33
4.6.9	TEST SAMPLE HOLDER.....	33
4.6.10	SIGNAL PROCESSING EQUIPMENT.....	34
4.6.11	LOUDSPEAKER.....	34
4.6.12	SIGNAL GENERATOR.....	34
5.0	ALTERNATE METHODS OF MEASUREMENT.....	38
5.1	CLOSE PROXIMITY METHOD.....	38
5.1.1	MEASUREMENT PRINCIPLE.....	39
5.1.2	TEST RESULTS.....	43
5.1.3	COMPARISION OF SURFACES.....	44
5.1.4	COMPARISION OF TYRES.....	44
5.1.5	EFFECT OF SPEED ON NOISE.....	45
5.2	IN SITU METHOD.....	46
5.2.1	SCOPE.....	46
5.2.2	GENERAL PRINCIPLE.....	47
5.2.3	SIGNAL SEPARATION TECHNIQUE.....	48
5.2.4	MEASUREMENT PROCEDURE.....	49
5.2.5	RADIUS OF MAXIMUM SAMPLED AREA.....	50
5.2.6	PRINCIPLE OF MEASUREMENT.....	51
5.3	STATISTICAL PASS BY METHOD.....	53
5.3.1	TRAFFIC NOISE.....	55
5.3.2	VEHICLE NOISE.....	55
5.3.3	TIRE/ROAD NOISE.....	55

5.3.4	POWER UNIT NOISE.....	55
5.3.5	ROAD SPEED.....	55
5.3.6	VEHICLE CATEGORIES.....	56
5.3.7	VEHICLE SOUND LEVEL.....	56
5.3.8	STATISTICAL PASS BY INDEX.....	57
5.3.9	MEASURING PROCEDURE.....	57
5.3.10	MEASURING PRINCIPLE.....	57
5.3.11	CONCLUSION.....	61
6.0	MEASUREMENT AND DISCUSSION OF RESULTS.....	72
6.1	TRACK SAMPLES.....	74
6.2	TESTING OF LABORATORY MANUFACTURED SAMPLES.....	76
7.0	CONCLUSION.....	110
	NOMENCLATURE.....	114

LIST OF FIGURES

4.1	Standing wave pattern in the impedance tube.....	35
4.2	Impedance tube set up.....	36
4.3	Dimensions of the two-microphone impedance tube built at Auburn University.....	37
5.1.1	Microphone layout for close-proximity method (trailer method).....	62
5.1.2	NCAT CPX trailer.....	63
5.1.3	UniRoyal tire.....	64
5.1.4	MasterCraft tire.....	64
5.1.5	Comparison of noise levels for different surfaces.....	65
5.1.6	Comparison of noise levels for each of the tires.....	66
5.1.7	Noise versus speed.....	67
5.2.1	Sketch of the essential components of the in-situ measurement set-up.....	68
5.2.2	Separation of the impulse response of the direct and the reflected path using time windows.....	69
5.2.3	Principle of the signal subtraction technique.....	70
5.3.1	Measurement Set-up for statistical pass-by method.....	71
6.1	Experimental setup of impedance tube.....	79
6.2	Experimental setup, 4-inch impedance tubes, asphalt cores “O” rings and metal back plates.....	80

6.3	The 3-inch thick hard surface dense track pavement samples.....	81
6.3	Comparison of sound absorption coefficients of different samples obtained using 6-inch tube.....	82
6.5	Absorption coefficient of sample S4 obtained using a 6-inch tube.....	83
6.6	Absorption coefficient of sample S5 obtained using a 6-inch tube.....	84
6.7	Absorption coefficient of sample S1 obtained using a 6-inch tube.....	85
6.8	Absorption coefficient of sample S11 obtained using a 6-inch tube.....	86
6.9	Absorption coefficient of sample N7 obtained using a 6-inch tube.....	87
6.10	Absorption coefficient of sample N1 obtained using a 6-inch tube.....	88
6.11	Absorption coefficient of sample NB obtained using 6-inch tube.....	89
6.12	Comparison of the sound absorption coefficients of hard samples measured in the 6-inch tube.....	90
6.13	OGFC graded coarse 1.5-inch thick 6-inch diameter porous cores.....	91
6.14	Sound absorption coefficients of OGFC 1-inch fine cores measured by a 6- inch tube.....	92
6.15	Sound absorption coefficients of OGFC 1.5-inch fine cores measured by a 6- inch tube.....	93
6.16	Comparison of sound absorption coefficients of OGFC fine 1.5-inch core and slab measured by 6-inch tube.....	94
6.17	Sound absorption coefficients of OGFC 2-inch fine measured by a 6-inch tube.....	95
6.18	Comparison of sound absorption coefficients of OGFC fine 2-inch core and slab measured by 6-inch tube.....	96

6.19	Sound absorption coefficients of OGFC 1-inch coarse cores measured by a 6-inch tube.....	97
6.20	Comparison of sound absorption coefficients of OGFC coarse 1-inch core and slab measured by 6-inch tube.....	98
6.21	Sound absorption coefficients of OGFC 1.5-inch coarse cores measured by 6-inch tube.....	99
6.21	Comparison of sound absorption coefficients of OGFC coarse 1.5-inch core and slab measured by 6-inch tube.....	100
6.22	Sound absorption coefficients of OGFC 2-inch coarse cores measured by a 6-inch tube.....	101
6.23	Comparison of sound absorption coefficients of OGFC coarse 2-inch core and slab measured by 6-inch tube.....	102
6.24	Comparison of sound absorption coefficients of OGFC slabs measured by the 6-inch tube.....	103
6.25	Experimental setup for in situ measurements of sound absorption coefficient of slabs.....	104
6.26	Comparison of sound absorption coefficients of OGFC cores measured in 6-inch tube.....	105
6.28.	Comparison of sound absorption coefficients of OGFC slabs measured by 6-inch and 4-inch tubes.....	106
6.29	Comparison of the sound absorption coefficient of OGFC aggregated fine slabs and cores.....	107

6.30	NCAT test track.....	108
6.31	NCAT tire noise measurement trailer set-up.....	109

CHAPTER 1
INTRODUCTION

Noise is one of the most serious environmental problems in modern societies. Practically all human activities create noise and the greater the level of development in a country the higher are the sound levels. This is true to a very great extent with regard to traffic noise. Owing to the increasing density of road traffic, higher mean speeds and vehicles that are in many cases noisier than in earlier days, vehicular traffic has grown into one of the largest sources of noise pollution in modern societies. Traffic noise is thus a very serious social problem. It is therefore of great importance to be able to assess with acceptable accuracy the effects of different measures taken with road surfaces with a view to reducing tire/road interaction noise.

Roadside noise levels have not substantially decreased in the last thirty years [1]. In the mean time, due to the spread of urban areas, the part of the population exposed to unhealthy noise levels has increased and has now reached almost 60 per cent in West European countries. As a response to people's complaints and as a result of the reduction of noise level limits, tire/road interaction noise has recently become the subject of a significant research effort.

Some of the laboratory procedures for the prediction of traffic noise are so accurate today that often they may predict noise levels that are more reliable and

representative then the noise level obtained when actually measurements are made at the specific site (in-situ methods). However, in some cases, large errors in the predictions occur. In such cases the tire/road noise is atypical of the condition assumed 'normal' in the prediction model, for instance when special road surfaces are used. This implies that tire/road noise is an important contributor to the overall traffic noise.

As tire/road noise is largely influenced by road surface characteristics, another implication is that prediction models should have a correction term for the influence of the road surface. Several methods indeed allow for this possibility. For instance the British procedure for Calculation of Road Traffic Noise [2] has a correction of up to +4dB(A) for deeply grooved cement concrete surfaces, and the Netherlands's Road Traffic Noise Calculation Procedure, allows for corrections up to +4.5dB(A).

In order to enable corrections to the tire/road noise prediction model, the road surface must be classified in some way. The Australian Standard contains a correction for the tire/road noise prediction model where the sand-patch method for texture measurement is recommended to supplement the road type classification [3].

There are few other mechanisms that affect the tire/road noise in addition to the ones that have been described above:

- The horn effect.
- The sound absorption of the road surface.
- The mechanical impedance effect.

The horn effect must be a fundamental component of any tire noise radiation model. A tire is a weak sound source. Between the curved tire tread, for and aft of the tire/road interface, and the road surface there is a space in the form of an acoustical horn which

increases the efficiency of sound radiated backwards and forwards [4]. This horn effect could be effectively eliminated when one of the surfaces of the horn is porous, such as when the road pavement is drainage asphalt.

The sound absorption effect occurs only with so-called drainage asphalt (porous or pervious asphalt are alternative names) when the surface has a significant sound absorption. It influences not only tire/road noise but also power-train noise [1]. The sound absorption effect is of great importance in the reduction of traffic noise. The stiffness of the road surface, or the matching of mechanical impedance tire-to-road, also influences the tread block or road texture impact. Impacts may be amplified by (stiff road surfaces) or attenuated by (soft road surfaces). It seems probable that rigid pavements like cement concrete may be somewhat noisier than flexible pavements like asphalt concrete, and that the noise may increase somewhat when a surface is aged by compaction.

For a complete road surface characterization with respect to noise one should, in light of the discussion in the previous section, measure the following quantities:

- The texture profile
- The sound absorption coefficient or sound propagation
- The mechanical stiffness or impedance.

In this research work, a laboratory method to determine the acoustical properties of various road surfaces has been discussed. The experimental technique used is a two-microphone impedance tube method, where absorption coefficients of different road surfaces were measured.

A summary of literature review on various methods that are used to determine the acoustical properties of road surfaces particularly the absorption coefficient is discussed

in Chapter 2. Chapter 3 presents the scope and motivation behind this thesis. Chapter 4 discusses the experimental laboratory method, which was used to determine the sound absorption coefficient of road surfaces. This chapter also includes results that were obtained using the impedance tube method set-up.

Chapter 5 discusses alternative methods that have been used to determine the absorption and mechanical properties of road surfaces. In this chapter the main features of the methods are presented along with some experimental results from various investigations. Although the methods are designed to give compatible results, they are not equivalent in all respects. Depending on their intended purposes, one or another could be more suitable as a reference procedure.

Chapter 5 also includes the experimental procedure and set-up for the CPX (close proximity) method along with some results from NCAT (the National Center for Asphalt Technology, Auburn). Pavement surfaces with different thicknesses, d , different air voids, V_a , and different aggregates (fine and coarse) have been investigated in NCAT. The relationship between air void ratio V_a , thickness d and peak frequency of the sound absorption coefficient α and its magnitude has been examined. Also some preliminary measurements of the A-weighted road/tire noise close to the tire have been made on some of the dense pavement surfaces, using the CPX (close proximity) method. This chapter also reviews the Statistical Pass-By Method (SPB) to determine the sound absorption properties of road surfaces and some results measured [8] using this method.

The discussions on results obtained using impedance-tube method are presented in Chapter 6. Conclusions on the results obtained and scope for future research work on the acoustical properties of road surfaces is given in Chapter 7.

CHAPTER 2

LITERATURE REVIEW

Throughout the world, sound caused by transportation systems is the number one noise complaint. Highway noise is one of the prime offenders. Engine (power train), exhaust, aerodynamic and pavement/tire noise all contribute to traffic noise.

Since 1973 the adverse noise effects of road proposals on the surrounding environment and possible ways of minimizing these effects have been more comprehensively taken into consideration before the road is built. The basis of assessing the effects of traffic noise was established from the outset, although the methodology has been improved in succeeding years. Because it is necessary to predict the effects of a scheme long before it is put into practice, assumptions have to be made about a number of factors that influence noise levels. In order to simplify the prediction process, the effects of most of these factors have been incorporated into statistical relationships established by measurements of traffic noise under different conditions.

The term *tire* was in use even before the pneumatic tire was first used. The term *tire* meant the outer part of the wheel. In the days of iron-shod wheels/tires, the interaction of the metal (tire as well as horse shoes) and stone (pavement) created noise that was concern to many. Complaints about such traffic noise were common already in the Roman Empire [1]. Nearly two thousand years later, in 1869, the problem seemed to

be about the same, as noted by Sir Norman Moore, a British physician, who gave a graphic description of the noise in a London street: *“Most of the streets were paved with granite sets and on them the wagons with iron-tired wheels made a din that disrupted conversation while they passed by. The roar of London by day was almost terrible – a never varying deep rumble that made a background to all other sounds”* [Crocker, 1984]. The problems led to trials with low noise road surfaces, already in the 19th century, like for example wooden block pavements that were both smoother and softer than the various stone pavements [1].

Tire/road noise has become a concern to more and more people these days and this type of noise now constitutes the major component problem in traffic noise in (at least) the highly industrialized countries [5]. Tire/road noise is mostly comprised of noise emitted from rolling tires as a result of the interaction between the tire and road surface. In principle, more than the tire may radiate this type of noise, most notably structure-borne sound may spread to the rim and parts of the vehicle body and radiate from there, and possibly also from part of the road surface. But radiation from the tire itself probably dominates. It is seen that there were very few papers published on this subject before about 1970, but very ambitious research programs in the US throughout the 1970's, with a few extensive projects also in the U.K., culminated in 1976 (San Francisco) and 1979 (Stockholm). The activities opened the eyes and ears of people and put tire/road noise permanently on the agenda; e.g. at Inter-Noise conferences.

But this does not mean that exterior tire/road noise was an insignificant environmental factor earlier times. At speeds above (say) 70 km/h, tire/road noise must have been the dominating type of noise already along the highways in 1950's but it seems

that almost nobody was aware of it. Engineers in the vehicle and tire industry were concerned with interior tire/road noise already in the 1930's, but the first major experimental study on exterior tire/road noise was published in 1955 [1].

2.1 Impedance tube:

In the last several years a number of new impedance measuring methods have been proposed. Initial studies were done using stationary microphone systems. The impedance of small acoustic filters used as mufflers for refrigeration compressors was measured using the gated sine wave method by Gately and Cohen [14]. This experimental method gave them an opportunity to measure the incident and reflected wave amplitudes, along with the phase shift between waves. Later Schmidt and Johnston measured the reflection coefficient of orifices using a pair of closely spaced microphones [5]. However, they had problems in determining the phase angle and therefore did not measure the acoustic impedance.

The “two-microphone” method was initially used by Melling to measure the acoustic impedance of perforates [7]. Singh and Katra [17] used a pulse technique to measure the reflection coefficient of small acoustic filters.

Seybert and Ross [9] were one among the first researchers to use a two-microphone, random-excitation technique to study the acoustic impedance of automotive mufflers. They proved that for a plane wave sound field, the incident and reflected waves could be separated by measuring the cross-spectrum between two microphones located at fixed positions in a long tube. In addition to the measurement of the acoustic impedance, this method can also be used to determine the incident and reflected sound power in a long

tube. Blaser and Chung also previously used this method to evaluate internal combustion engine exhaust systems [5].

The remainder of this thesis discusses the application of some other methods that are used to determine the acoustic impedance of materials.

In the United States, the Federal Highway Administration has published the noise standards for highway projects as 23CFR772 [20]. The FHWA Noise Abatement Criteria states that noise mitigation must be considered for residential areas when the A-weighted sound pressure levels approach or exceed 67 dB (A). To accomplish this, many areas in the United States are building large sound barrier walls at a cost of one to five million dollars per roadway mile [10]. Noise barriers are most common abatement strategy. Other strategies such as alterations of horizontal/vertical alignment, traffic controls, greenbelts and insulation of structures are also used to reduce noise. Each of these noise reduction measures will add significant cost to a project. In addition, each is limited in the amount of noise reduction that is possible and in many cases cannot be used for practical reasons. For examples, noise barriers cannot be used if driveways are present.

It has been shown that modification of pavement surface type and/or texture can result in significant tire/pavement noise reductions. European highway agencies have found that the proper selection of the pavement surface can be an appropriate noise abatement procedure. Specifically, they have identified that a low noise road surface can be built at the same time considering safety, durability and cost using one of the following approaches [11]: 1) A surface with a smooth surface texture using small maximum size aggregate 2) A porous surface, such as an open graded friction course

(OGFC) with a high air void content or 3) A pavement-wearing surface with an inherent low stiffness at the tire/pavement interface.

The purpose of this thesis is to present the results of the study of tire/pavement noise and procedures that can be used for this purpose. This thesis describes an analysis of testing conducted at Auburn University acoustical laboratory during January 2002 to April 2003.

In summary, it is anticipated that the use of various methods such as SPB, CPX and impedance tube, together with other methods under development, will help to accelerate the introduction of progressively quieter road surfaces around the world. In addition, the standard measurement procedures being developed by ISO will lead to improvements in the specification of noise reducing road surfaces and in assessing their conformity of production. These assessment procedures together with the tire noise type approval test could provide the authorities with a range of tools to encourage industry to develop complementary designs of tyres and road surfaces that will substantially reduce the problem of tire noise.

CHAPTER 3

MOTIVATION AND SCOPE OF RESEARCH WORK

In last several years, a considerable amount of research and development work has been conducted to reduce noise and vibration in modern cars and trucks. Significant improvements have been made in reducing noise from power trains, exhaust and wind turbulence. Nowadays tire/road interaction noise is receiving increasing attention. The tire/road interaction noise generation mechanisms are complicated.

The two main noise sources in modern cars and trucks are caused by the tire/road interaction (noise emitted from a rolling tire as a result of the interaction between the tire and the road surface) and power train (engine and exhaust pipe induced noise). Substantial noise reductions have been achieved with power train noise. Tire/road noise is generated from vibrations caused by the impact and release of tread blocks entering and leaving the tire/road contact patch. These acoustic sources are then differentially amplified by the tire/road geometry ('horn effect'), resulting in far-field noise. The amplification is strongest in the 'horn' between the tire belt and the road surface, so that contributions from local vibrations in this region dominate the far field noise. Both tire/road and power unit noise have strong relationships to vehicle speed. Tire/road noise levels increase approximately logarithmically with speed, which means that on a logarithmic speed scale, noise levels increase linearly with speed.

At low speeds power unit noise dominates, while at high speeds tire/road noise dominates, and there is a certain “crossover speed” where the contributions are about the same.

Speed influence

The relationship between the vehicle speed and the tire noise can be represented as,

$$L = A + B \log(v) \quad (3.1)$$

where,

L = sound pressure level (SPL) in dB,

v = Vehicle speed in km/h and

A and B are speed coefficients (constants).

The noise resulting from the contact between the tire and the road becomes predominant at driving speeds above 50 km/h. There is therefore an explicit need for methods of tire/road noise calculation, which relate the sound levels caused by road vehicles to the parameters of the road and traffic. Many such methods have been published in recent years, but most of them are fairly approximate and do not permit studies of all the parameters that are of significance.

When vehicle noise is measured according to the present international standards, the driving condition is such that power-train noise (engine and exhaust noise) generally dominates over tire/road noise. The purpose of such measurements is primarily to measure the maximum noise a vehicle can emit during urban use. However, during most of the time during non-urban use, tire/road noise dominates over power-train noise [6]. This is true for practically all cars and for many, if not most, trucks.

Also in urban driving, tire/road noise may sometimes be important. This can be illustrated by the finding that when cars were designed to satisfy the noise emission limit of 77 dB (A), as measured by ISO 362 and as required in Europe in 1988, tire/road noise contributed significantly to overall noise, despite the extreme acceleration and resulting high power output of the engines during this test. When satisfying the stringent Swiss limits of 75 dB (A), tire/road noise even appears to contribute as much as all the other sources together. In line with increased awareness of the importance of tire/road noise, the need for a standardized measurement method has become pressing.

Researchers have found that one way to reduce tire/road interaction noise is by the use of porous road pavement surfaces. Such surfaces have the advantage that they not only reduce the tire/road noise at the point of its generation, but they also attenuate it (and the power plant noise) by absorption of sound as it propagates to nearby residential areas. Such surfaces have the further advantage that they drain water well and reduce the splash up behind vehicles during heavy rainfalls [12].

The sound absorption of porous road pavement surfaces is affected by several geometrical and other parameters. These include:

- 1) The *thickness* d of the porous layer,
- 2) The *residual air voids content*, Ω *air voids* (V_a) often just called “air voids” or “porosity”,
- 3) The *airflow resistance per unit length*, R ,
- 4) The *tortuosity*, q , and
- 5) The *coarseness of the aggregate mix* (use of small or large chips aggregate, etc).

The residual air void content Ω is the proportion of air in the total pavement mix (by volume). For most common dense asphalt mixes, V_a is about 5%, while for new porous mixes, the air void content Ω air voids V_a varies from about 15 to 30%. The airflow resistance R is the resistance experienced by air when it passes through open pores in the pavement. The tortuosity or “shape factor as it is sometimes known” is a measure of the shape of the air void passages (whether they are almost straight or twisted and winding and whether they slowly or rapidly change cross section area) and the effect this has on the pavement sound absorption properties [12].

Von Meier [13] has made theoretical studies of the effect of air void content and flow resistance on the sound absorption coefficient “ α ” of porous surfaces. He found that both the air void content and flow resistance have a strong effect on the peak values of the absorption coefficient of a 40 mm thick porous surface with a tortuosity value of 5. The high air void content leads to higher values of the absorption coefficient α at both of the absorption peaks predicted for such surfaces, while higher values of air flow resistance R also initially lead to higher values of the absorption coefficient at the peaks, but after a certain value of R is reached, the sound absorption peak values “ α ” start to decline.

Several in situ methods are already in use to measure the acoustical characteristics of tire/road interaction mechanism but there is scope to improve the laboratory methods of measuring the acoustical properties of road surfaces. In addition there is a need for more experimental data to be obtained on the acoustical properties of different road surfaces.

The objective of the research work in this thesis is to develop an experimental methodology to determine the acoustical properties of various road surfaces. The experimental technique used was a two-microphone impedance tube method, where absorption coefficients of different road surfaces were measured. The impedance tube used for measurements was constructed in the Auburn University workshop and the validity of the impedance tube was verified by measuring sound absorption characteristics of known materials like fiberglass and metal surfaces. Two different sizes of impedance tube were constructed one with a 4-inch and another with a 6-inch internal diameter. The 6-inch tube allows the absorption of a large core sample surface to be determined, but only up to a frequency of about 1250 Hz. The 4-inch tube allows the absorption coefficient to be determined up to a frequency of about 1950 Hz. The effect of sound absorption coefficient on the dense and porous road surfaces is studied.

All the measurements were carried out at the Auburn University Sound and Vibration Research laboratory using a 4-channel B&K pulse system analyzer and two ½ inch G.R.A.S. microphones. Funds were provided by the National Center for Asphalt Technology (NCAT) in partial support of this project.

CHAPTER 4

IMPEDANCE TUBE METHOD

4.1 Introduction

The acoustically relevant parameters and criteria measured in this research are related in the first place to the noise generating mechanisms of tire/noise. With regard to the road surface these parameters are:

- Acoustic absorption coefficient.
- Acoustic reflection coefficient.
- Normalized impedance.

These acoustical properties can be measured in a variety of ways both in situ and in the laboratory. This chapter discusses, in brief, different laboratory methods for the measurement of the acoustical properties of road surfaces. The advantages and disadvantages of each technique are discussed. The Impedance tube method to measure the acoustical properties of road surfaces was used in this research work. The subsequent sections in this chapter describe in detail the theory, construction and testing of an acoustical impedance measurement tube.

A number of alternate measurement techniques can be used to quantify the acoustic impedance of materials or structures, but most often the determination of the

properties is made in an impedance tube. This is because in a tube, acoustic phenomena become one-dimensional, and up to a certain frequency and bandwidth sound waves can only propagate in one direction. This makes the experimental set-up relatively simple. Different alternate methods of measuring acoustic impedance are discussed in brief in Chapter 5.

4.2 Laboratory Methods of Measurement Techniques

The acoustical laboratory measurement techniques can be divided into three categories:

- Reverberant field methods.
- Free-field methods
- Impedance tube methods (Kundt's tube)

4.2.1 Reverberant Field Method

The so-called reverberant field method is a well-known technique used to measure sound absorption coefficient with waves at random incidence. Experiments are performed in a reverberation chamber in which a diffuse sound field is generated.

There are a number of standards available for the procedure as well as for the geometry and dimensions of the test chamber. Usually a sound pressure field is generated with a uniform energy density. This is achieved with loudspeakers that are placed in the corners of such chambers and a number of diffusers are used to reduce standing waves in the chamber. A relatively large sample of the sound absorbing material (several m^2) is placed in the chamber and for a given frequency band the reverberation time T_{60} is measured. T_{60} is the time during which the sound pressure level has dropped 60 dB after

the loudspeakers have been shut down [20]. The same procedure is performed without the sample and the difference is related to the sound absorption coefficient.

For highly sound absorbing materials the absorption coefficient can exceed a value of one because of the simple Sabine formula used for the calculation. This can also be the case if the sound field is non-diffuse. Various standards state that at least 20 modes of vibration in the chamber are required in the lowest frequency band. As a result the room volume must be quite large. Nevertheless considerable differences have been observed for measurements on the same test materials in different reverberation chambers.

Although it is the only method to apply diffuse sound fields, it is concluded that the reverberation field method is less suitable for testing samples, which include broadband resonators.

4.2.2 Free Field Method

Free field methods are commonly used for radiation measurements of sources of sound. The free field condition indicates that waves only propagate directly from the source of sound. This condition can be realized in an anechoic chamber. For such situations, outdoor measurements above a reflecting plane can be made, or a semi-anechoic chamber can be used, in which the floor is a reflecting plane.

Some authors have proposed methods to measure the acoustic properties of sound absorbing materials under free field conditions. In general the methods are suited for measurements with oblique incident waves. One technique is known as the pulse technique. A short signal is generated and the direct and the reflected waves are separated in order to calculate the reflection coefficient. It is noted that the sample has to be placed

outside the near field, which can pose a lower limit on the frequency range of interest, and on the dimensions of the samples (several m^2). Another technique uses two microphones placed close to the sound-absorbing surface. With this method it is possible to calculate the normal impedance at the surface exposed to obliquely incident waves. The area of the test material can be much smaller (1 m^2). For lower frequencies, however, the size of an anechoic chamber may be a restricting factor because the sample should be placed outside the near field of the sound source.

The possibility to measure the acoustic behavior of sound absorbing materials exposed obliquely incident waves is a strong advantage of the free field method. It was already mentioned that with obliquely incident sound waves, the shear waves that propagate in the sound absorbing material cause it to have a different acoustic behavior. However, for the materials tested with the impedance tube, the shear waves were not present. Therefore it will be shown that it is suitable to use the impedance tube technique to measure the normal impedance.

Earlier techniques made use of the measured standing wave ratio (SWR) for a specific frequency in the tube. By means of a movable microphone, the ratio of sound pressure maximum to the sound pressure minimum is determined. This ratio is then used to calculate the reflection coefficient and the acoustical impedance. An advantage of this method is that it is not necessary to calibrate the microphone. Drawbacks are: 1). The complex set-up required with a movable probe and 2). The time needed to find the maximum and minimum sound pressure levels at each frequency of interest.

4.2.3 Impedance Tube Method (Kundt's Tube)

In 1980 Chung and Blazer presented a technique, which is based on the transfer function between two fixed microphones located at two different positions in the tube wall [14]. This method will be called the 2p method. The standing wave pattern in their case was built up from a broadband stationary noise signal. By using the measured transfer function, the incident and reflected waves can be recovered mathematically. From these the reflection coefficient of the sample can be calculated for the same frequency band as the broadband signal. The impedance and absorption coefficient can be calculated as well. The method is as accurate as the SWR method and considerably faster. The transfer function method has proven to be reliable and has been standardized in the ISO standard 10534-1 [15].

4.3 Impedance Tube Theory

Two methods are employed for acoustical impedance measurements using an impedance tube. One technique uses continuous white noise to excite two-microphones and the other uses transient sound excitation to excite a single microphone. Acoustics theory can be used to derive equations for the two methods. In this research work, the first method i.e. two-microphone method, which is the most commonly used method now, was used.

Usually the acoustical sample is put at one end of a tube and a loudspeaker is mounted at the other end. The loudspeaker generates sound and this results in a forward traveling sound wave. A part of the sound is reflected, causing a backward traveling sound wave. The reflection coefficient is determined by measuring sound is traveling in the forward and backward direction.

Imagine that the sample in the tube is fully sound reflecting, so that all the sound that travels along the tube is reflected at the end. In such a case the sound intensity (the net flow of sound energy in one direction) in the tube will be zero. If on the other hand the sample is fully sound absorbing, the sound intensity will be large. How large the sound intensity is depends on the amount of noise, which is generated by the loudspeaker. The ratio of the sound intensity to the energy density is zero for a full reflecting sample.

During any measurement process, in general one is interested in the sound absorption coefficient α , (which is the fraction of the total incident sound energy which is dissipated in the porous material), the reflection coefficient R , or the normal surface impedance Z_n . The incident sound field can be classified into three types: 1) normal incidence 2) oblique incidence and 3) random incidence.

Typically the absorption coefficient of a material increases with increasing angle of incidence up to a certain angle. Beyond this angle a decrease in the absorption coefficient is usually observed. One explanation for this is the contribution of the so-called shear waves that propagate in the flexible porous material. As a result the absorption coefficient at normal incidence is slightly less than the absorption coefficient measured at random incidence for porous materials. The normal impedance on the other hand is a complex vector that is oriented normal to the surface of the porous material and directed inward. In this case one can speak of the normal surface impedance of a material measured with oblique incident sound waves.

For sound-absorbing materials the impedance measured with the impedance tube method depends strongly on the thickness of the material because the sound waves reflect at the backing plate. Therefore some authors advise the use of acoustic properties that are

independent of the test configuration such as the characteristic impedance and the propagation coefficient in the material. One technique to derive these two coefficients is to measure the surface impedance of the material with two different thicknesses.

For low frequencies the impedance tube method may not give accurate results because an airtight fit of the sample is needed and at the same time the sample has to be able to vibrate freely. This may also be a problem for higher frequencies when laminated materials or materials covered with a screen (for example a perforated sheet) are used. Furthermore, for a non-zero transverse contraction ratio (Poisson's coefficient) it is unlikely that a small sample is representative for a large area. For rock and glass wool, however, Poisson's coefficient is approximately zero.

The theory underlying the two-microphone method involves the decomposition of a broadband stationary random signal (generated by an acoustical driver) into its incident and reflected components by the use of a simple transfer function relation between the sound pressure at two locations on the tube wall as depicted in Fig 4.2. This wave decomposition is made by a determination of the complex reflection coefficient, from which acoustical properties such as the acoustical impedance and the sound absorption coefficient are evaluated. Assume that a pipe of cross sectional area S and length L . The pipe is terminated at $x=L$ by a mechanical impedance Z_{mL} . The sound source produces a plane wave that propagates along the impedance tube. Then the sound pressure wave in the pipe will be of the form,

$$P = Ae^{i[\omega t + k(L-x)]} + Be^{i[\omega t - k(L-x)]}, \quad (4.1)$$

where A and B are determined by the boundary conditions at $x = 0$ and $x = L$. Using Euler's equation

$$\rho \left(\frac{\delta u}{\delta t} \right) = -\nabla p. \quad (4.2)$$

One may obtain the particle velocity in the tube,

$$u = \frac{1}{\rho c} \left(A e^{i[\omega t + k(L-x)]} + B e^{i[\omega t - k(L-x)]} \right). \quad (4.3)$$

The acoustical impedance of the plane waves in the tube may be expressed as,

$$Z_A(x) = \frac{p}{u} S = \frac{\rho c}{S} \left(\frac{A e^{i[\omega t + k(L-x)]} + B e^{i[\omega t - k(L-x)]}}{A e^{i[\omega t + k(L-x)]} - B e^{i[\omega t - k(L-x)]}} \right). \quad (4.4)$$

The mechanical impedance load at $x = L$ may be written in terms of this acoustical impedance as,

$$Z_L(x) = S^2 Z_A = \rho c S \left(\frac{A+B}{A-B} \right) = \rho c S \left(\frac{1 + \left(\frac{B}{A} \right)}{1 - \left(\frac{B}{A} \right)} \right). \quad (4.5)$$

If we chose to write,

$$A = A$$

$$B = B e^{i\theta}, \quad (4.6)$$

Then,

$$Z_L(x) = \rho c S \left(\frac{1 + \left(\frac{B}{A} \right) e^{i\theta}}{1 - \left(\frac{B}{A} \right) e^{i\theta}} \right). \quad (4.7)$$

Thus, given the ratio of incident to reflected amplitudes, and the phase angle θ , the acoustical impedance of the sample may be determined. Substitution of Eq. 4.5 in Eq. 4.1 and solving for the sound pressure amplitude of the wave, one obtains

$$P = |p| = \left\{ (A+B)^2 \cos^2 \left[k(L-x) - \frac{\theta}{2} \right] + (A-B)^2 \sin^2 \left[k(L-x) - \frac{\theta}{2} \right] \right\}^{1/2}. \quad (4.8)$$

This sound pressure amplitude is shown in Fig 4.1. The Fig 4.1a shows the pressure amplitude in the pipe with a rigid termination at $x=L$. All of the sound energy incident upon the termination is reflected with the same sample. However, there may be some absorption along the walls as the waves travel back and forth along the pipe. The Fig 4.1b represents the case when the pipe is terminated at $x= L$ with some acoustic absorbing material. Now the material absorbs some of the incident sound energy so that the reflected waves do not have the same amplitude as incident wave. In addition the absorbing material introduces a phase shift into the reflected wave.

The sound pressure amplitude at an antinode (maximum pressure) is $A+B$, and the sound pressure amplitude at a pressure node (minimum pressure) is $A-B$. It is not possible to measure A or B directly. However, we can measure $A+B$ and $A-B$ using the standing wave tube.

We define the ratio of the sound pressure maximum to the sound pressure minimum as the standing wave ratio.

$$SWR = \frac{A+B}{A-B}, \quad (4.9)$$

which may be arranged to provide the sound power reflection coefficient,

$$R = \frac{B}{A} = \frac{SWR-1}{SWR+1}. \quad (4.10)$$

A sound pressure minimum occurs when,

$$\cos \left[k(L-x) - \frac{\theta}{2} \right] = 0 \text{ and } \sin \left[k(L-x) - \frac{\theta}{2} \right] = 1, \quad (4.11)$$

Which requires that

$$k(L-x) - \frac{\theta}{2} = \left(n - \frac{1}{2}\right)\pi, \quad (4.12)$$

or,

$$\theta = 2k(L-x) - (2n-1)\pi, \quad (4.13)$$

Where the quantity $(L-x)$ equals the distance from the test sample to the first pressure minimum ($n=1$) as shown in Fig 4.1.

The sound power absorption coefficient for the test sample at a specific frequency is given by,

$$\alpha = 1 - R^2 = 1 - \frac{(SWR-1)^2}{(SWR+1)^2}. \quad (4.14)$$

As was the case for the impedance, the absorption coefficient is a function of frequency, and measurements over the frequency range of interest are usually required.

4.4 Experimental Procedure

The test sample is mounted at one end of a straight, rigid, smooth and airtight impedance tube. Plane waves are generated in the tube with the help of a loudspeaker (random, pseudo-random sequence, or chirp) fixed at the other end. The complex acoustical transfer function between the two microphone signals is determined and used to compute the normal incidence complex reflection factor, the normal-incidence absorption coefficient, and the impedance ratio of the test material. These quantities are determined as functions of frequency with a frequency resolution, which is determined from the sampling frequency, and the record length of the Brüel and Kjaer Pulse system used for the measurements. The usable frequency range depends on the width of the tube

and the spacings between the microphones. An extended frequency range may be obtained from the combination of measurements with varying widths and spacings between the microphones.

The measurement method is based on the fact that the sound reflection factor, at normal incidence, r , can be determined from the measured transfer function H_{12} between two microphone positions in front of the material tested. See Fig 4.2.

The sound pressures of the incident wave p_i and the reflected wave p_R are, respectively:

$$p_I = \widehat{p}_I e^{jk_0 x} \quad (4.15)$$

and

$$p_R = \widehat{p}_R e^{-jk_0 x} \quad (4.16)$$

where

\widehat{p}_I and \widehat{p}_R are the magnitudes of p_I and p_R at the reference plane ($x=0$);

and $k_0 = k_0' - jk_0''$ is a complex wave number.

The sound pressures p_1 and p_2 at the two microphone positions are

$$p_1 = \widehat{p}_I e^{jk_0 x_1} + \widehat{p}_R e^{-jk_0 x_1} , \quad (4.17)$$

and

$$p_2 = \widehat{p}_I e^{jk_0 x_2} + \widehat{p}_R e^{-jk_0 x_2} . \quad (4.18)$$

The transfer function, H_1 , for the incident wave alone is:

$$H_1 = \frac{P_{21}}{P_{11}} = e^{-jk_0(x_1-x_2)} = e^{-jk_0 s} , \quad (4.19)$$

where the separation between the two microphones is $s = x_1 - x_2$.

Similarly, the transfer function H_R for the reflected wave alone is:

$$H_R = \frac{P_{2R}}{P_{1R}} = e^{jk_0(x_1 - x_2)} = e^{jk_0s} . \quad (4.20)$$

The transfer function H_R for the total sound field may now be obtained by using equations and that $\widehat{p}_R = r\widehat{p}_I$,

$$H_{12} = \frac{p_2}{p_1} = \frac{e^{jk_0x_2} + re^{-jk_0x_2}}{e^{jk_0x_1} + re^{-jk_0x_1}} . \quad (4.21)$$

Rearranging Eq. 4.21 to yield r ,

$$r = \frac{H_{12} - H_I}{H_R - H_{12}} e^{2jk_0x_1} . \quad (4.22)$$

The normal incidence sound absorption coefficient is:

$$\alpha = 1 - |r|^2 . \quad (4.23)$$

the specific acoustical impedance ratio is:

$$\frac{Z}{\rho c_0} = \frac{R}{\rho c_0} + \frac{jX}{\rho c_0} = \frac{(1+r)}{(1-r)} , \quad (4.24)$$

where

R Is the real component of the impedance

X is the imaginary component of the impedance and

ρc_0 is the characteristic impedance.

4.5 Experimental Setup

The impedance tube is straight with a uniform cross sectional (diameter or cross dimension within $\pm 0.2\%$) and with rigid, smooth, non-porous walls without holes or slits (except for the microphone positions) in the last section. The walls are massive and thick enough so that they are not excited into vibration by the sound signal and do not have any vibration resonances in the working frequency range of the tube. For tubes with metal walls, a thickness of about 5% of the diameter is recommended.

The length of the tube is 4 ft and the diameters are 4 and 6 inches to fit the diameters of the standard road core samples. The metal chosen for the impedance tube was aluminum in accordance with the ISO standard chosen and to keep within the available funding for the project. The test specimen provided was tightly fitted to one end of the tube-using O-rings. The diameter of the O-rings was varied according to the diameter of the tube. The width of the sample could be varied and the number of O-rings to be used was selected accordingly. A metal spacer was placed behind the sample when a sample of smaller width is tested.

The O-rings were fitted onto the tube first by making a circular groove in the tube. The samples were then tightly fitted into the tube. Two microphones were fitted into the tube wall to measure the sound pressures. These microphones were further connected to the Brüel & Kjær Pulse system that is used in the analysis of the data collected.

The type and the diameter of the microphones were selected in accordance with the ISO [16] and ASTM standards [18]. O-rings are also used to fit the microphones to the impedance tube. The sound source was connected to the other end of the impedance tube. The sound source was enclosed in a wooden box to avoid any leakage of sound. The

sound source along with the wooden box was fitted to the impedance tube through a flange, which was welded to the end of the tube.

4.6 Construction of the Impedance Tube

The apparatus is essentially a metal tube with a test sample at one end and a loudspeaker (sound source) at the other. The impedance tube used is straight, with a constant cross-section (to within 0.2 %) and with rigid, smooth, non-porous walls without holes or slits in the test section. The tube is massive and sufficiently rigid to avoid;

1. Transmission of noise into the tube from outside.
2. Vibration excitation by the sound source or from background sources (e.g., doors closing).

Two microphones whose type and diameters were chosen in accordance with the ISO standard 10534 and fitted into the ports provided in the wall of the impedance tube. The tube should be packed with acoustical absorbing materials that provide enough absorption to make the SWR constant within 2 dB over the working range of the tube.

4.6.1 Working Frequency Range

The dimensions of the setup determine the working frequency range. The lower frequency limit depends on the microphone spacing. It was 200 Hz in these experiments.

The upper frequency limit depends on the diameter of the tube:

$$f_u < \frac{Kc}{d}, \quad (4.25)$$

where

c = speed of sound, d = diameter, m, and K = constant, 0.586.

For the 6-inch diameter tube, the theoretical upper frequency limit is 1318 Hz. However, we observed that the plane wave assumption did not appear valid for frequencies higher than 1250 Hz. So for our tests, the working frequency range was set to be from 200 Hz to 1250 Hz. For the 4-inch diameter tube, the theoretical upper frequency limit for the tube is 1978 Hz. For some thin samples, the first absorption peak occurs higher than 1250 Hz. So the smaller 4-inch tube can be used for thin samples. In this study the sound absorption of the samples measured for the same pavement type with the two different tubes was compared.

The working frequency range is,

$$f_l < f < f_u. \quad (4.26)$$

where,

f = operating frequency hertz, f_l = Lower working frequency of the tube, hertz, f_u = Upper working frequency of the tube, hertz, f_l is limited by the accuracy of the signal processing equipment, f_u is chosen to avoid the occurrence of the non – plane wave mode propagation.

4.6.2 High-Frequency Limit (f_u)

The condition for f_u

$$d < 0.58\lambda_u, \quad (4.27)$$

$$f_u d < 0.58c_0. \quad (4.28)$$

For circular tubes with the inside diameter ‘ d ’ in meters and f_u in hertz.

4.6.3 Low-Frequency Limit (f_l)

The condition for f_l

$$f_l > \frac{0.75(343)}{(l-d)}. \quad (4.29)$$

Measurements at frequencies greater than $c/4l$, where l is the tube length, will provide reliable data. According to the ISO standard 10534, the length and the cutoff frequencies should be calculated as follows (6-inch diameter tube):

$$f_l > \frac{0.75(343)}{(l-d)}, \quad (4.30)$$

$$f_l > \frac{0.75(343)}{(1.2192 - 0.1524)}, \quad (4.31)$$

$$f_l > 241.14 \text{ Hz}, \quad (4.32)$$

$$f_u < \frac{0.586(343)}{d}, \quad (4.33)$$

$$f_u < \frac{0.586(343)}{0.1524}, \quad (4.34)$$

$$f_u < 1318.88 \text{ Hz} \quad (4.35)$$

For the 6-inch dia of the tube the upper and lower cutoff frequencies are calculated as,

$$241.14 \text{ Hz} < f < 1318.88 \text{ Hz} \quad (4.36)$$

For the 4-inch dia tube the upper and lower cutoff frequencies are calculated in the same manner:

$$f_l > \frac{0.75(343)}{(l-d)}, \quad (4.37)$$

$$f_l > \frac{0.75(343)}{1.2192 - 0.1016}, \quad (4.38)$$

$$f_l > 230.18 \text{ Hz} \quad (4.39)$$

$$f_u < \frac{0.586(343)}{d}, \quad (4.40)$$

$$f_u < \frac{0.586(343)}{0.1016}, \quad (4.41)$$

$$f_u < 1978.32 \text{ Hz} \quad (4.42)$$

For the 4-inch diameter tube, the upper and lower cutoff frequencies are calculated as,

$$230.18 \text{ Hz} < f < 1978.32 \text{ Hz} \quad (4.43)$$

The spacing S in meters between the microphones is chosen so that,

$$f_u S < 0.45c_0, \quad (4.44)$$

$$S \ll \frac{c_0}{2} f_u. \quad (4.45)$$

For the 6-inch tube, $S = 4$ inch

For the 4-inch tube, $S = 2.7$ inch

4.6.4 Length of the Impedance Tube

The length of the tube was also related to the frequencies at which measurements are made. The tube must be long enough to contain that part of the standing wave pattern needed for measurement. That is, it must be long enough to contain at least one and preferably two sound pressure minima. To ensure that at least two minima can be observed in the tube, its length should be such that,

$$f > \frac{0.75c}{(l-d)}. \quad (4.46)$$

where,

l = length of tube, m.

The length of the tube in this particular case is 4 ft.

4.6.5 Sound Source

The sound source used was a loudspeaker mounted at the end of the impedance tube. According to the ISO and ASTM Standards the surface of the loudspeaker membrane must cover at least two-thirds of the cross sectional area of the impedance tube. The loudspeaker axis was made co-axial with the tube. The loudspeaker was contained in a sound-insulating box in order to avoid airborne cross talk to the microphone. Elastic vibration insulation was applied between the impedance tube and the frame of the loud speaker as well as the loudspeaker box, and also between the impedance tube and the transmission element in order to avoid structure borne sound excitation of the impedance tube.

4.6.6 Microphones

Microphones of identical type were used at each location. The diameter of the microphones was small compared to c_0/f_u .

4.6.7 Microphone Type

The microphones were pressure-type precision microphones in accordance with American National Standards Institute [18]. Free-field types are used in a plane-wave tube over a more restricted frequency range, as shown in manufacturer's catalogs. 1/4-in microphones are ideal for this application, since they can tolerate very high sound-pressure levels, and their size versus the wavelengths of sound being measured makes them easy to install without causing response problems.

4.6.8 Positions of the Microphones

Each microphone was mounted with its diaphragm flush with the interior of the tube. A small recess that is often necessary was provided. The recess is kept small and identical for both the microphone mountings. The microphone grid was sealed tightly to the microphone housing and a seal was made between the microphone and the mounting hole. O-rings of suitable diameter were used to fit the microphones tightly to the microphone holder.

4.6.9 Test Sample Holder

The sample holder constructed is an extension of the metal impedance tube and the sample was fitted snugly into the tube. O-rings were used at different positions at the end of the tube to fit the sample tightly. Metal backup plates were used for the samples, which were short in length. The backplate of the sample holder was rigid and was fixed tightly to the tube since it serves as a rigid termination in many measurements. A metal plate of thickness of about 20mm was used.

4.6.10 Signal Processing Equipment

The signal processing system used was a Brüel and Kjaer Pulse system of Type 3560. The system was used to measure the sound pressures at two-microphone locations and to calculate the transfer function H_{12} between them. A generator capable of producing the required source signal compatible with the analyzing system was also used.

4.6.11 Loudspeaker

A membrane loudspeaker of the required diameter was located at the opposite end of the tube from the test sample. The surface of the loudspeaker membrane is at least two-thirds

of the cross-sectional area of the impedance tube. The loudspeaker axis was mounted to the tube coaxially.

The loudspeaker was contained in a wooden insulating box in order to avoid airborne flanking transmission to the microphones. Elastic vibration insulation was applied between the impedance tube and the frame of the loudspeaker as well as to the loudspeaker box in order to avoid structure-borne sound excitation of the impedance tube.

4.6.12 Signal Generator

A signal generator was used to generate a stationary signal with a flat spectral density within the frequency range of interest. It was used to generate white noise as required.

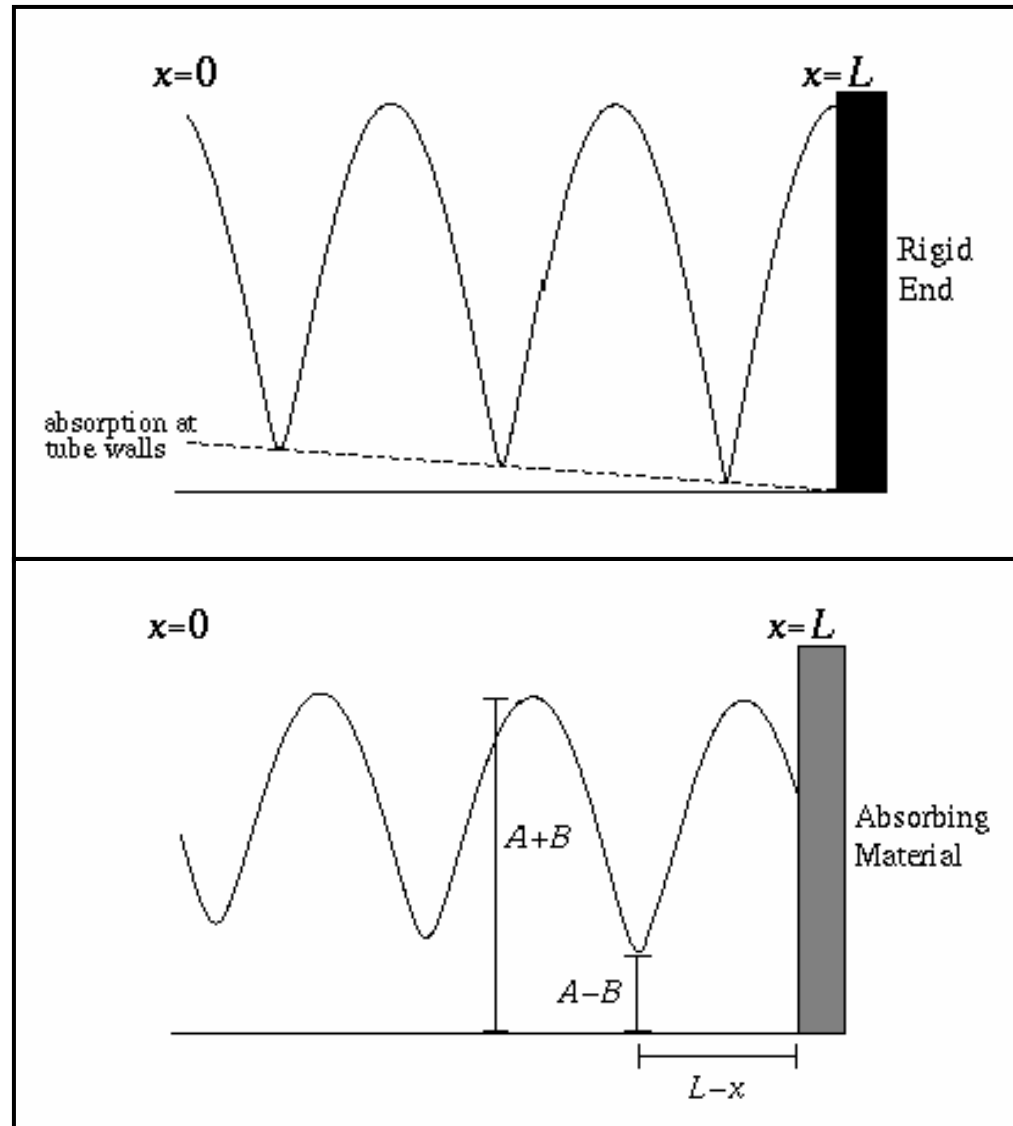


Figure 4.1 a and b Standing wave pattern in the impedance tube

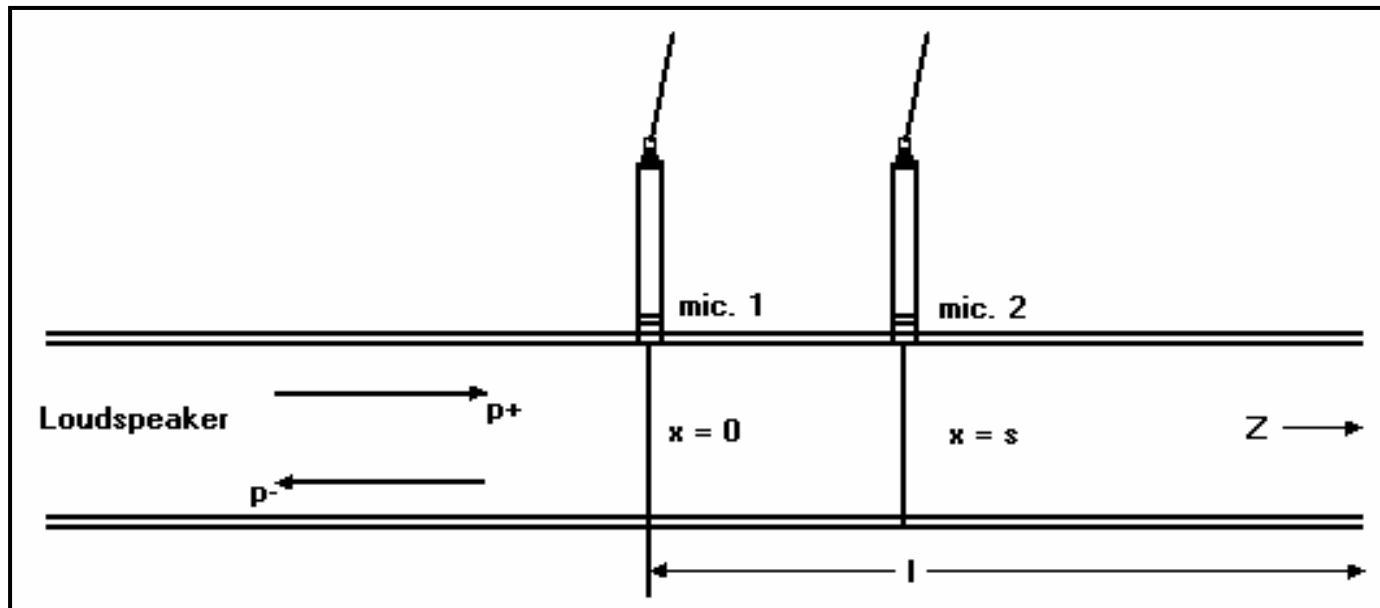


Figure 4.2 Impedance tube set up

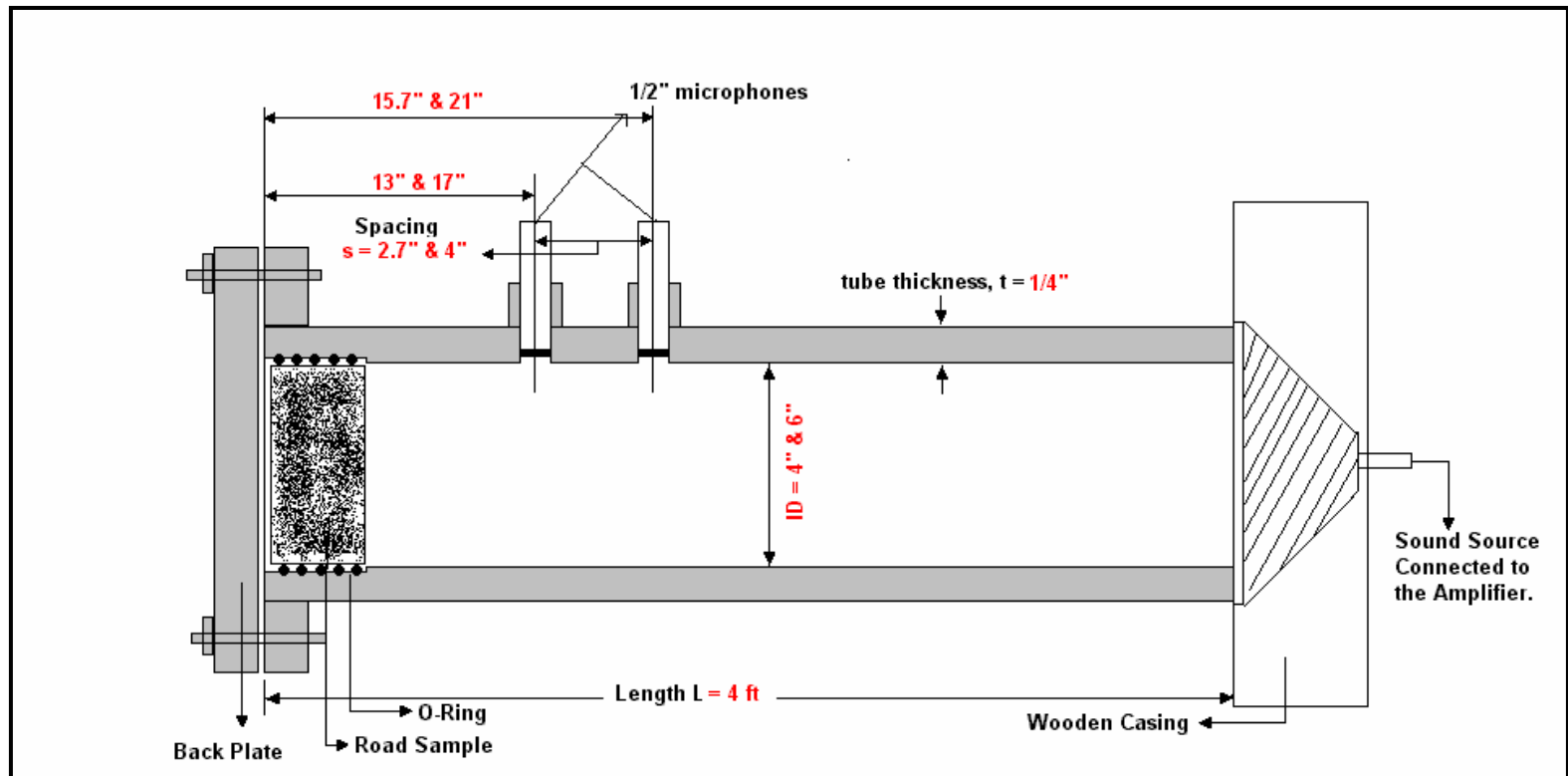


Figure 4.3 Dimensions of the two-microphone impedance tube built at Auburn University

CHAPTER 5

ALTERNATE METHODS OF MEASUREMENT

This chapter discusses different alternate methods to measure acoustical properties of road surfaces and tire/road interaction noise.

5.1 Close Proximity Method

This chapter describes the close proximity method, which is also sometimes known as the trailer method that is used to determine tire/road interaction noise. This section also includes details of the construction of the trailer at Auburn University and the measurements made using this approach.

The FHWA noise criteria state that noise abatement must be considered for residential areas when the traffic noise levels approach or exceed 67 dB (A) [3]. To reduce traffic noise to this level, many areas in the United States are building large sound barrier walls at a cost of one to five million dollars per roadway mile. Research in Europe and in the United States has indicated that it is possible to build pavement surfaces that will reduce traffic noise. In January 2002, the National Center for Asphalt Technology (NCAT) initiated a research study with the objective to develop safe, quiet and durable asphalt pavement surfaces. The first step towards accomplishing this objective was to develop a fast and scientifically reliable method for measuring the acoustical characteristics of pavement surfaces.

This chapter describes a method of evaluating different road surfaces with respect to their influence on traffic noise, under conditions when tire/road noise dominates. The interpretation of the results applies to free-flowing traffic traveling on essentially level roads at constant speeds of 50 km/h and upwards. In such cases tire/road noise is assumed to dominate (although in some countries tire/road noise may not dominate at 50 km/h when the percentage of heavy vehicles is high). For other driving conditions where traffic is not freely flowing, such as junctions and/or under high acceleration, and where the traffic is congested, the influence of the road surface on noise emission is more complex. The noise situation is also complicated in 1) the case for roads with high longitudinal gradients and 2) a high proportion of heavy vehicles.

The emission and propagation of road traffic noise generally depends on road surface characteristics, notably on texture and porosity. Both these characteristics influence the generation of tire/road noise and, in addition, the sound absorption properties of the road surface can influence the propagation of sound, particularly when the propagation takes place close to the surface. Power unit noise, which is usually generated at a greater height above the road surface than tire/road noise, may also be affected during propagation by the sound absorption characteristics of the road surface. These effects lead to differences in sound levels, associated with a given traffic flow and comparison, from different road surfaces of up to 15 dB which can have a substantial impact on the environment alongside a road.

5.1.1 Measurement Principle

In the “Close-Proximity (CPX) method”, the average A-weighted sound pressure levels emitted by two of the four specified reference tires are measured over arbitrary or a

specified road distance, together with the vehicle testing speed, by at least two microphones, located close to the tires. For this purpose, a special test vehicle, which is either self-powered or towed behind another vehicle, is used. In the latter case the test vehicle is a trailer. Reference tires are mounted on the test vehicle, either one by one, or a few at a time. According to the ISO standard [21], four uniquely different reference tires have to be selected in order to represent the tire/road characteristics, which are to be studied.

For the sake of economical and practical reasons, this method is not used with tires designed for heavy vehicles. It is known that road surface sound emission characteristics depend on the tire used, including knowledge of whether the tire is intended for light or heavy vehicles. The results obtained with this method, therefore, best describe conditions when sound from light vehicles constitutes the major part of traffic noise. This often occurs when the heavy vehicle proportion is less than 10%. However, by the selection of one of the reference tires, having properties sensitive to road surface noise characteristics considered to be similar to those of heavy vehicle tires, the effect of the latter on road surface ranking can also be considered.

Since the source of tire/road noise is close to the tire/road interface, a substantial part of the propagation effect due to acoustically absorptive surfaces is included in the microphone signal. This conclusion is supported by model calculations and the results of the CPX validation experiment.

The tests are performed with the intention of determining the “tire/road sound level” L_{tr} , at one or more of the reference speeds (50, 80 and 110 km/h). This can be met by testing

at, or close to one of the reference speeds, or by testing over a wider speed range and using an appropriate method for normalizing for speed deviations.

CPX method consists of placing microphones near the tire/pavement interface to directly measure the tire/pavement noise levels. Different approaches with the close-proximity method were developed at General Motors in the USA and in Europe. ISO Standard 11819 -2 defines the close proximity approach, which is in very close agreement with the method used in Europe. In this method the sound pressure level is measured. Engineers at General Motors have developed a technique that uses sound intensity to evaluate noise radiated at the tire/pavement interface. In this method, the sound intensity level generated by the tire is measured. This approach, while more complicated, eliminates some of the difficulties inherent in making near field measurements of noise near a complicated source such as a tire.

In the close-proximity method the microphones are mounted as shown in Fig 5.1.1. They are mounted inside an acoustical chamber (each side of the chamber is covered with acoustical sound absorbing material). The purpose of this is to eliminate the noise from traffic during testing.

There has been a concern about whether traffic noise can be predicted based on noise measurements made at the tire/pavement interface. Both the power train and tire/pavement noise are strongly related to vehicle speed. At low speeds power train noise dominates while at high speeds tire/pavement noise dominates for most of the automobiles.

In CPX method this method for each reference tire and each individual test run with that tire, the average sound pressure levels over short road pavement measurement

segments each of 20 m, together with the corresponding vehicle speeds are recorded. The sound pressure level of each segment is normalized by the reference speed using a simple correction procedure. Averaging is then carried out according to the purpose of the measurement (measuring a particular segment or a number of consecutive segments – a section). The resulting average sound level for the two mandatory microphones at that reference speed is called the “tire/road sound pressure level”, L_{tr} . There will be one L_{tr} for each reference tire and each reference speed.

The CPX method may be used in two variants, depending on the number of reference tires used, and depending on the purpose of the measurement. The “investigatory method” is the main method and relies on using all four-reference tires. The other method is the “Survey method” which relies on using only two of the reference tires. The “investigatory method” has the best measuring precision but takes more time to conduct than the “Survey method”. The latter method may be better suited to survey long distances of roads.

For the purpose of reporting the acoustical characteristics of road surfaces, the tire/road levels for the selected reference tires may be averaged to give a single “index” which constitutes the final result. This index is called the “Close-Proximity Sound Index (CPXI)” and can be used for comparison of road surfaces.

The CPX method consists of placing microphones near the tire/pavement interface to measure directly the tire/pavement noise levels. In the CPX method the sound pressure level is measured using microphones mounted inside an acoustical chamber (each side of the chamber is covered with acoustical sound absorbing material)

as shown in Fig 5.11. The purpose of the acoustical chamber is to eliminate the noise from other sources of sound while the tests are being conducted.

Auburn University in association with the National Center for Asphalt Technology (NCAT) has designed and built two CPX noise trailers. The first was built for the Arizona Department of Transportation (ADOT) and was delivered in late January 2002. This trailer is now being used by ADOT to evaluate a number of pavement surfaces in Arizona. In September 2002, the second trailer was delivered to NCAT. Figure 5.1.2 presents a picture of the trailer.

During October 2002, NCAT used the NCAT CPX trailer to test nine pavement surfaces for the Michigan DOT. At each site, noise measurements were made at three different speeds: 45, 60 and 70 mph. At each site, measurements were made with two different tires. Figs 3 and 4 present photographs of the tread pattern for the two tires: a MasterCraft tire and a UniRoyal tire. They were chosen to provide a range of tread patterns. As can be seen from these figures the MasterCraft tire has the denser tire tread pattern.

5.1.2 Test Results

Table 5.1 presents the results of the measurements. The comparison of the different sections is based on the noise measurements made at 60 mph. 60 mph data are available for all of the test sections.

Table 5.1 - Noise Data

	City	Route	Surface Type	Noise Levels (dB (A))			
				Tire	45 mph	60 mph	70 mph
1	Lansing	I-96 E	Concrete	MasterCraft	97.0	100.8	102.3
				UniRoyal	95.2	98.8	100.8
				UniRoyal	96.0	99.1	100.5
2	Coldwater	I-69 S	SMA	MasterCraft	95.1	98.2	100.2
				UniRoyal	94.0	97.8	98.7
3	Coldwater	I-69 S	Longitudinal	MasterCraft	97.0	100.5	102.7

			Tined Concrete	UniRoyal	95.8	99.9	101.7
4	Coldwater	I-69 S	Transverse Tined Concrete	MasterCraft	97.5	100.6	102.8
				UniRoyal	96.8	100.6	102.2
5	Detroit	I-96 E	Concrete	MasterCraft	95.1	99.3	101.06
				UniRoyal	93.8	97.2	99.3
6	Detroit	I-96 E	SMA	MasterCraft	94.4	98.4	100.3
				UniRoyal	93.8	96.7	98.5
7	Detroit	I-96 E	Dense Graded Asphalt	MasterCraft	94.8	98.8	100.6
				UniRoyal	94.1	97.2	99.2
8	Detroit	I-275 N	Superpave	MasterCraft	96.1	99.9	101.1
				UniRoyal	95.1	98.7	100.7
9	Detroit	I-275 N	Concrete	MasterCraft	94.6	98.9	100.4
				UniRoyal	93.6	96.6	98.7

5.1.3 Comparison of Surfaces

Figure 5.1.5 shows a graphical result of the noise levels measured for all of the sections. It ranks the pavements from the quietest to the noisiest. The quietest pavement was the mix in Detroit and the noisiest surface was the transverse tined concrete surface at Coldwater. Three types of pavements were tested: dense-graded asphalt, SMA, and Portland cement concrete. For each pavement section the noise level used for comparison purposes was an average noise level for the two tires. The average noise values for the three surfaces at 60 mph was:

- Stone Matrix Asphalt (SMA) – 97.6 dB (A)
- Dense Graded Asphalt – 98.6 dB (A)
- Portland Cement Concrete – 99.4 dB (A)

For the Portland Cement Concrete surface, the noisiest surface was the transverse tined surface (100.6 dB (A)) and the quietest section was the diamond ground surface (97.7 dB (A)). The diamond grinding of the surface brought the noise level for the concrete pavement down to the average level of a dense graded asphalt pavement [22].

5.1.4 Comparison of Tires

The average noise level for all the pavements at 60 mph was 99.0 dB (A). The average noise level for the MasterCraft tire was 99.4 dB (A) and for the UniRoyal tire was 97.9 dB (A). This is expected since the MasterCraft tire has the most dense tire pattern. Figure 5.1.6 shows the noise levels measured for each of the sections and for each tire. The chart presents the noise levels for each of the sections by tire type. Note that the two tires result in a different ranking of the tire/road surface noise. It is felt that the cause of this is the interaction of the different pavement textures and the different tire tread patterns. Work should be done using the NCAT test track surfaces and additional tires to evaluate this concept.

5.1.5 Effect of Speed on Noise

The measurements on all but three sections were made at three speeds – 45 mph, 60 mph and 70 mph. Three sections were not tested at either the high or low speed due to safety concerns. All of the sections were tested at 60 mph. Figure 7 presents the results of the speed versus noise for three pavement types. There were insufficient data to show results for the Nova Chip sections. The speed versus noise relationship for the PCC had a slightly steeper slope than the two HMA surfaces (0.22 vs. 0.20). Note also that for both the SMA and the DGA the slope for speed versus noise was about the same.

Based on the testing conducted by the Department of Transportation in Michigan [22], it was concluded that the pavement types can be rated as follows with regard to noise levels. This ranking is based on using an average of the results from the two tires. The ranking is different for the two tires. It is thought that the reason for this is the interaction between the texture of the tire and the texture of the pavement surface.

1. SMA
2. Dense Graded Asphalt
3. PCC

5.2 In Situ Method

In this section an alternative method is described for the measurement of sound absorption properties of road surfaces in situ. The discussion includes a review of ISO Standard 13472 [23], which describes a test method for measuring, in situ, of the sound absorption coefficient of road surfaces as a function of frequency under normal incidence sound. The in situ method provides a means of evaluating the sound absorption characteristics of a road surface without damaging the surface. It is intended to be used during road construction, road maintenance and other traffic noise studies.

The method is based on free-field propagation of the test signal from a source to the road surface and back to a receiver, and uses a road surface of approximately 3 m² and a frequency range, in one-third-octave bands, from 250 Hz to 4 kHz. The measurement results of the in situ method are comparable with the results of impedance tube methods, performed on bore cores taken from the surface. The measurement results of the in situ method are in general not comparable with the results of the reverberation room method (ISO 354), because the method described in this part of ISO 13472 uses a directional sound field, while the reverberation room method assumes a diffuse sound field.

5.2.1 Scope

The in situ method is intended for the following applications:

- Determination of the sound absorption properties of test tracks laid out according to ISO Standard 10844, with limitations, and other standards.
- Determination of the sound absorption properties of road surfaces in actual use.
- Comparison of sound absorption design specifications of road surfaces with actual performance data of the surface after the construction work.

The complex reflection factor can also be determined by this method.

5.2.2 General Principal

In this method a sound source, driven by a signal generator, is placed above the surface under test, and a microphone is positioned between the source and the test surface. The method is based on the assessment of the transfer function between the output of the signal generator and the output of the microphone. This transfer function is composed of two parts, one resulting from the direct sound path (from the signal generator through the amplifier and loudspeaker to the microphone) and a second part resulting from the reflected sound path (from the signal generator through the amplifier, loudspeaker and surface under test to the microphone).

The overall impulse response containing the direct and reflected sound is measured in the time domain. This overall impulse response consists of the impulse response of the direct sound path and, after some delay due to the greater distance of travel, the impulse response of the reflected sound path as shown in the Fig 5.2.2.

With suitable time domain processing, these responses can be separated. Using Fourier transforms, the transfer functions of both the direct and reflected paths are obtained ($H_i(f)$ and $H_r(f)$). The ratio of the squared modulus of these functions gives the

sound power reflection factor $Q_W(f)$ from which the sound absorption coefficient can be calculated as discussed below, apart from a factor K_r due to geometrical spreading.

The key components of the test set up shown in Fig 5.1.1 are given below

1. Sound source
2. Microphone
3. Microphone amplifier
4. Surface under test
5. Loudspeaker amplifier
6. Impulse response time windows and Fourier transform
7. Signal generation
8. Analyzer or computer

5.2.3 Signal Separation Techniques

In the following, a test procedure is described to explain how the sound source and the microphone should be positioned above the surface, which is under test, and how the overall impulse response is measured.

The impulse response consists of a direct sound path component, a reflected path component resulting from the surface under test and other parasitic components. The separation of those different components can be achieved in two different ways.

1) Temporal separation: If the geometry is arranged so that a sufficient time delay exists between the arrival of the direct and reflected signals, the relevant components can be extracted from the overall impulse response by application of time windows. Figure 5.2.2 shows a simple separation technique in which the geometry is arranged so that the reflected sound component occurs after the direct sound has decayed to zero.

2) Signal subtraction technique: The impulse response of the direct sound path is not extracted from the overall impulse response; instead, it is removed from the overall impulse response by subtraction of an identical signal.

The distance d_m between the microphone and the surface of the test sample can be made relatively small. For source and microphone distances from the surface of reference of the test sample, this part of the standard requires the following values: $d_s = 1.25\text{m}$ and $d_m = 0.25\text{m}$. These values are kept constant during the averaging process (within $\pm 0.005\text{m}$). The direct impulse response has to be exactly known in shape, amplitude and time delay. In principle, this can be obtained by performing a free-field measurement using the same geometrical configuration of the loudspeaker and microphone. In particular, the distance between them is kept constant. Using a stable mechanical connection between the sound source and the measuring microphone can fulfill this requirement. In order to avoid temperature differences during the measurement process, the measurements are performed within a short time (less than 10 min).

5.2.4 Measurement Procedure

The measurement is taken in an essentially free field, i.e. a field that is free from all reflections other than that caused by the test surface. However, a time window can be used to cancel out reflections which arrive after a certain period of time, and which thus originate from locations further away than a certain set distance. The road surface and meteorological conditions are checked to ensure compliance with the specifications. The equipment is then positioned on the site as specified in the ISO standard [23]. The radius of the maximum sampled area is specified as discussed below. It is then necessary to check that no reflecting objects exist inside the maximum area sampled. The test signal is

then generated from the selected sound source. A sample is obtained of the total signal as received by the microphone with a sampling frequency. The microphone response data are repeatedly averaged until a stable impulse response function is obtained (at least 50 averages). The free-field impulse response is recorded with the measurement set-up removed from any reflecting surface, which could influence the measurement and keeping the same geometrical configuration.

The impulse response of the reflected path is then isolated using the signal subtraction method. A suitable temporal window cancels parasitic reflections. The power spectra of the two signals extracted using time windows are then computed using Fourier transforms. The sound power reflection factor is then calculated taking into account the correction for the geometrical spreading factor. The road surface sound absorption coefficient is then computed by linear averaging narrow band absorption measurements in one-third-octave bands. Measurements are obtained at different points on the road surface.

5.2.5 Radius of the Maximum Sampled Area

The surface area, contained within the plane of reflection that must remain free of reflecting objects, which could cause parasitic reflections, is called the maximum sampled area. For normal incidence, a circle bounds the maximum sampled area with its centre at the point of incidence and radius r , in metres, given by the relationship:

$$r = \frac{1}{d_s + d_m + cT_w} \sqrt{\left(d_s + d_m + \frac{cT_w}{2}\right) \left(d_s + \frac{cT_w}{2}\right) (2d_m + cT_w) cT_w}, \quad (5.1)$$

where

d_s = Distance from the sound source to the reflecting plane (m),

d_m = Distance from the microphone to the reflecting plane (m),

c = Speed of sound in air, (m/s),

T_w = Width of the temporal window used to isolate the sound pressure wave reflected by the surface under test (s).

5.2.6 Principle of the Measurement:

The source emits a sound wave that travels past the microphone position to the surface under test where it is reflected. The microphone, placed between the sound source and the test surface, detects the direct sound pressure wave traveling from the sound source to the surface under test, followed by the sound pressure wave reflected by the surface under test. The overall microphone response, $h_m(t)$ is described by:

$$h_m(t) = h_i(t) + K_r h_i(t) * r_p(t - \tau) + \sum_j K_{r,j} h_i(t) * r_{p,j}(t - \tau_j) + h_n(t), \quad (5.2)$$

where

$h_i(t)$ = Impulse response of the direct path,

$r_p(t)$ = Reflection factor of the surface under test,

$h_n(t)$ = Background noise response,

* = Convolution sign,

j = Parasitic reflections,

K_r = Geometrical spreading factor accounting for the path length difference between the direct and reflected paths ,

$$K_r = \frac{d_s - d_m}{d_s + d_m}, \quad (5.3)$$

where

d_s = Distance between the sound source and the reflecting plane,

d_m = Distance between the microphone and the reflecting plane,

$\Delta\tau$ = Delay time, resulting from the path length difference between the direct and reflected paths, as detected by the microphone;

$$\Delta\tau = \frac{2d_m}{c}, \quad (5.4)$$

where

c = speed of sound in air.

The overall microphone response $h_m(t)$ contains the impulse response of the sound reflected by the surface under test:

$$h_r(t) = K_r H_i(t) * r_p(t - \Delta\tau). \quad (5.5)$$

The impulse response of the direct system $h_r(t)$ and impulse response of the sound reflected from the surface under test $h_i(t)$ can be extracted from the overall microphone response in the time domain by using a suitable windowing function, provided that the amplitude of $h_i(t)$ decays to an insignificant value with respect to $h_r(t)$ within the delay time $\Delta\tau$.

Alternatively, the impulse response of the direct system can be measured in a free field, keeping the distance of the microphone from the sound source strictly constant, then the road surface response can be measured using the subtraction technique as described previously. Fourier transformation of the preceding expression for $h_r(t)$ yields the sound power reflection factor in the frequency domain:

$$|Q_p(f)|^2 = \frac{1}{K_r^2} \left| \frac{H_r(f)}{H_i(f)} \right|^2, \quad (5.6)$$

where

$H_r(f)$ = Transfer function of the reflected path (from the signal generator through the amplifier, loudspeaker and reflection of the surface under test to the microphone), and

$H_i(f)$ = Transfer function of the direct path (from the signal generator through the amplifier and loudspeaker to the microphone).

From here, the sound absorption coefficient can be computed:

$$\alpha(f) = 1 - |Q_p(f)|^2 = 1 - \frac{1}{K_r^2} \left| \frac{H_r(f)}{H_i(f)} \right|^2. \quad (5.7)$$

This method provides a means of evaluating the sound absorption coefficient of a road surface without damaging the surface. It is intended to be used during road construction, road maintenance and other traffic noise studies.

5.3 Statistical Pass by Method

This section describes a method of comparing traffic noise on different road surfaces for various compositions of road traffic for the purpose of evaluating the acoustical properties of different road surfaces. This section discusses an ISO standard 11819-1 Part –1, a standard method for comparing noise characteristics of road surfaces, that gives road and environment authorities a tool for establishing common practices or limits on the use of surfacing needed to meet certain noise criteria. The statistical pass by method (SPB) as per the ISO standard 11819 part-1 involves the simultaneous measurement of the noise and the speed of individual vehicles in a traffic stream as they

pass by a selected location. Microphones are mounted by the roadside usually 7.5 m, but not more than 15 m, from the centre of the road lane as shown in the Fig 5.2.1. The purpose has been to develop methods that are simple to use, easy to understand, and have moderate requirements with regard to the availability of instrumentation. Sound pressure levels representing either light or heavy vehicles at selected speeds are assigned to a certain road surface. The method is applicable to traffic traveling at constant speed, i.e. free flowing conditions at posted speeds of 50km/h and upwards. For other driving conditions, where traffic is not free flowing, such as at junctions and where the traffic is congested, the road surface is of less importance.

The statistical pass-by (SPB) method is intended to be used for two main purposes. First it may be used to classify surfaces in typical and good condition as a type according to their influence on traffic noise (surface classification) and secondly, it may be used to evaluate the influence on traffic noise of different surfaces at particular sites irrespective of condition and age. This later type of application may be useful for example where a road is to be resurfaced and “before” and “after” measurements are required in order to assess the differences in traffic noise following resurfacing. However, due to severe requirements on the acoustical environment at the site, the method cannot generally be used at any given site.

The emission and propagation of road traffic noise depends greatly on the road surface characteristics, notably on texture and porosity. Both these characteristics influence the generation of tire/road noise and in addition, the porosity can influence the propagation of sound, particularly when the propagation takes place close to the surface. Power unit noise, which is usually generated at a greater height above the road surface

than the tire/road noise, may also be affected during propagation by the porosity characteristics of the road surface. These effects lead to differences in sound levels, associated with a given traffic flow and composition, from different road surfaces of up to 15 dB, which can have a substantial impact on the environment quality alongside a road. It is therefore important to be able to measure this influence by a standardized method and to arrive at a quantitative ranking of road surfaces with respect to traffic noise. For the purpose of the ISO standard 11819 discussed in this chapter the following definitions apply;

5.3.1 Traffic Noise

Overall noise emitted by the traffic running on the road under study.

5.3.2 Vehicle Noise

Total noise from an individual vehicle that consists of two major components, power unit noise and tire/road noise.

5.3.3 Tire/road Noise

Noise generated by the tire/road interaction.

5.3.4 Power Unit Noise

Noise generated by the vehicle engine, exhaust system, air intake, fans, transmission, etc.

5.3.5 Road Speed Categories

Three categories of roads are defined with respect to the range of speeds at which the traffic flows and these are usually associated with certain areas (urban, suburban, rural, etc.)

“Low” road speed category:

Conditions, which relate to traffic operating at an average speed of 45 km/h to 64 km/h.
These conditions are usually associated with urban traffic.

“Medium” road speed category:

Conditions, which relate to traffic operating at an average speed of 65 km/h to 99 km/h.
These conditions are mostly found in suburban areas or on rural highways.

“High” road speed category

Conditions that relate to cars operating at an average speed of 100 km/h or more, heavy vehicles may operate at lower average speed due to speed restrictions. These conditions are usually associated with motorway traffic in rural or suburban areas.

5.3.6 Vehicle Categories

A vehicle category consists of vehicles that have certain common features easy to identify in the traffic stream, such as the number of axels and the size. The common features are assumed to correspond to similarities in their sound emission when driven under the same operating conditions. The following vehicle categories are considered to be sufficient for the description of the noise characteristics of road surfaces and are used in Part 1 of ISO 11819.

Category No. 1 – cars

Passenger cars excluding other light vehicles.

Category No. 2 – heavy vehicles

All trucks, buses and coaches with at least two axels and more than four wheels. This category consists of categories 2a and 2b together.

Category No. 2a – dual-axle heavy vehicles

Trucks, buses and coaches with two axels and more than four wheels

Category No. 2b – multi-axle heavy vehicles

Trucks, buses and coaches with more than two axels

5.3.7 Vehicle Sound Level, L_{veh}

Maximum A-weighted sound pressure level determined at a reference speed from a regression line of the maximum A-weighted sound pressure level versus the logarithm speed, calculated for each vehicle category.

5.3.8 Statistical Pass-By Index (SPBI)

Noise index for comparison of road surfaces, that is based on the vehicle sound levels and takes into account the mix and speeds of vehicles.

5.3.9 Measuring Procedure

The following measurement procedures are also followed during the pass by method that is discussed in the ISO standard.

5.3.9.1 Microphone position

The horizontal distance from the microphone position to the centre of the lane in which the vehicles to be measured travel shall be $7.5 \text{ m} \pm 0.1 \text{ m}$ in accordance with the ISO standard.

5.3.10 Measuring principle

The measuring principle from ISO Standard 11819 for determining the statistical pass by index for different category vehicles is discussed in the following section. The statistical pass-by method consists of placing microphones at a defined distance from the vehicle path at the side of the roadway. The statistical pass by (SBP) is governed in the United States by procedures developed by the John A. Volpe National Transportation Systems Center. It calls for placing microphones 50 feet from the center of the vehicle lane and at

a height of 5 feet above the pavement and requires that the noise characteristics and speed of a prescribed number of vehicles be evaluated. The statistical pass-by procedure is time consuming to conduct, the results can vary based on the traffic mix (even if the vehicle types are the same, the differences in tires can cause problems), and very specific acoustical conditions must be met to conduct these measurements. The roadway must be essentially straight and level, there is a limit on the background noise, no acoustical reflective surfaces are allowed within 30 feet of the microphone position, and a relatively uniform traffic speed is required. The result of these restrictions is that a limited number of pavement surfaces can be tested economically.

In accordance with the ISO standard 11819, in the statistical pass by (SPB) method, the maximum A-weighted sound pressure levels of a statistically significant number of individual vehicle pass-bys are to be measured at a specified roadside location together with the vehicle speeds. Each measured vehicle is classified into one of three vehicle categories, 1) “cars”, 2) “dual –axle heavy vehicles” and 3) “multi-axle heavy vehicles”. Other vehicle categories are not used for this evaluation, since they do not provide any additional information regarding the influence of the road surface on the tire/road noise generation.

For each of three speed ranges that is, 1) “low” road speed category, 2) “medium road speed category” and 3) “high road speed category”, as well as for each of the three vehicle categories, a nominated reference speed is given. Each individual pass-by level together with its vehicle speed is recorded, and a regression line of the maximum A-weighted sound pressure level versus the logarithm of speed is calculated for each vehicle category. From this the average maximum A-weighted sound pressure level is determined

at the reference speed. This level is called the vehicle sound level, L_{veh} . For the purpose of reporting the acoustical performance of road surfaces, the vehicle sound levels for cars, dual-axle heavy vehicles and multi-axle heavy vehicles are added on a sound power, assuming certain proportions of these vehicle categories, to give a single “index” which constitutes the final result. This index is called the statistical pass-by index (SBPI) and can be used for the comparison of road surfaces so that their influence on the sound pressure level of mixed traffic flow can be determined. It is not suitable for determining actual traffic noise levels.

Determination of statistical pass-by index (SBPI) according to ISO standard 11819:

In order to obtain an aggregate (overall) level of road surface influence on traffic noise for a mix of vehicles, a statistical pass-by index shall be calculated as follows:

$$SPBI = 10 \log \left[W_1 10^{\frac{L_1}{10}} + W_{2a} \left(\frac{v_1}{v_{2a}} \right) 10^{\frac{L_{2a}}{10}} + W_{2b} \left(\frac{v_1}{v_{2b}} \right) 10^{\frac{L_{2b}}{10}} \right], \text{ dB} \quad (5.8)$$

where,

SBPI = Statistical pass-by index, for a standard mix of light and heavy vehicles.

L_1 , L_{2a} and L_{2b} are the vehicle sound levels for vehicle categories as discussed above. W_1 , W_{2a} and W_{2b} are the weighting factors, which are equivalent to the assumed proportions of vehicle categories in the traffic, and V_1 , V_{2a} and V_{2b} are the reference speeds of individual vehicle categories.

The measurement of the tire/pavement noise at the interface using the CPX method is faster, more practical and more economical than the SPB method [24], but it is limited in that it is relevant only in cases where tire/road noise dominates and the power unit noise can be neglected. The reference speeds for the vehicle categories in the road

speed categories are specified in the Table 5.3.1. Note that the reference speeds are the same for the two heavy vehicle groups.

The ordinate sound level of the regression line for each category of vehicle at the corresponding reference speed is taken to be the vehicle sound level, L_{veh} . In this way, for a certain road site, three L_{veh} values are obtained: for 1) cars, 2) dual-axle heavy vehicles and 3) multi-axle heavy vehicles.

The values for weighting factors vary depending on the road surface type. They also vary depending on the country and with time of day and night. The values shown in Table 5.3.1 above represent most cases, which allow simple comparisons of road surfaces. SPBI is not an equivalent level (L_{eq}) of traffic noise, but can be used to describe the relative influence of the road surface on such levels [38]. The SPBI is an index obtained by adding “energetically” adding the L_{veh} values together, with each L_{veh} weighted in accordance with the expected typical proportion of the vehicle category in question. The index will have a numerical value close to the main L_{veh} levels [39]. It is valid for cases where speeds of cars and heavy vehicles are as given in Table 5.3.1. The index cannot be used for estimation of effects of speed.

Table 5.3.1

Reference speeds and weighting factors in the different road speed categories

Vehicle Category		Road Speed Category					
		Low		Medium		High	
Name	No.	Ref speed (km/h)	W_X	Ref speed (km/h)	W_X	Ref speed (km/h)	W_X
Cars	1	50	0.900	80	0.800	110	0.700

Dual-axle heavy vehicles	2a	50	0.075	70	0.100	85	0.075
Multi-axle heavy vehicles	2b	50	0.025	70	0.100	85	0.225

5.3.11 Conclusion

The statistical pass-by method can be used to classify surfaces in typical and good condition according to their influence on traffic noise. An advantage of this method is that it includes all of the noise generated including engine and exhaust noise. But, due to severe requirements on the acoustical environment on the measurement site, it cannot be used for new or rebuilt surfaces at any arbitrary location or in most urban areas where noise is a significant problem.

Advantages of method

- Eliminate the variability of noise emissions from different vehicles of each type.
- Noise measurements near the receptors along the roadway can be made and it is more representative of actual traffic conditions.

Disadvantages to method

- Test section requirements are: flat, straight section of a road at an open site with no large reflecting objects in the immediate vicinity.
- Measurements are taken at a specific location; the results can be only related to short test sections of road surface. Inhomogeneous road surface cannot be evaluated.

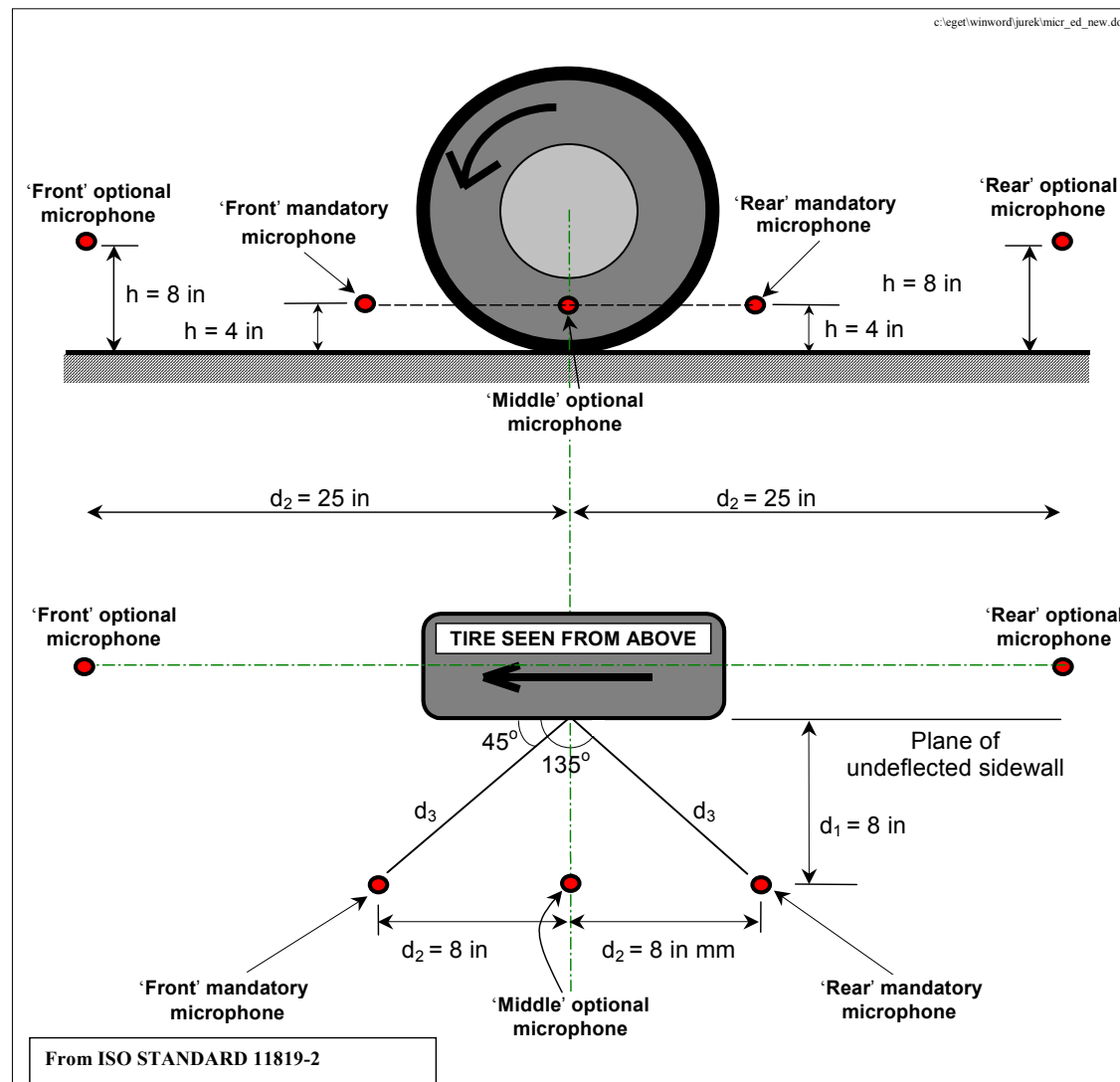


Figure 5.1.1. Microphone layout for close-proximity method (trailer method)



Figure 5.1.2 – NCAT CPX trailer



Figure 5.1.3 – UniRoyal tire



Figure 5.1.4- MasterCraft tire

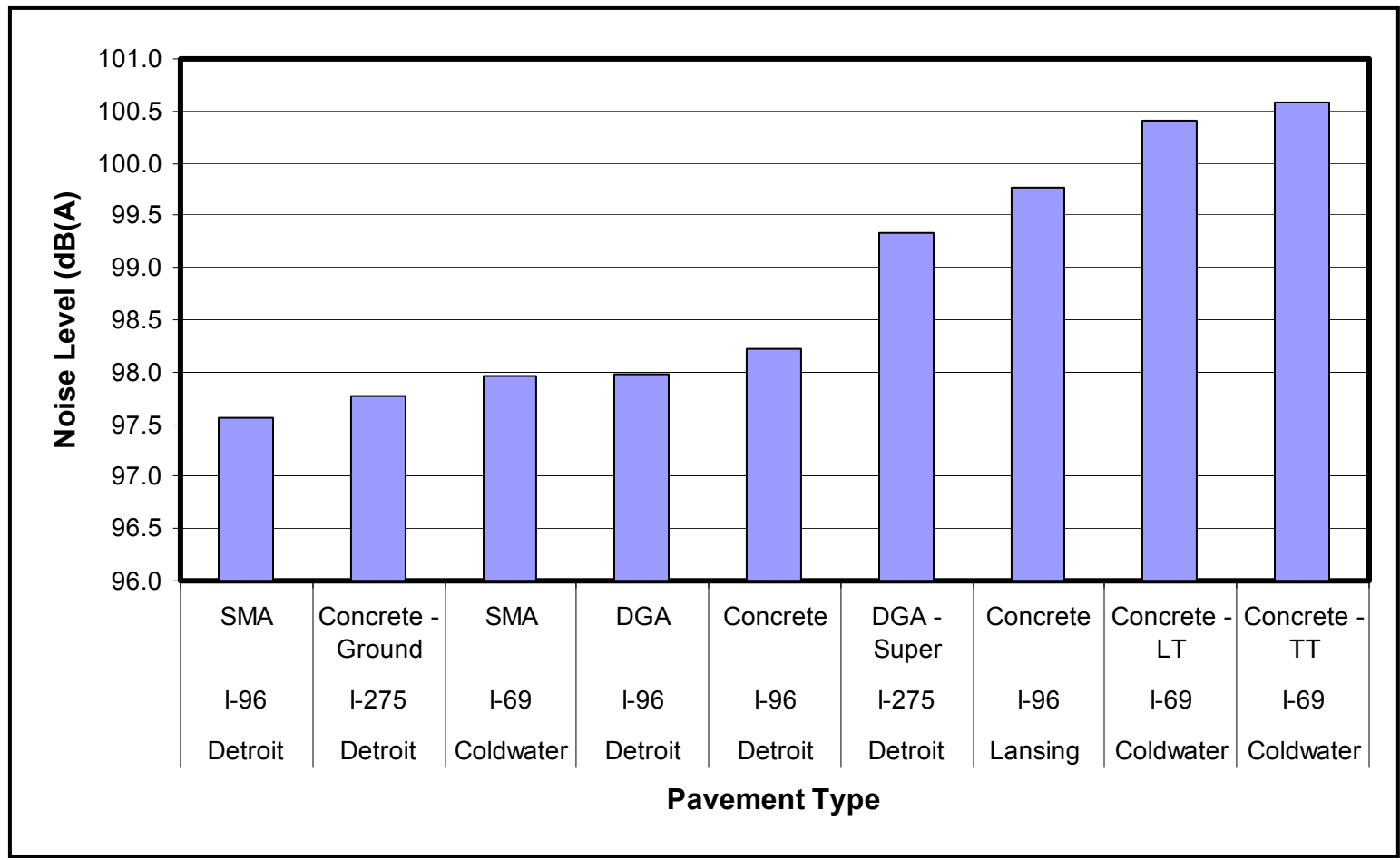


Figure 5.1.5 – Comparison of noise levels for different surfaces

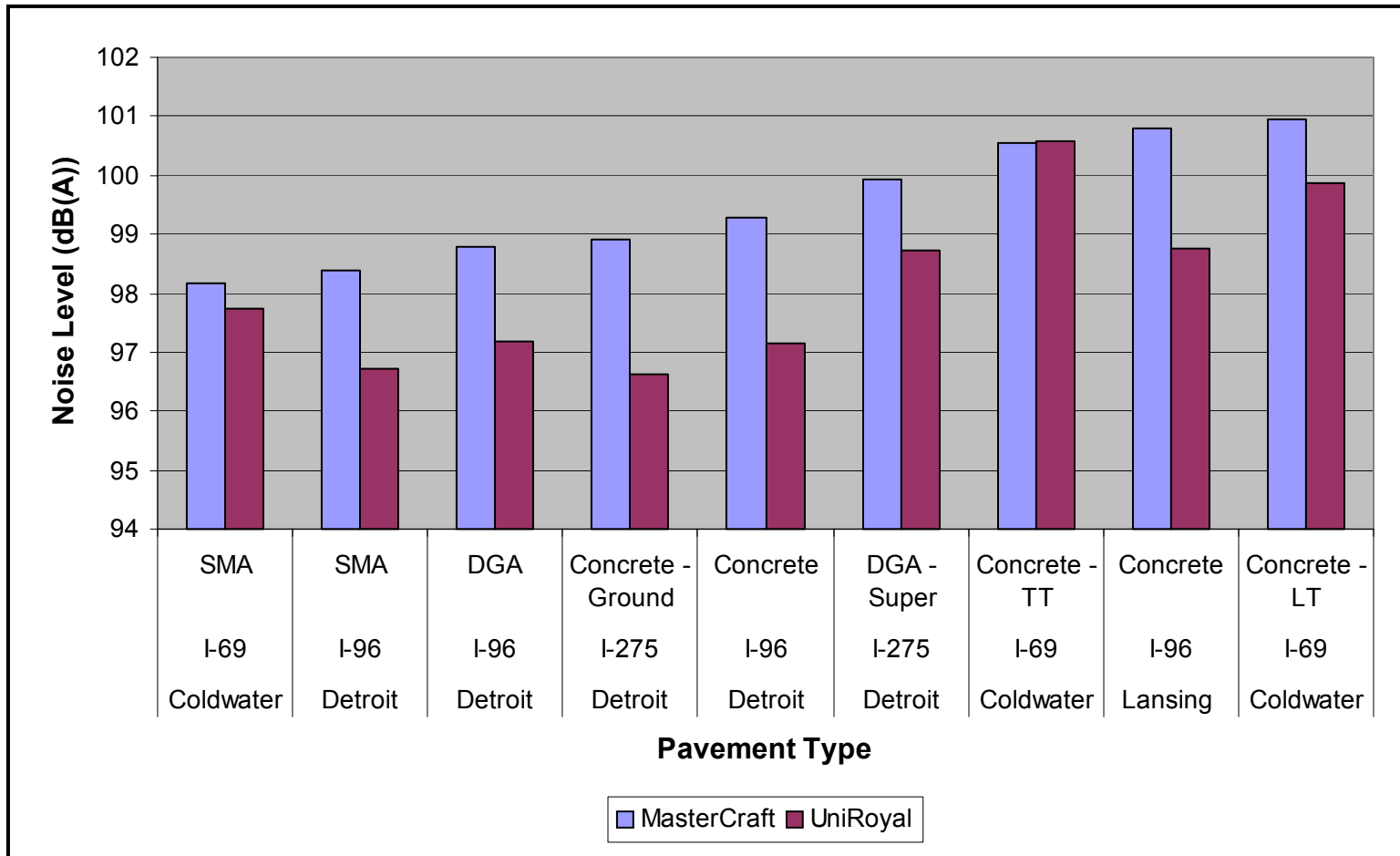


Figure 5.1.6 – Comparison of noise levels for each of the tires

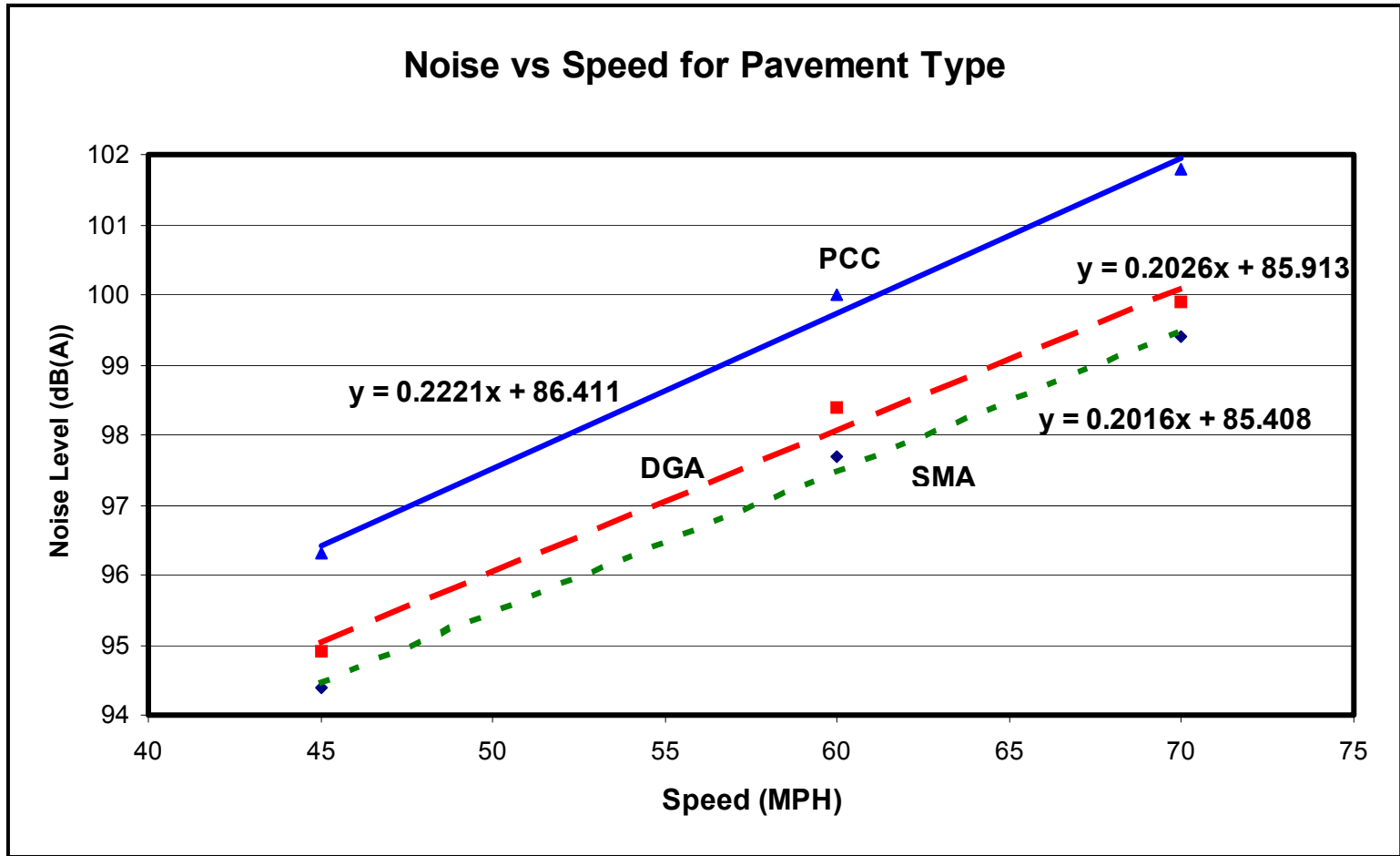


Figure 5.1.7 – Noise versus speed

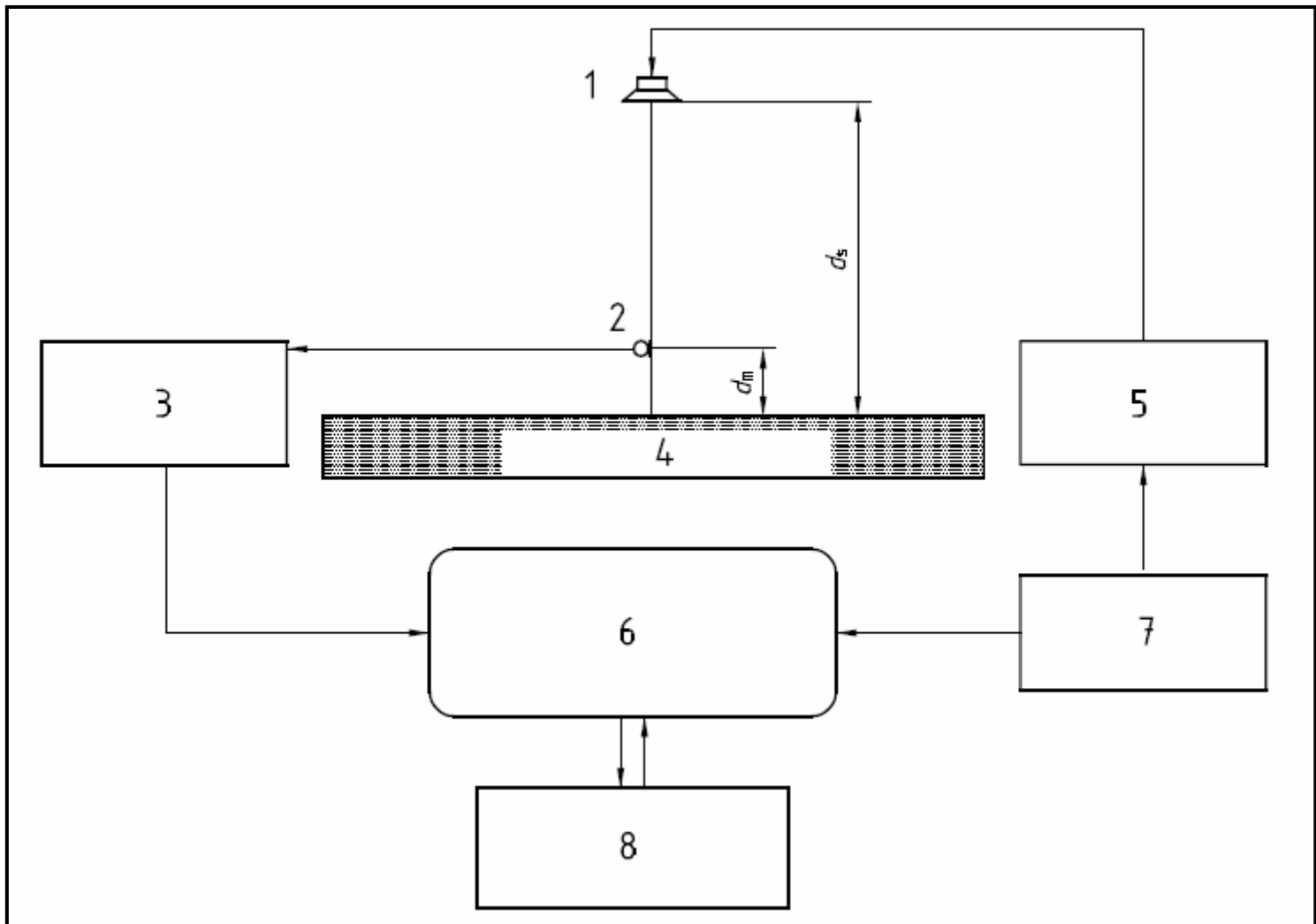


Figure 5.2.1 - Sketch of the essential components of the in-situ measurement set-up

Key:

1. Direct component
2. Reflected component
3. Time window ($T_{w,direct} = T_{w,reflected}$)

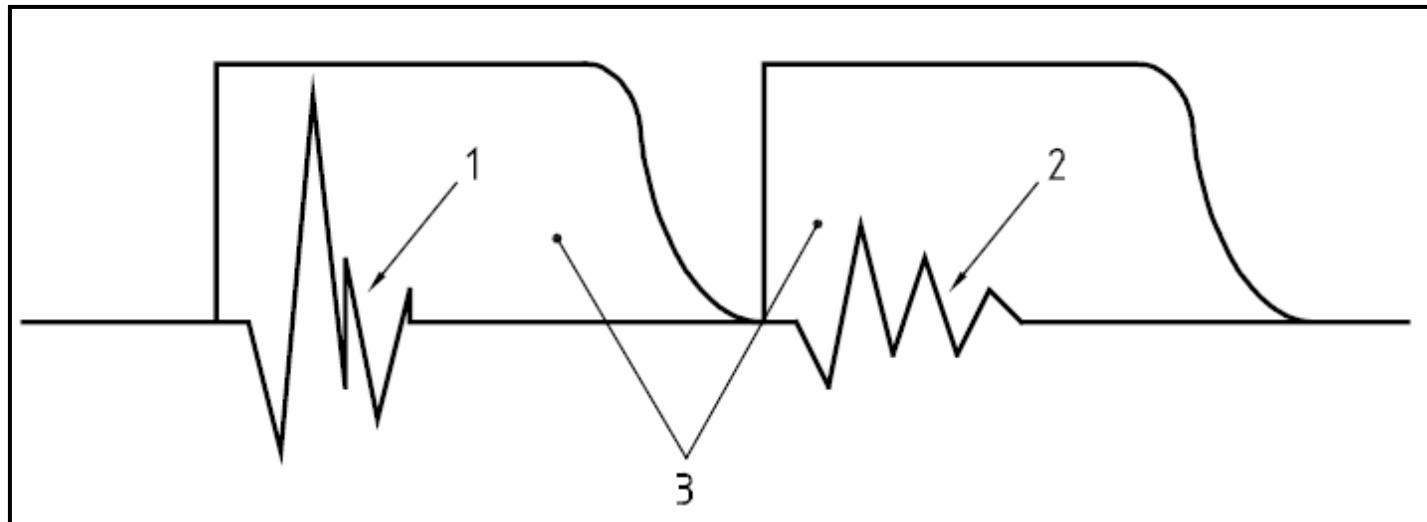


Figure 5.2.2 - Separation of the impulse response of the direct and the reflected path using time windows.

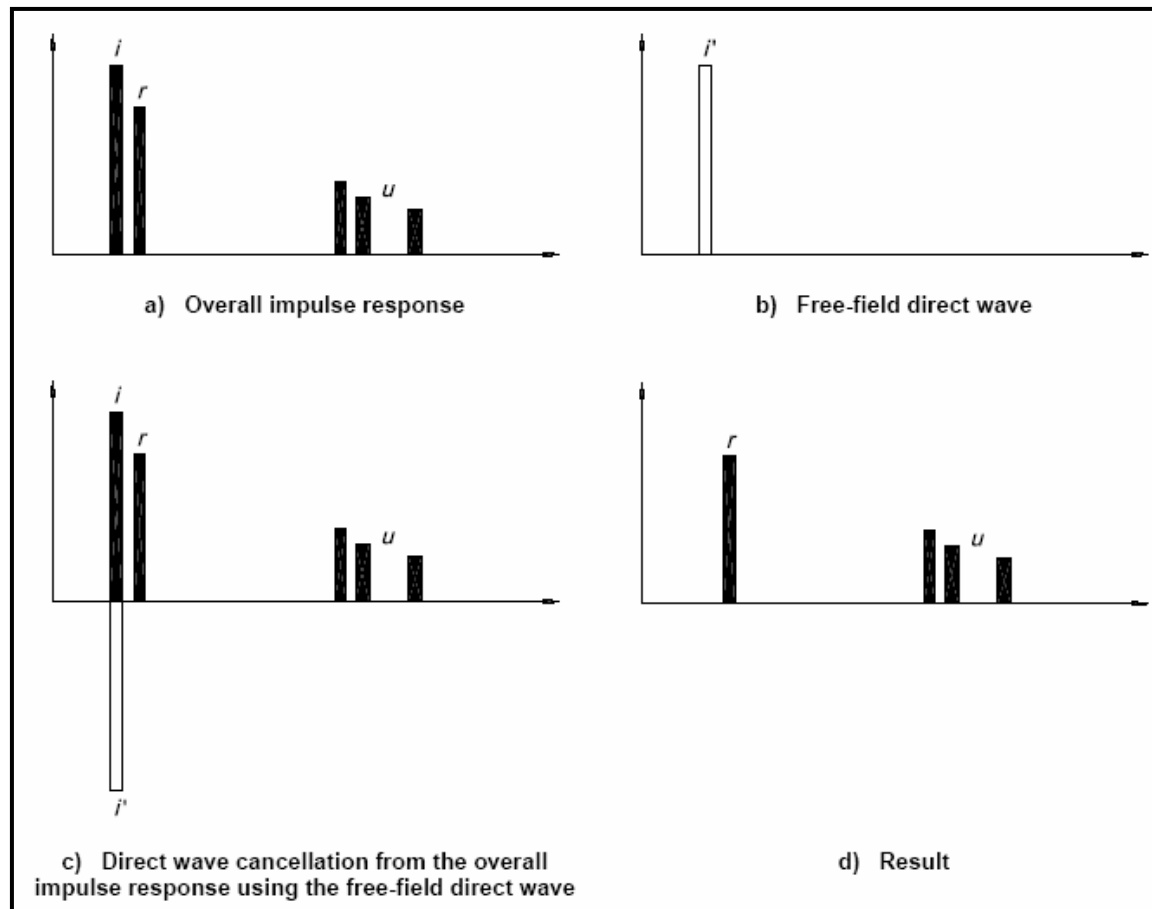


Figure 5.2.3 Principle of the signal subtraction technique I = direct incident wave, r = reflected wave, u = unwanted parasitic reflections i' = free-field direct wave

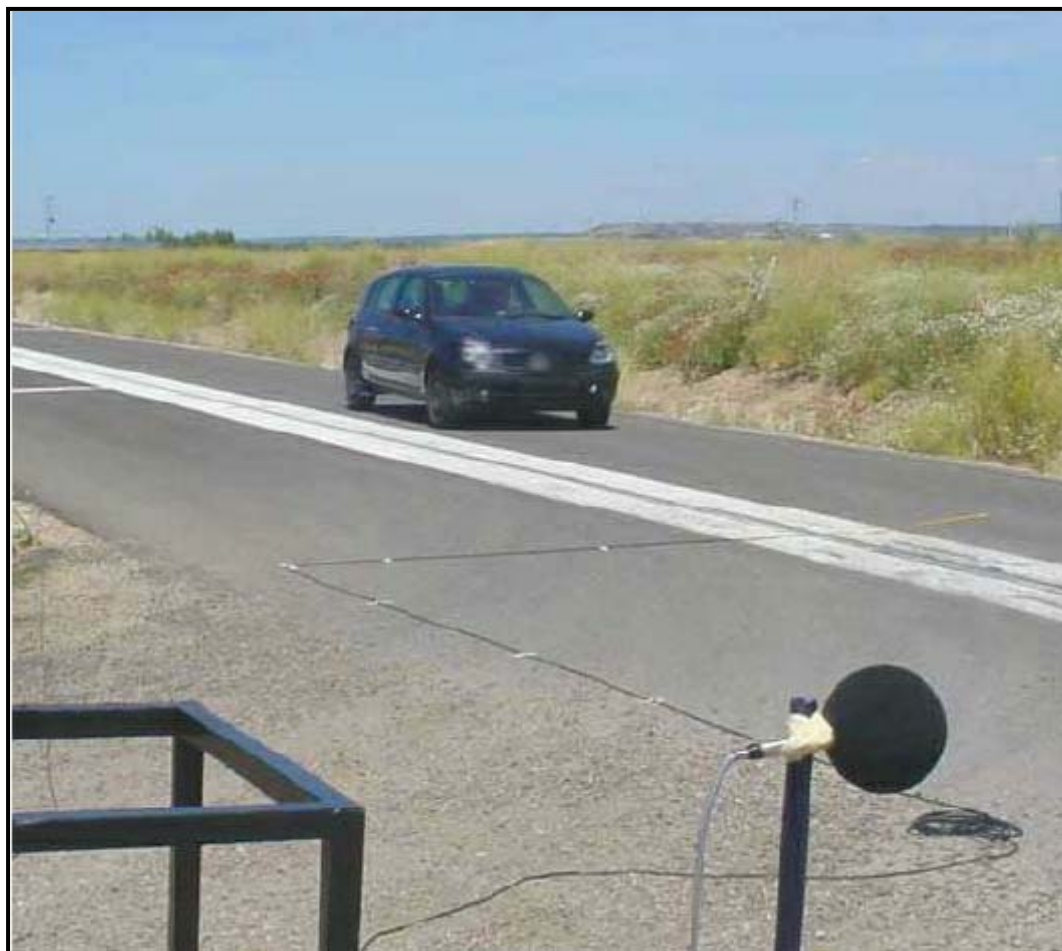


Figure 5.3.1. Measurement Set-up for statistical pass-by method

CHAPTER 6

MEASUREMENTS AND DISCUSSION OF RESULTS

The test sample is mounted at one end of a straight, rigid, smooth and airtight impedance tube. Plane waves are generated in the tube with the help of the loudspeaker (random, pseudo-random sequence, or chirp) fixed at the other end. The complex acoustical transfer function of the two microphone signals is determined and used to compute the normal incidence complex reflection factor, the normal-incidence absorption coefficient, and the impedance ratio of the test material. These quantities are determined as functions of frequency. The frequency resolution, which is determined from the sampling frequency and the record length of the Brüel and Kjaer Pulse system, is used for the measurements. The usable frequency range depends on the width of the tube and the spacing between the microphones. An extended frequency range may be obtained from the combination of measurements with varying widths and spacings between the microphones.

Two identical microphones are mounted in the tube wall to measure the sound pressure at two longitudinal locations simultaneously. The Brüel and Kjaer Pulse system is used to calculate the normal incidence absorption coefficient α by processing an array of complex data from the measured transfer function. Figure 6.1 illustrates the experimental setup for the test equipment. Figure 6.2 shows the 4-inch diameter tube,

asphalt cores, “O”-rings and metal backing plates. Also shown is the Brüel & Kjaer Pulse system. In the background the 6-inch diameter tube can be seen in a vertical orientation.

The dimensions of the test setup determine the working frequency range. The lower frequency limit depends on the microphone spacing. For frequencies lower than this limit, the microphone spacing is only a small part of the wavelength. Measurements at frequencies below this limit will cause unacceptable phase errors between the two microphones. The low frequency limit was 200 Hz in these experiments. The upper frequency limit depends on the diameter of the tube:

$$f_u < \frac{Kc}{d}, \quad (6.1)$$

where

c = Speed of sound (meter/second), d = Diameter (meter) and K = constant, 0.586.

For higher frequencies, the sound waves in the tube are no longer plane waves. For the 6-inch diameter tube, the theoretical upper frequency limit is 1318 Hz. However, it was observed that the plane wave assumption did not appear valid for frequencies higher than 1250 Hz. So in the tests, the working frequency range was set to be from 200 Hz to 1250 Hz.

For the 4-inch diameter tube, the theoretical upper frequency limit for the tube is 1978 Hz. For some thin samples, whose thicknesses were 1-inch and 1.5-inch, the first absorption peak occurs higher than 1250 Hz. So the smaller 4-inch tube can be used for thin samples. In this study the sound absorption of the samples measured for the same pavement type with the two different tubes was compared.

To test the accuracy of the equipment, the impedance tube was used to measure the absorption coefficient, reflection coefficient and impedance of fiberglass material, a highly porous material. Measurements were also taken with a metal block as a sample. Following are the results that were obtained for the road test samples.

Samples for this study were obtained from two sources. Samples of an in-service pavement were taken from the National Center for Asphalt Technology (NCAT) test Track. The NCAT pavement test track was constructed in Opelika, Alabama (near Auburn University) in 2000. The test track is a 2.7 km (1.7 mile) oval track consisting of 46 different flexible (hot mix asphalt) pavement sections (26 in tangents and 20 in curves). Each test section is approximately 61 m (200 feet) in length. Cores were taken from six of those sections and tested using the equipment described in the previous chapters. The samples used in these tests are listed with thickness and air void measurements in Table 6.1. Test results using the NCAT tire noise measurement trailer are also shown.

TABLE 6.1

Properties of dense pavement core samples studied, measured air voids V_a and sound levels L_A measured on test track for different pavement types

Section name	Type of mix	Thickness of core d (mm)	Air void V_a (%)	A-weighted sound pressure measured using NCAT CPX Trailer, dB.
N1	Super pave	76.20	4.82	92.7
N7	Super pave	76.20	3.31	93.9
N13	SMA	76.20	3.00	94.6
S1	Super pave	76.20	3.43	90.9
S4	Super pave	76.20	4.08	92.5
S5	Super pave	76.20	3.90	93.2

6.1 Track Samples

The thickness of the hard pavement samples studied was 3 inches, as shown in Figure 6.3. The first peaks of sound absorption are in the working frequency range of the 6-inch tube. In each of the different hard pavement types studied, six samples were tested using the 6-inch tube and the average absorption coefficient of these samples was calculated.

Figure 6.4 shows the absorption coefficient measured for a very hard surface material and a highly absorptive material. It is observed the absorption coefficient of fiberglass material is close to 1.0 which is expected because of the high absorptive property of the fiberglass material. It is also noted that the absorption coefficient of very hard material such as metal plate is close to zero as most of the sound gets reflected back from the hard surface. The absorption coefficient was also measured keeping the impedance tube open. An absorption coefficient value close to 1.0 was obtained which proved the validity of the impedance tube method.

Figures 6.5 to 6.11 show the absorption coefficient of different road samples that were measured using a 6-inch tube.

Figure 6.12 compares the sound absorption coefficients of these different pavements. As expected, the most porous pavement, N13, has a much higher overall magnitude of absorption than the other pavements. However, the overall absorption coefficient magnitude is much less than one. There are two peaks for all of the pavements, presumably because the thickness of these samples is 3 inches. The Open Graded Fine Core (OGFC) samples tested are not as thick as these samples, so only single peaks are observed. The second, third and higher frequency peaks would be above the upper frequency limit of our impedance tube plane wave capability limit.

The sound absorption, the mechanical properties and the tire noise were measured for the dense pavement samples. So far the tire noise has not been measured for the porous surfaces. Tire noise measurements will be made on such porous surfaces when they have been laid and become available on the test track.

6.2 Testing of Laboratory Manufactured Slabs

Slabs were manufactured in the laboratory for the evaluation of the effect of different thicknesses and gradations of OGFC materials. The slabs consisted of a 2-½ inch dense graded Superpave mix with an OGFC placed on top. Two OGFC gradations were used, a 9.5 mm (3/8 inch), and a 15.9 mm (5/8 inch) mix, or referred to here as fine and coarse aggregates. Three different thickness layers were used (1 inch, 1 ½ inch and 2 inch). In order to make in-situ measurements and to avoid having to cut circular samples from road pavements, the impedance tube was mounted vertically on the asphalt slabs, and the sound absorption coefficients were measured by using the same procedure.

Figures 6.14 to 6.22 show the measurements obtained for the fine and coarse samples with the test sample as a core and also obtained by mounting the 6-inch tube directly on the test slab. It can be seen that the sound absorption coefficients measured on the slabs and with samples in the impedance tube are very similar, except for lower frequencies.

To study how serious the sound leakage was from the interface between the vertically mounted tube and the slabs, a rubber “O” ring and some grease were applied to seal the metal collar at the lower end of the tube to the pavement slabs. However, it was observed that the measured absorption coefficient results were not very different for the conditions: (a) no seal, (b) with only “O”-ring, and (c) with “O”-ring and grease.

On each slab, the absorption coefficient α was measured at four different positions and an average of the sound absorption-frequency curve was calculated for each pavement. The porosity on the surface is not distributed uniformly over each block. And the acoustical properties are of course dependent on the surface of the samples. Different sound absorption coefficients were observed at different positions on each pavement block.

The frequencies of the peak sound absorption of the fine aggregate samples are seen to be slightly lower than those of the coarse aggregate samples. And the peaks for the fine aggregate samples are broader. Figure 6.25 compares the results obtained for the six slabs.

The thinner the sample, the higher the frequency at which the peak absorption occurs. Especially for the 1-inch thick slabs, the frequency of the first absorption peak is higher than 1250 Hz. So a 4-inch diameter tube was utilized for measurements with these slabs. With the 4-inch tube, the absorption coefficient can be measured up to 1.95 kHz. Then the peaks, which could not be measured with the 6-inch tube, could be observed.

The pavement surface area tested with the 4-inch tube is less than one-half of that tested with the 6-inch tube. So the individual surface properties of the samples have more of an effect on the sound absorption results than when the 6-inch tube is used. Satisfactory results were obtained after more surface averages were made. The results obtained with the 4-inch tube have the same shape and peaks at almost the same frequencies as those obtained with the 6-inch tube, even though the magnitudes vary by about 10%. See Fig 6.28. A comparison of the sound absorption coefficients of the OGFC coarse 1-inch core and the slab measured with 6-inch tube is shown in Fig 6.20.

After the in-situ tests were completed, cores were cut from the slabs. And more measurements of sound absorption were carried out with the impedance tubes. Figure 6.21 shows the results. Figure 6.22 shows a comparison of the absorption coefficients of the fine aggregate pavement samples measured both with the in-situ tube tests and the two different diameter laboratory impedance tube core tests. For the comparison of the one-inch thick porous pavements the 4-inch impedance tube was used. And for the thinner two-inch and 1.5-inch thick porous pavements the 6-inch diameter impedance tube was used. The results are seen to be very similar, considering the different boundary conditions in the different tests. Figure 6.30 shows the NCAT test track used for the tire noise measurements on the dense pavements. Figure 6.31 shows the NCAT trailer used for the CPX tire noise tests.

Comparing Figures 6.20 and 6.22, we can see that the sound absorption coefficients measured on the slabs and with core sample in the impedance tube are very similar, except that about 10 to 50 Hz shifts the peaks measured in the tube to a lower frequency. The absorption coefficient of more OGFC samples was measured in the 4-inch tube as well. Similar results were obtained as shown in Figure 6.19.

In contrast to the dense track samples, the sound absorption coefficients of the OGFC samples have values close to 1.0 in some particular frequency ranges. For the 2-inch thick samples, the peak sound absorption frequency is about 900 Hz, which coincides with the noise generated by automobiles in interstate travel. The sound absorption peak is fairly broad, so it is attractive to use such a porous surface to reduce tire/road noise. Additionally, as we have seen in the preceding parts of the chapter, the porosity of the

OGFC samples is much higher than those of the track samples, so that they possess not only good sound absorption properties, but good drainage properties as well.

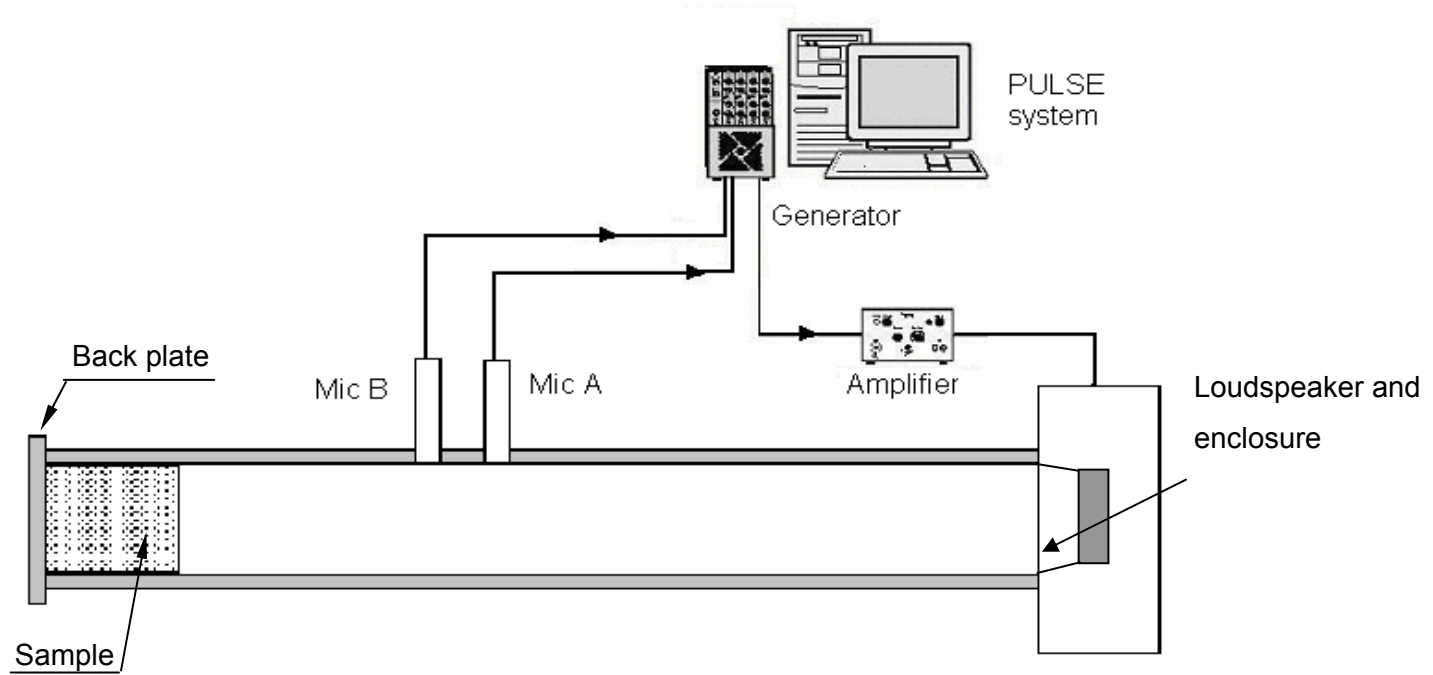


Figure 6.1. Experimental setup of impedance tube



Figure 6.2. Experimental setup, 4-inch impedance tubes, asphalt cores, “O” rings and metal back plates. Shown as well is the Brüel & Kjaer Pulse System. The 6-Inch tube can also be seen in the back ground.



Figure 6.3. The 3-inch thick hard surface dense track pavement samples

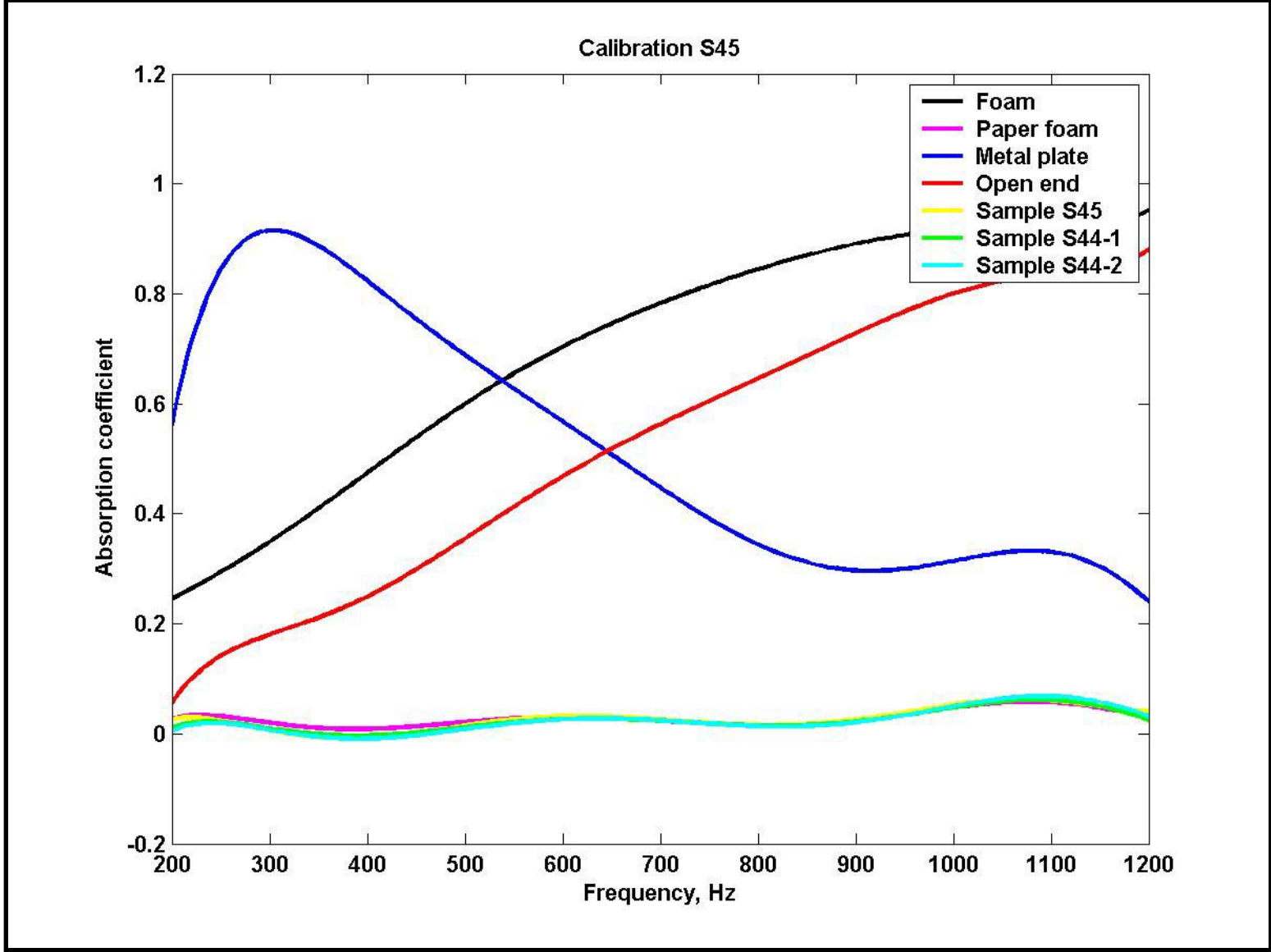


Figure 6.4 Comparison of sound absorption coefficients of different samples using 6-inch tube

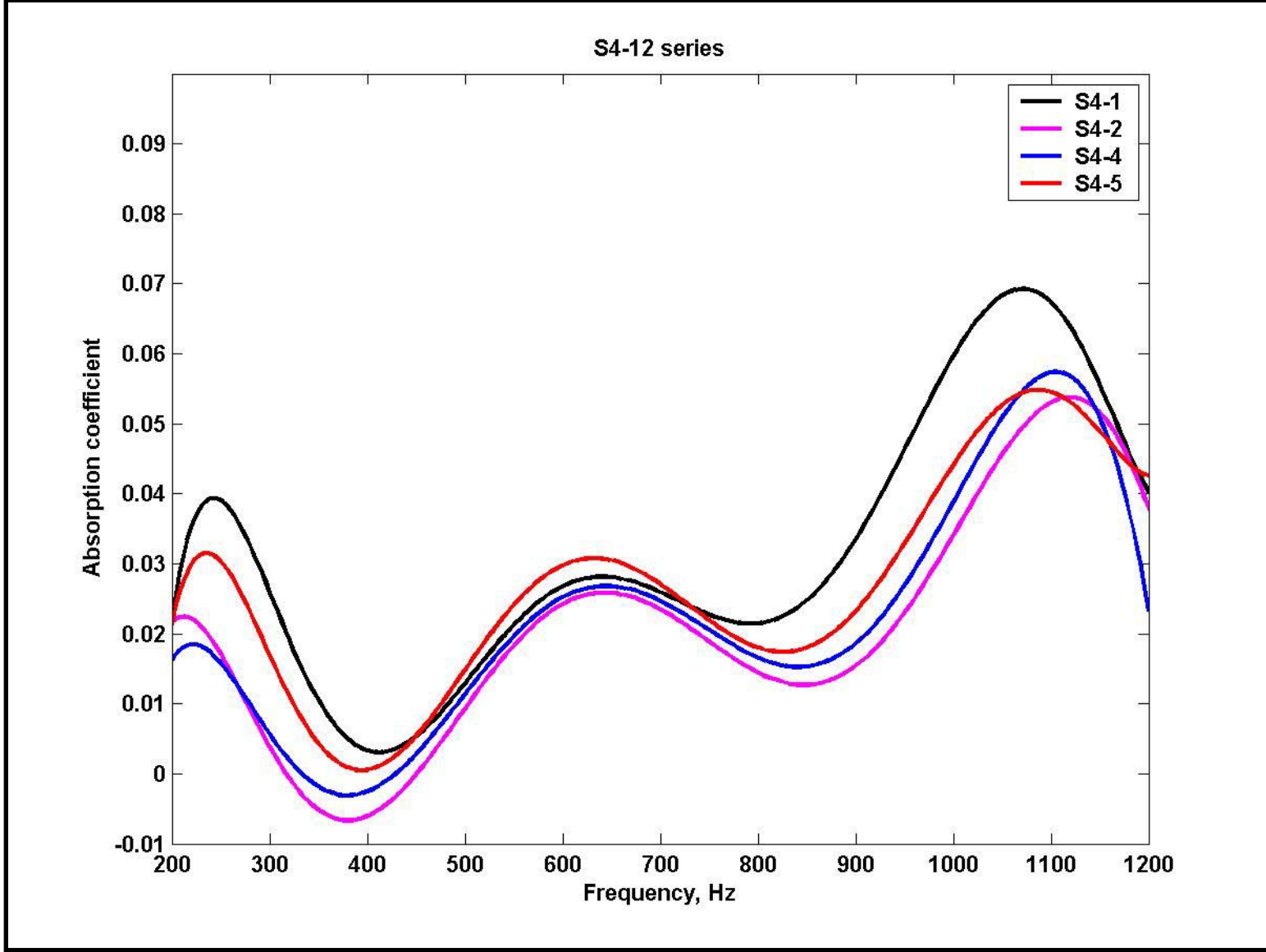


Figure 6.5 Absorption coefficient of sample S4 using a 6-inch tube

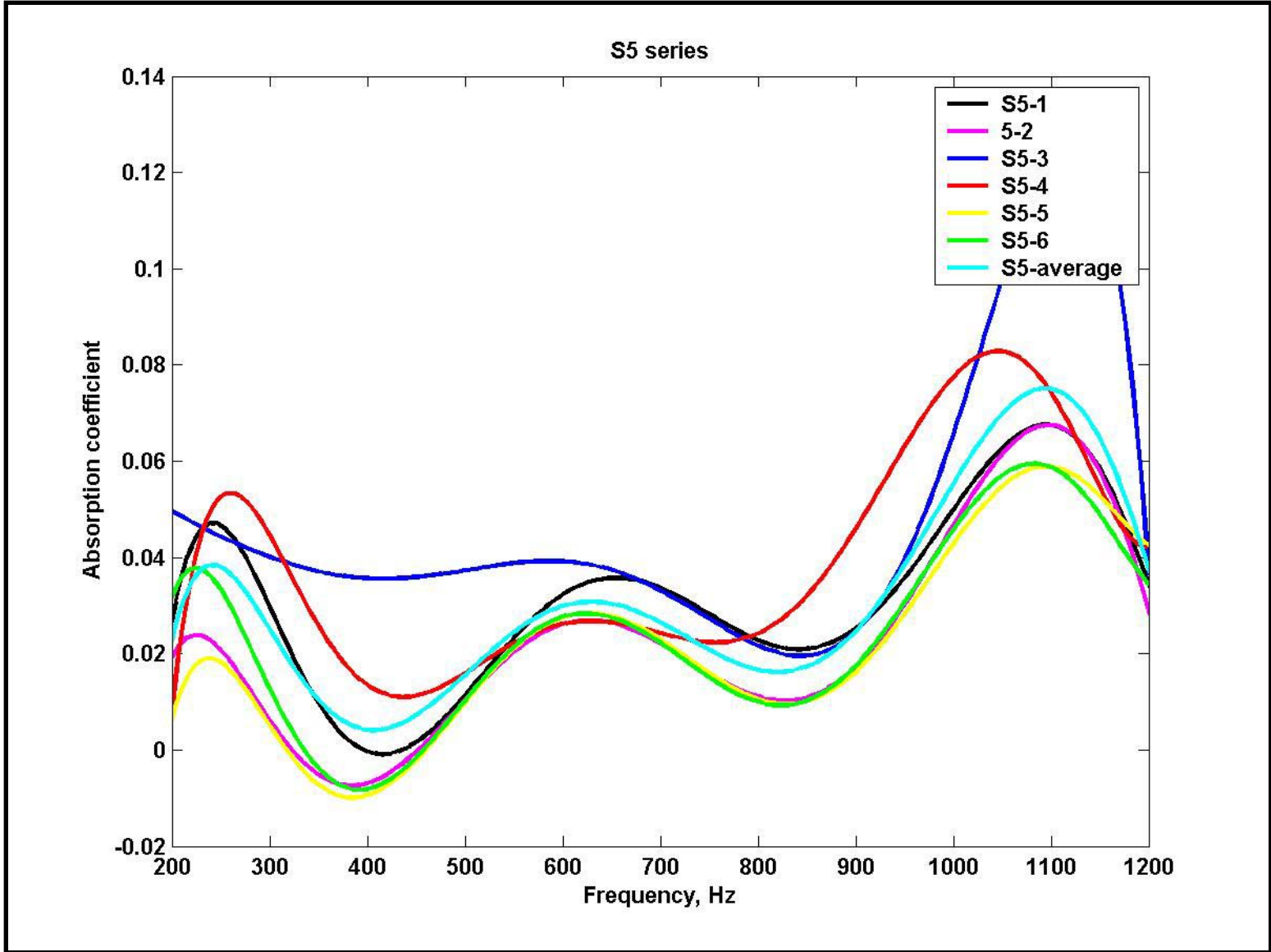


Figure 6.6 Absorption coefficient of sample S5 using 6-inch tube

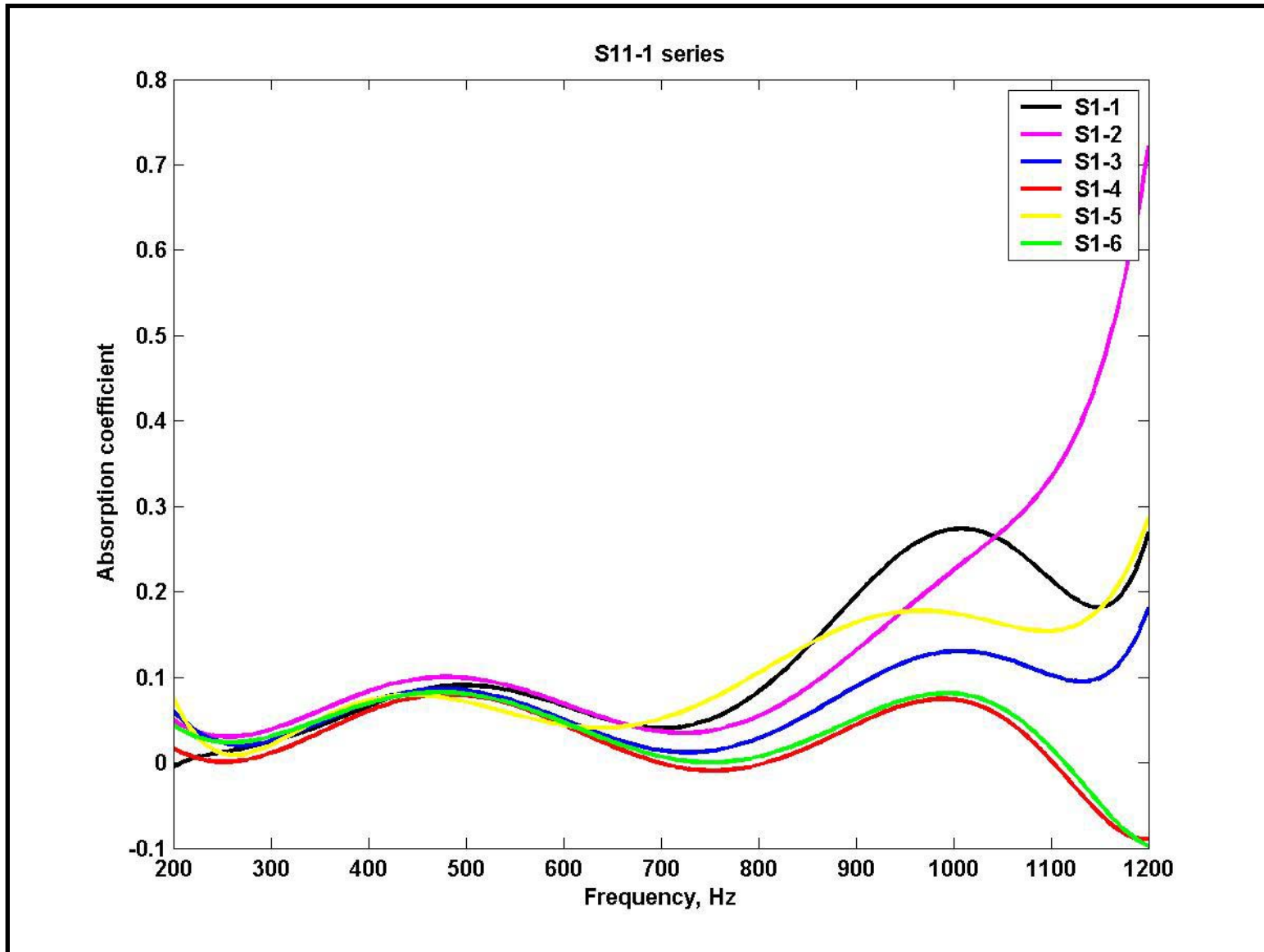


Figure 6.7 Absorption coefficient of sample S1 using 6-inch tube

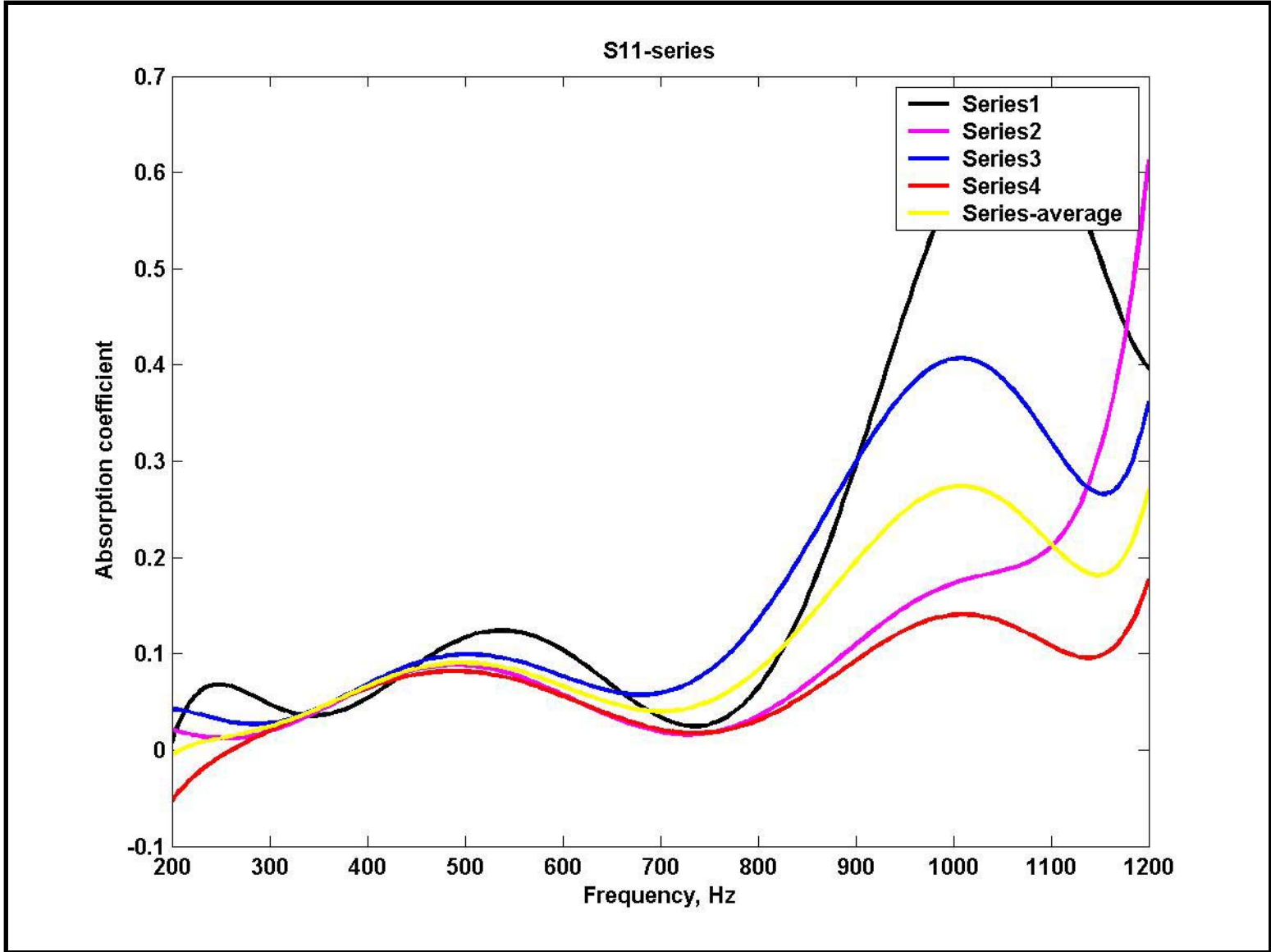


Figure 6.8 Absorption coefficient of sample S11 using 6-inch tube

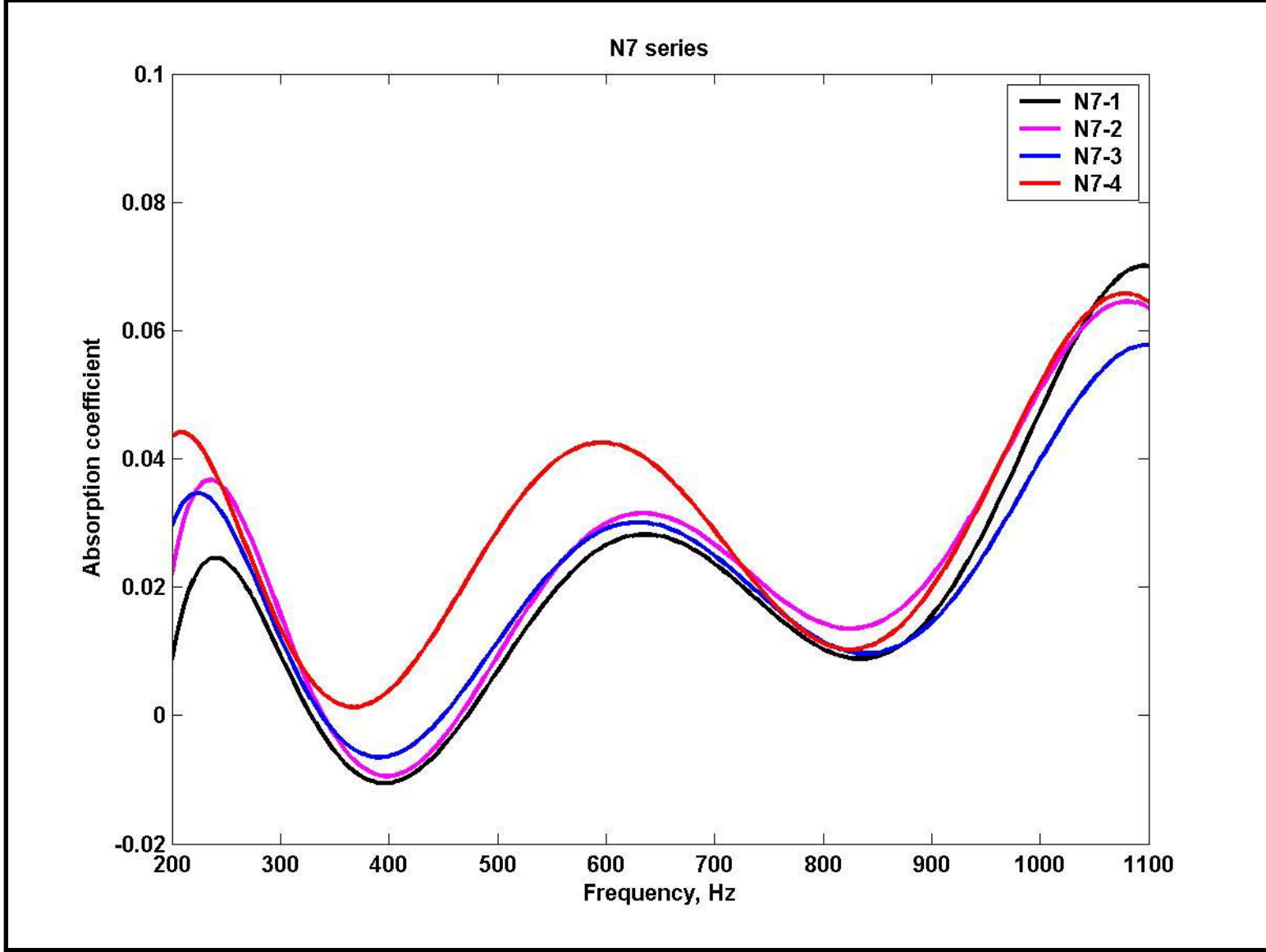


Figure 6.9 Absorption coefficient of sample N7 using 6-inch tube

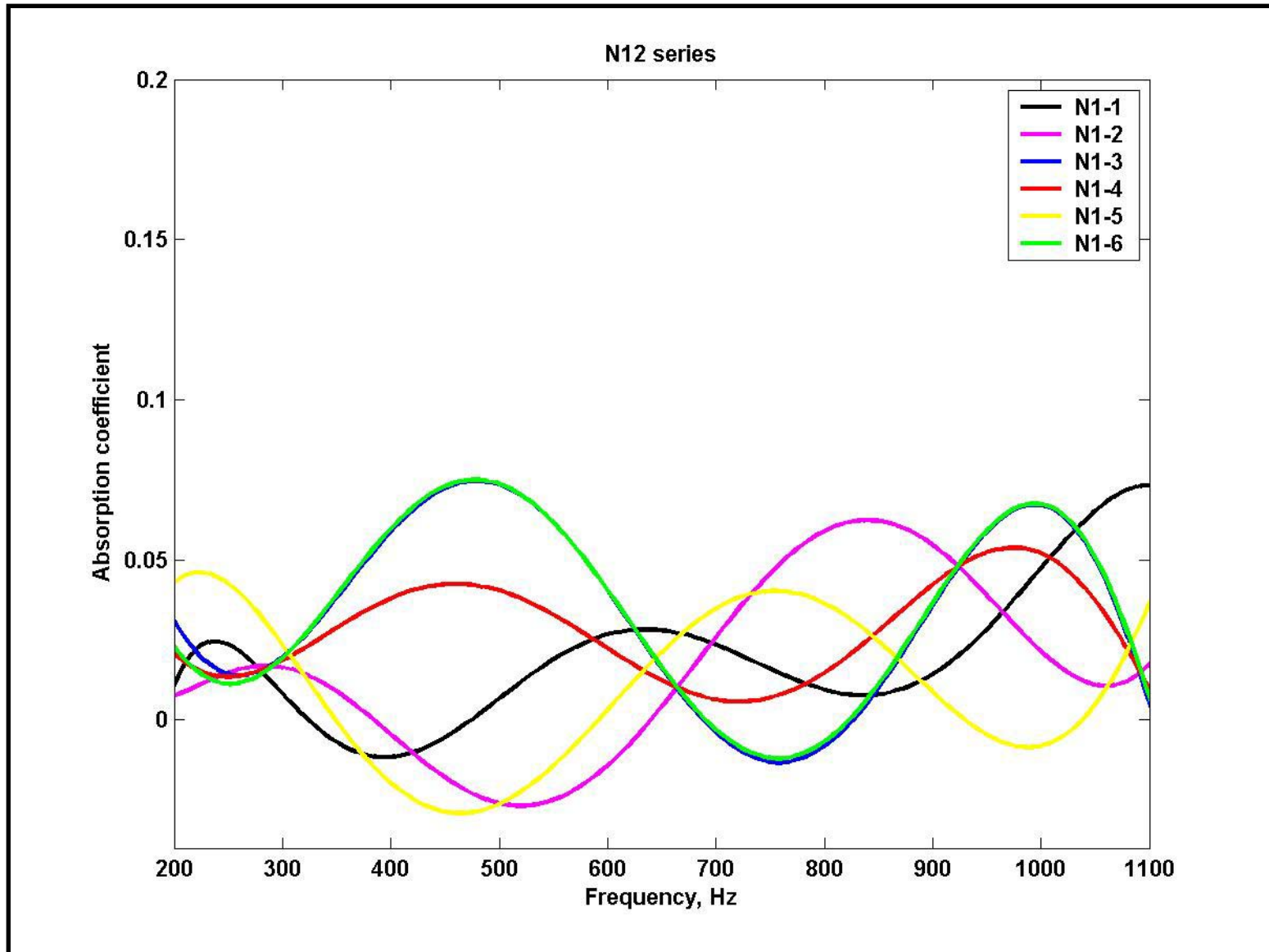


Figure 6.10 Absorption coefficient of sample N1 using 6-inch tube

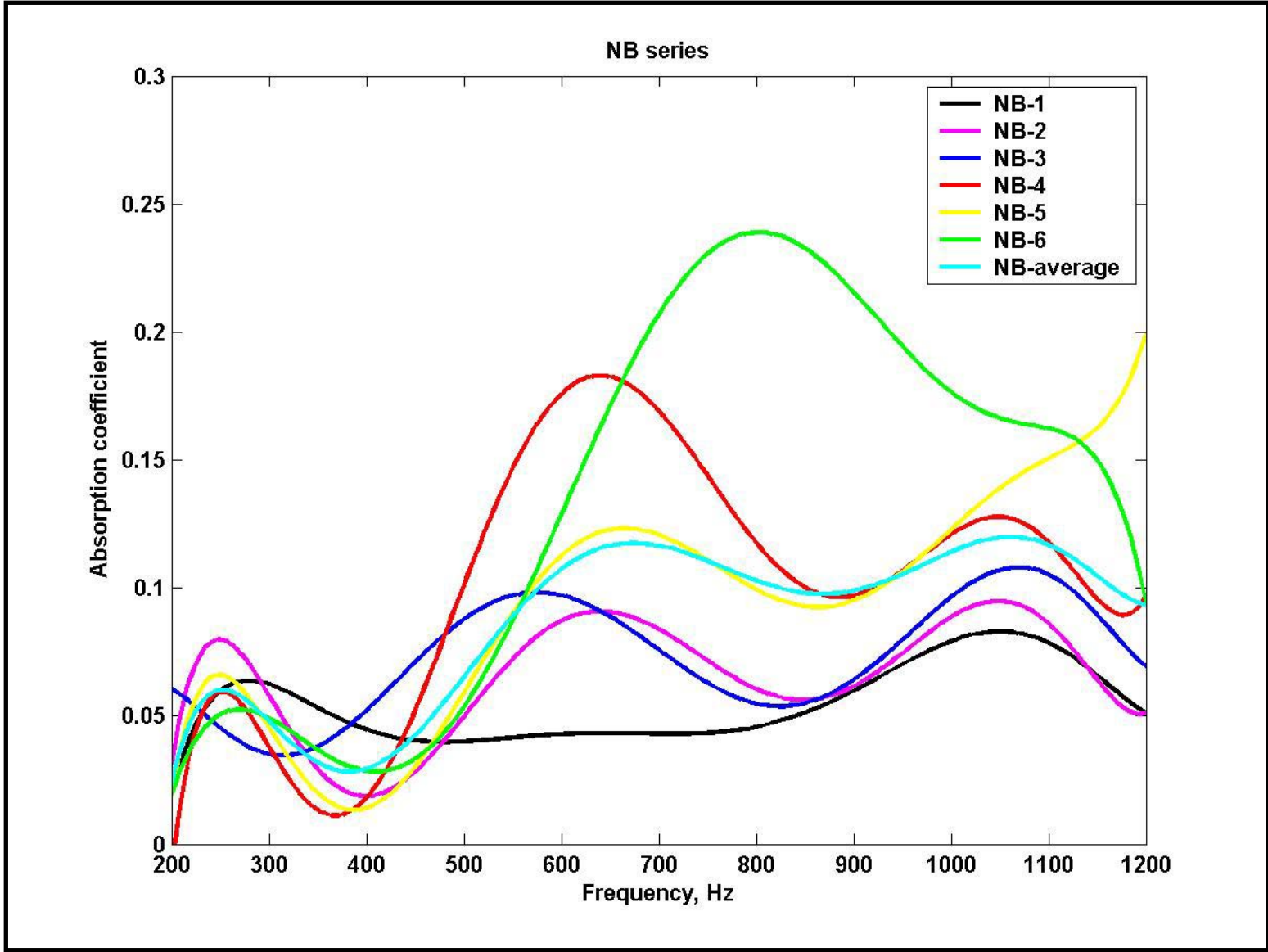


Figure 6.11 Absorption coefficient of sample NB using 6-inch tube

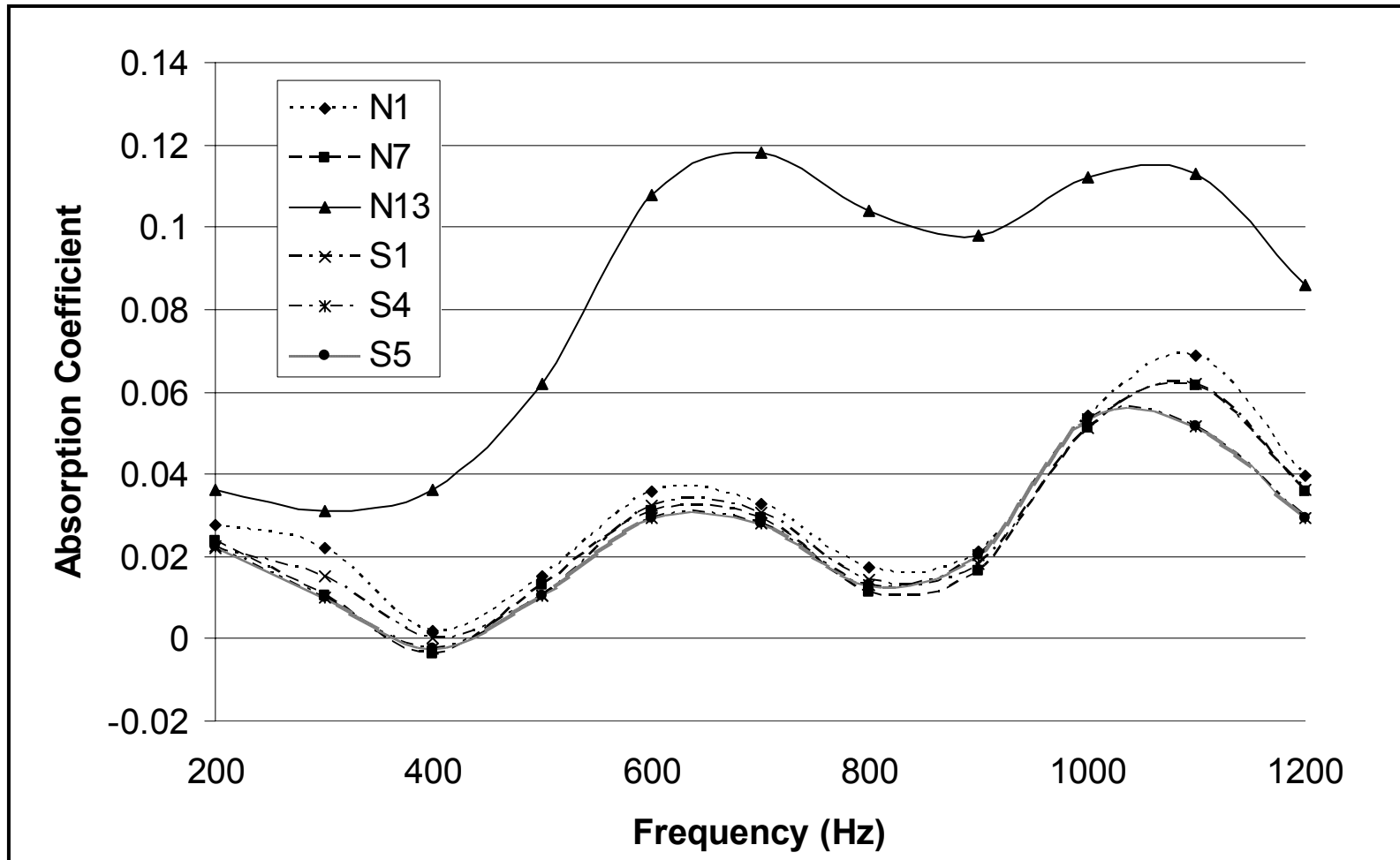


Figure 6.12. Comparison of the sound absorption coefficients of hard samples measured in the 6-inch tube



Figure 6.13. OGFC graded coarse 1.5-inch thick 6-inch diameter porous cores

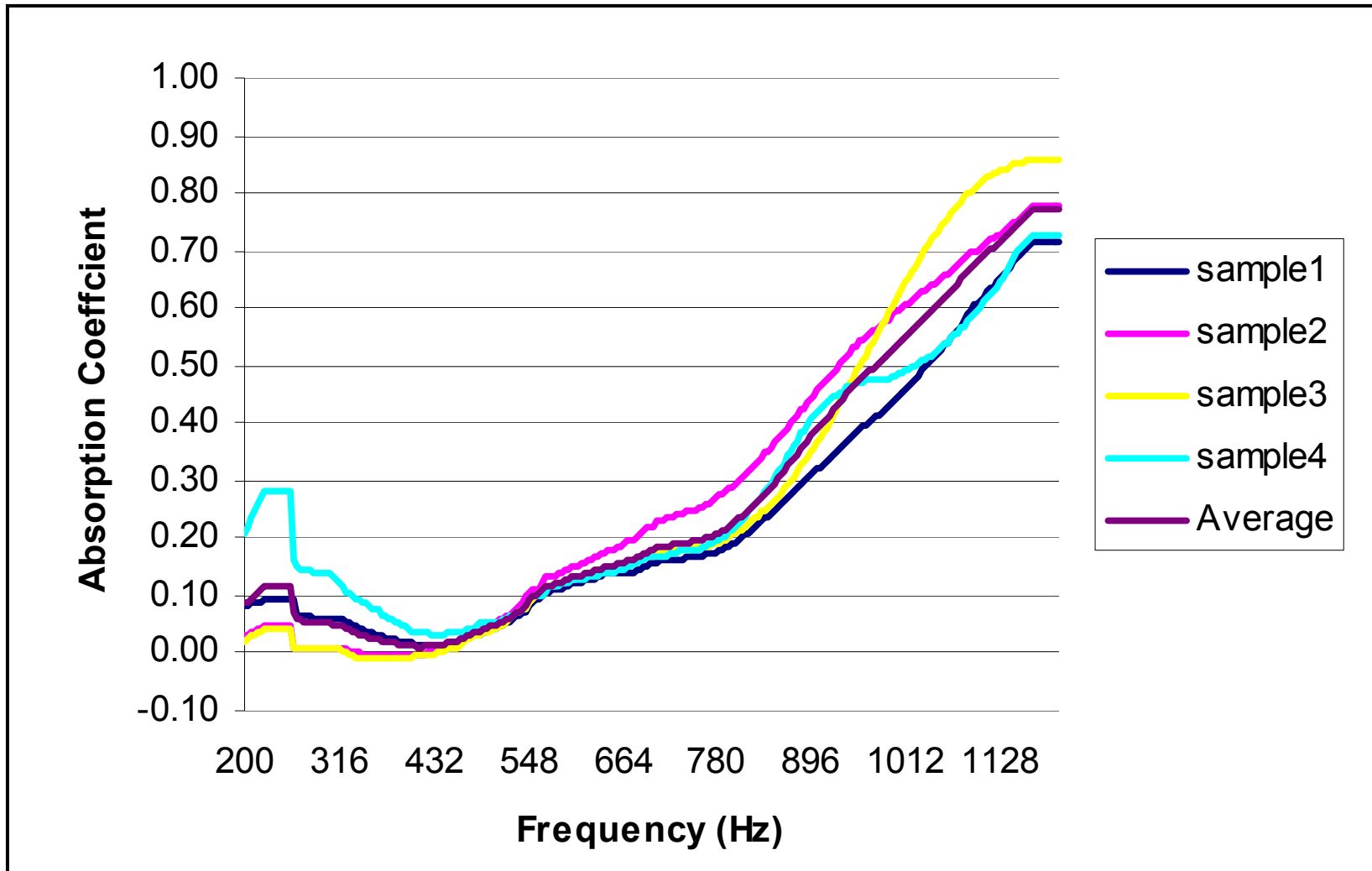


Figure 6.14 Sound absorption coefficients of OGFC 1-inch fine cores measured by a 6-inch tube

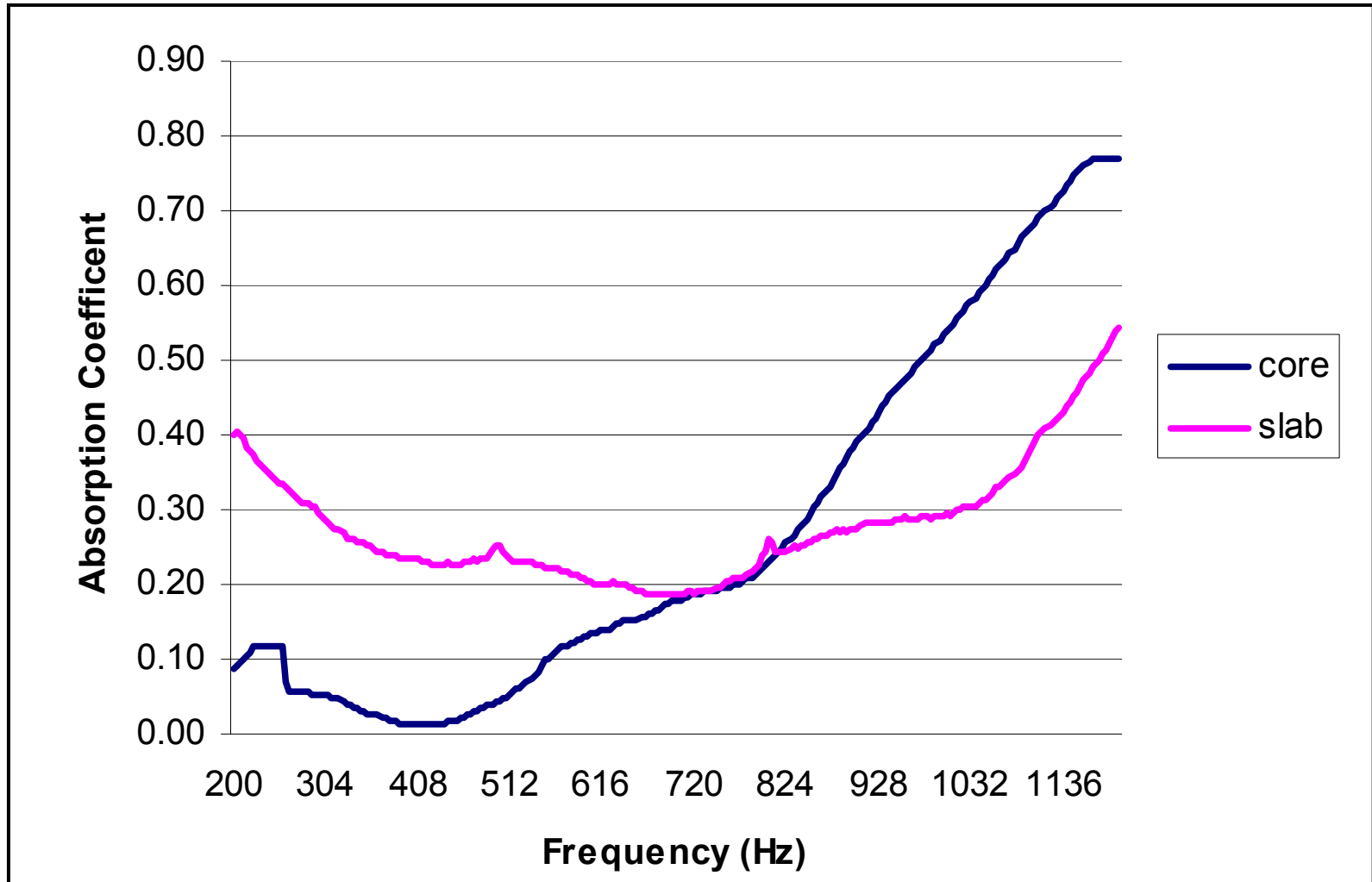


Figure 6.15 Sound absorption coefficients of OGFC 1.5-inch fine cores measured by a 6-inch tube

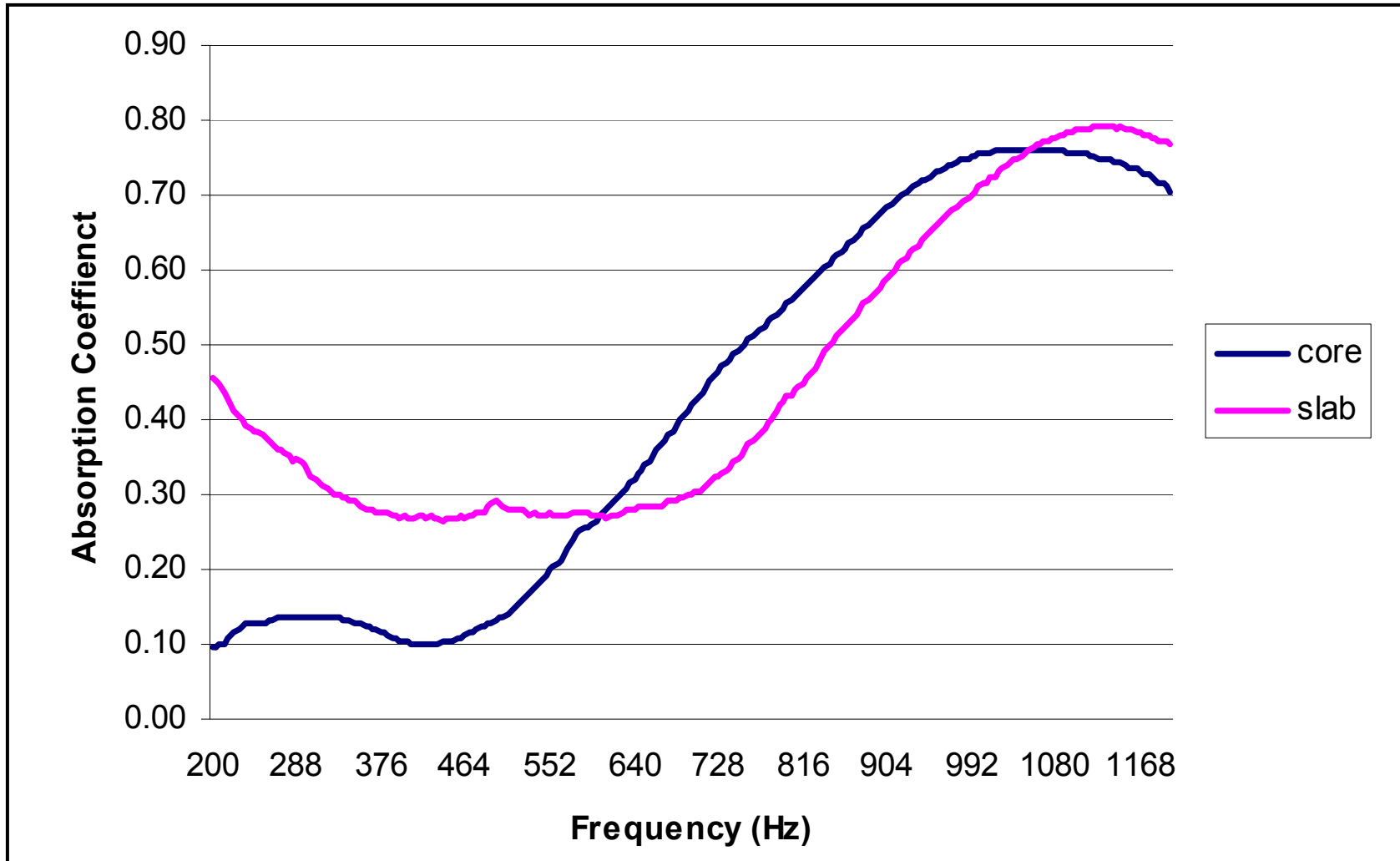


Figure 6.16: Comparison of sound absorption coefficients of OGFC fine 1.5-inch core and slab measured by 6-inch tube

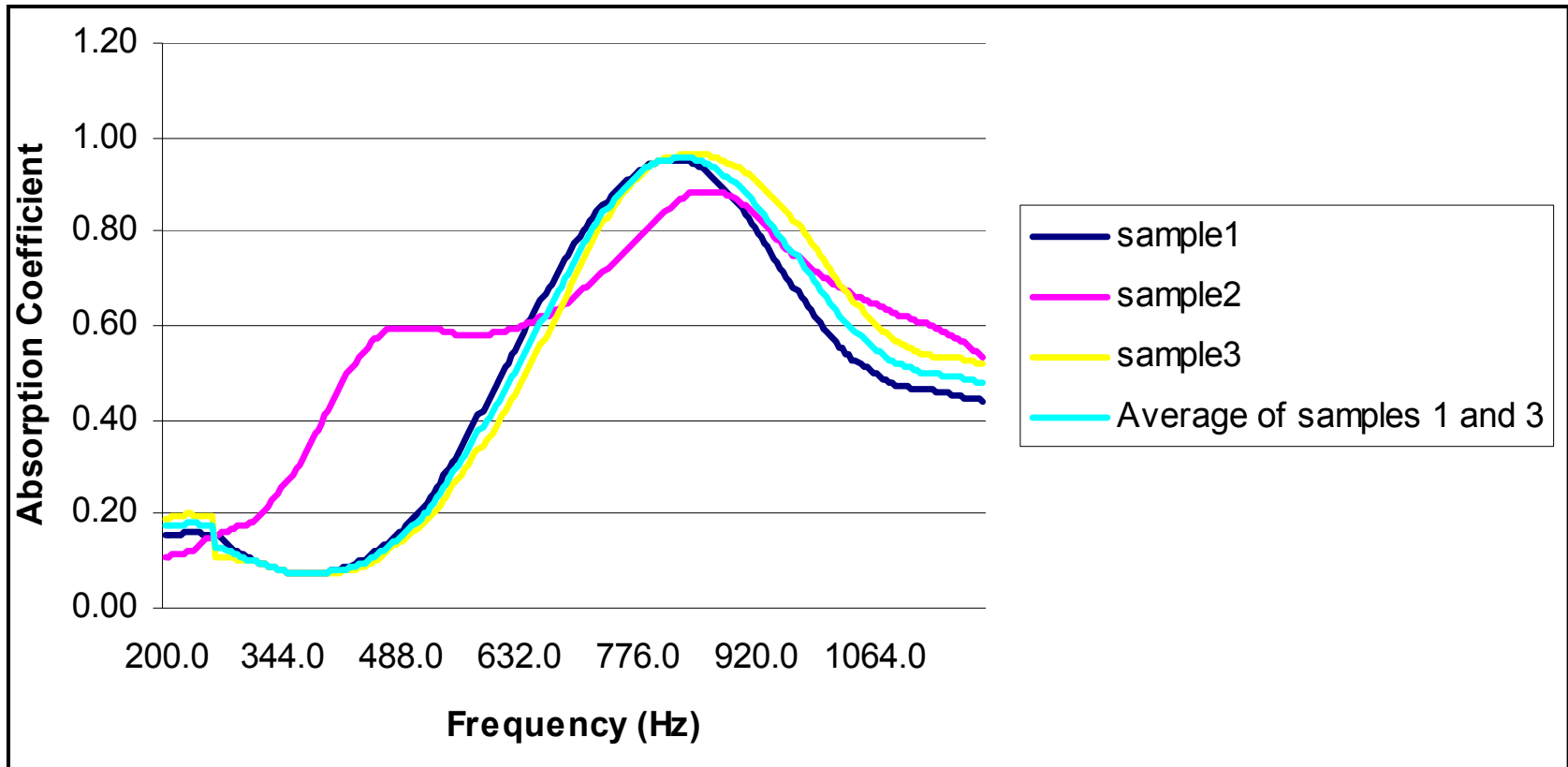


Figure 6.17 Sound absorption coefficients of OGFC 2-inch fine cores measured by a 6-inch tube

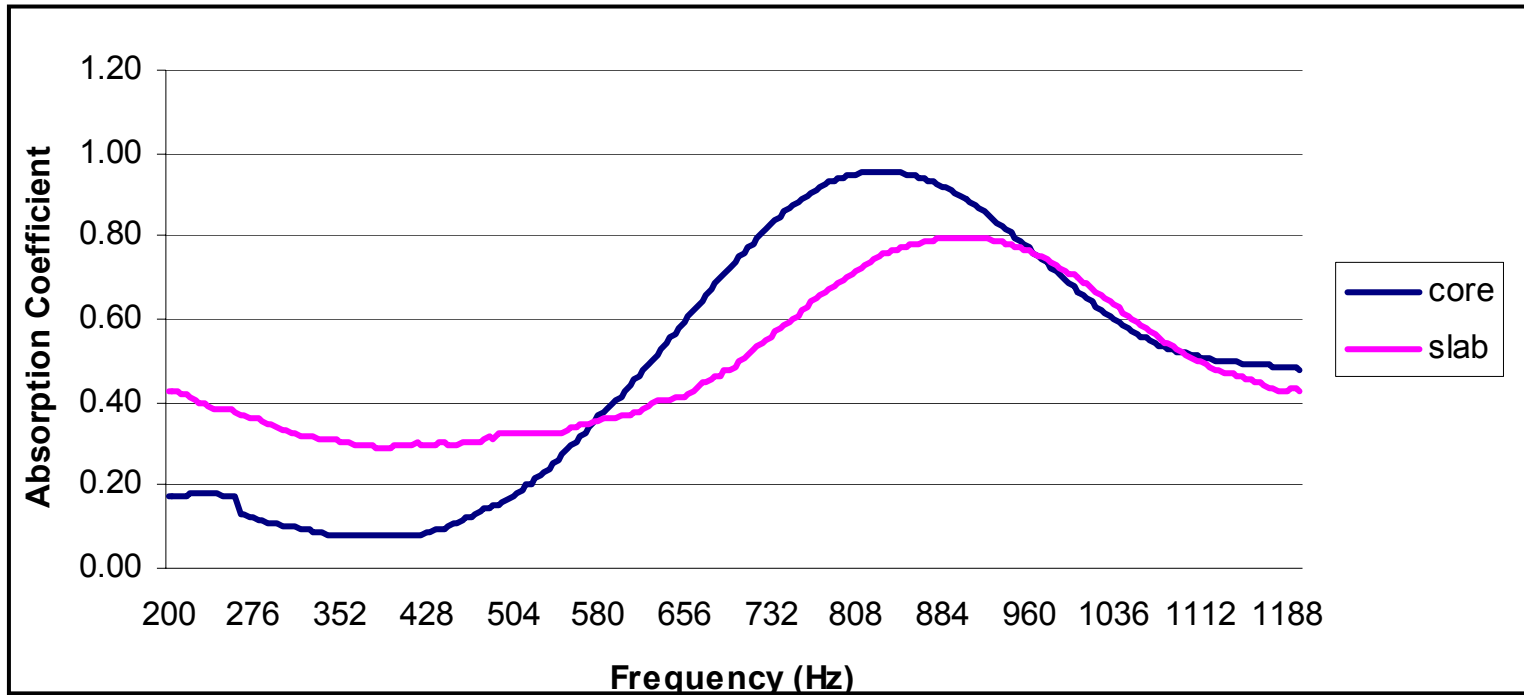


Figure 6.18 Comparison of sound absorption coefficients of OGFC fine 2-inch core and slab measured by 6-inch tube

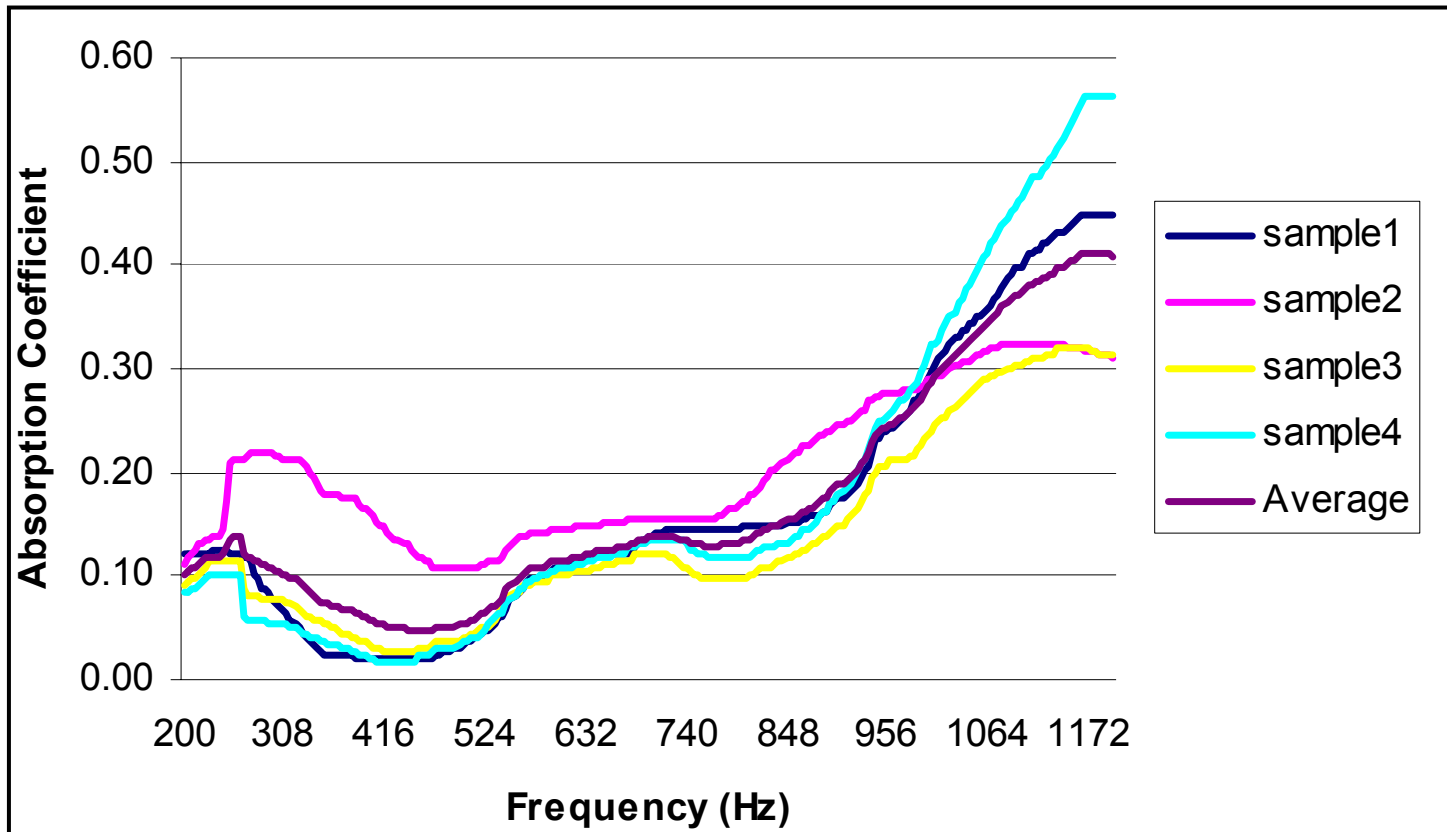


Figure 6.19 Sound absorption coefficients of OGFC 1-inch coarse cores measured by a 6-inch tube

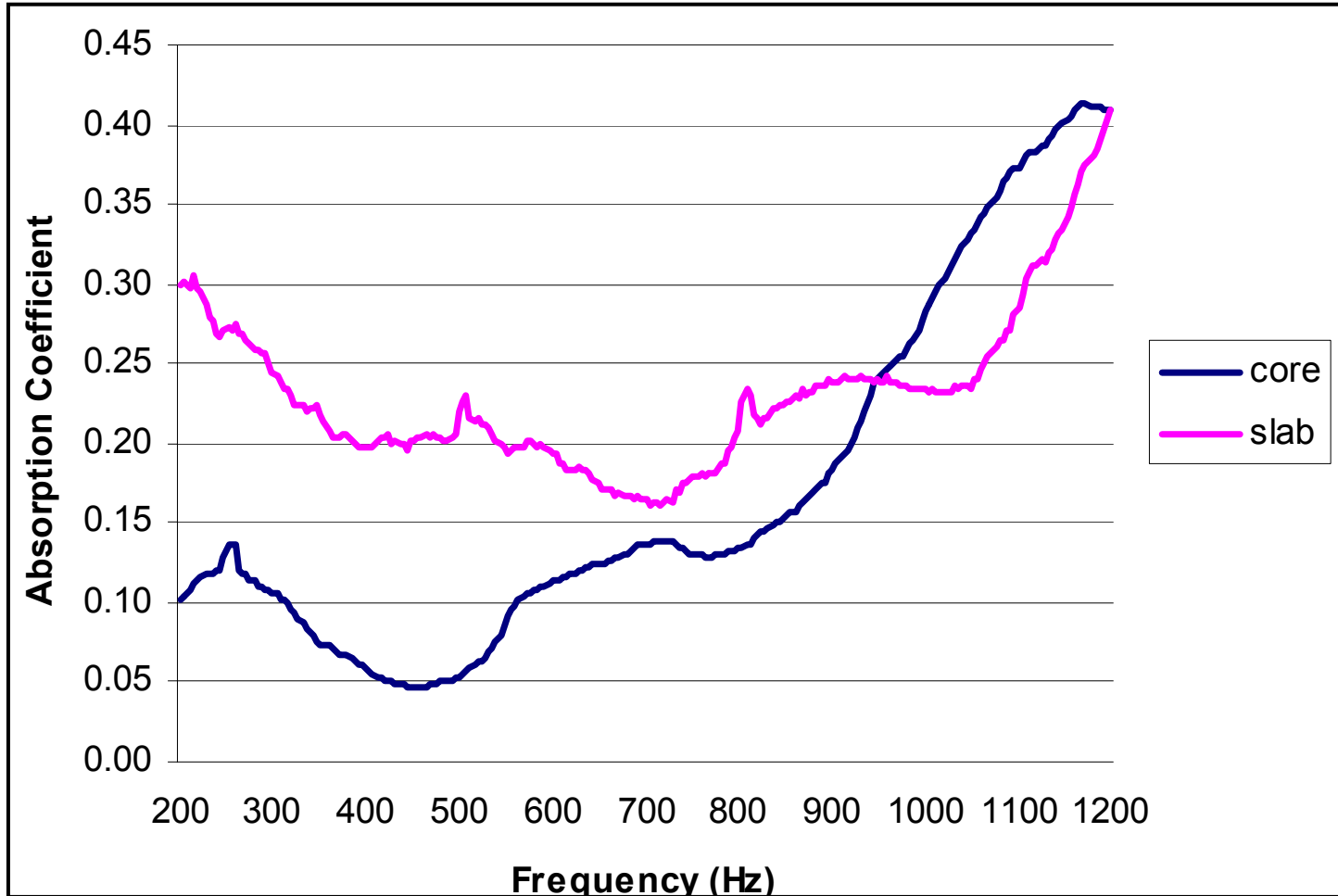


Figure 6.20 Comparison of sound absorption coefficients of OGFC coarse 1-inch core and slab measured by 6-inch tube

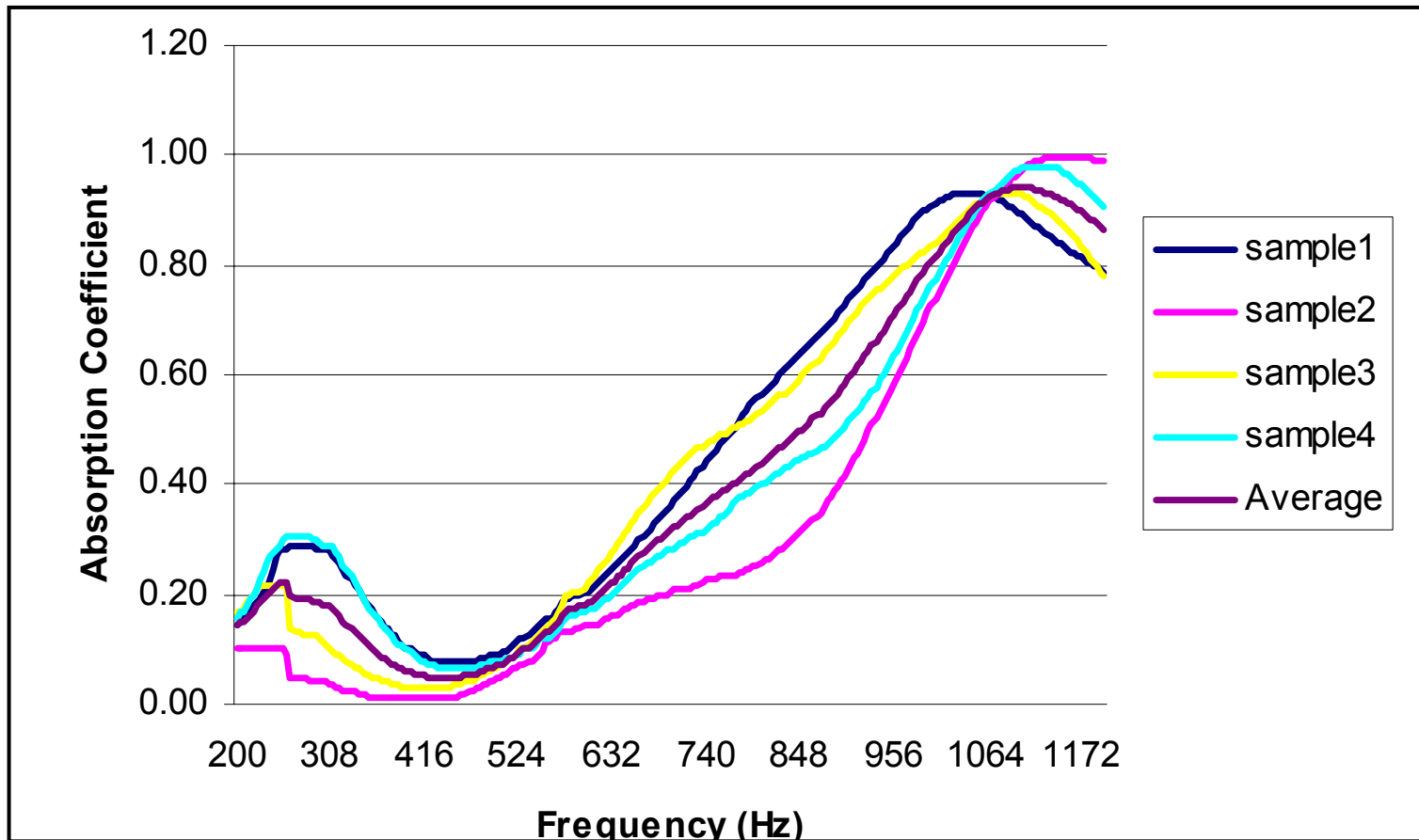


Figure 6.21 Sound absorption coefficients of OGFC 1.5-inch coarse cores measured by 6-inch tube

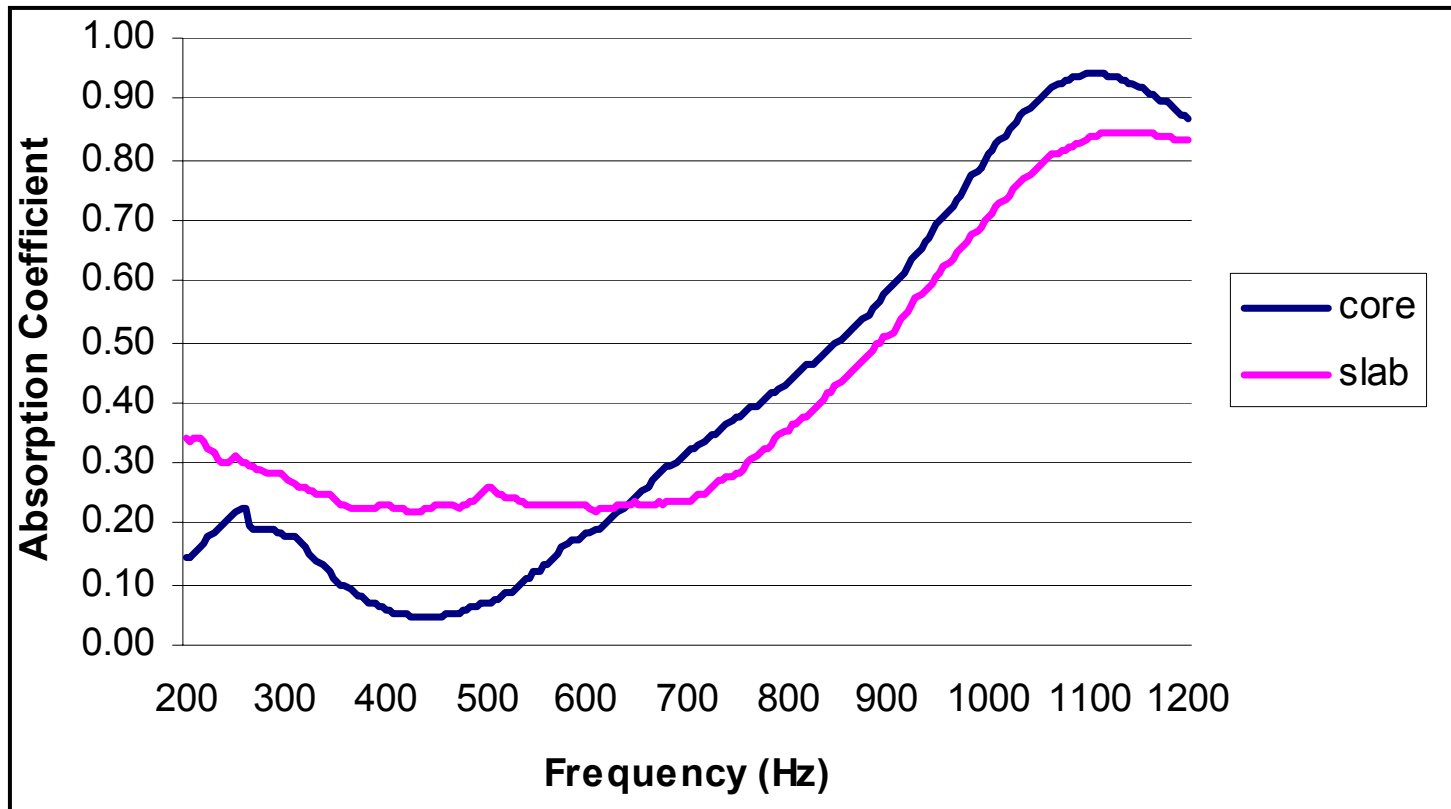


Figure 6.22 Comparison of sound absorption coefficients of OGFC coarse 1.5-inch core and slab measured by 6-inch tube

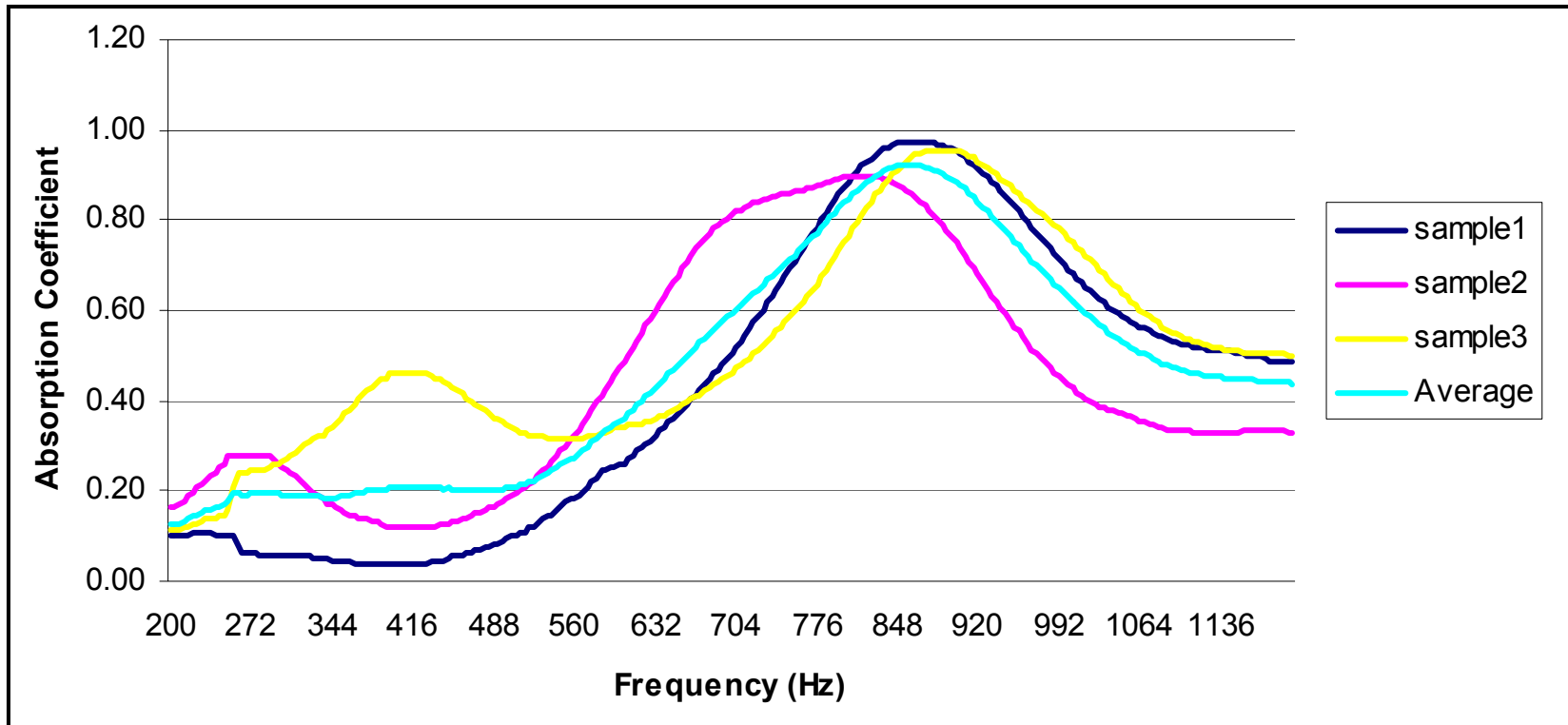


Figure 6.23 Sound absorption coefficients of OGFC 2-inch coarse cores measured by a 6-inch tube

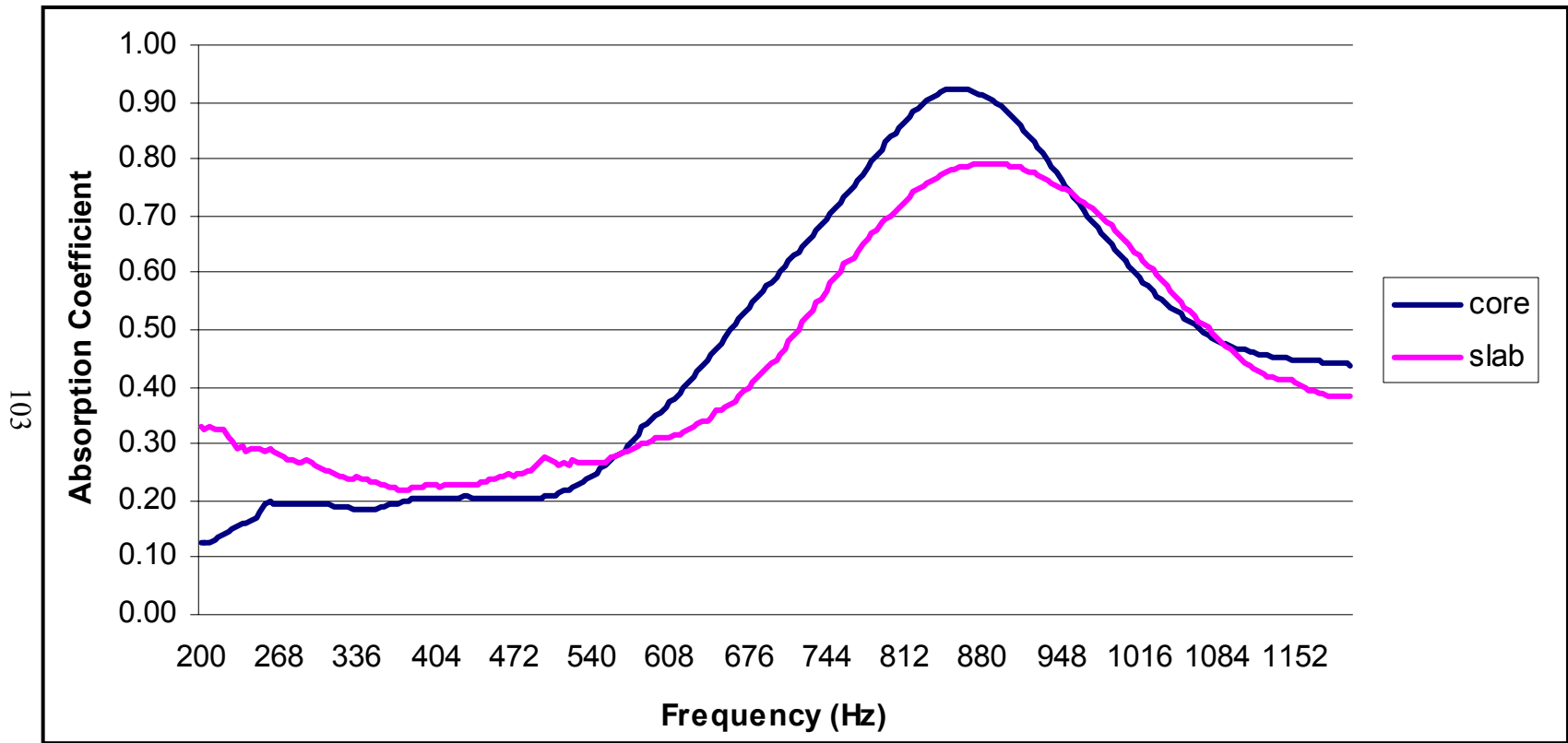


Figure 6.24 Comparison of sound absorption coefficients of OGFC coarse 2-inch core and slab measured by 6-inch tube

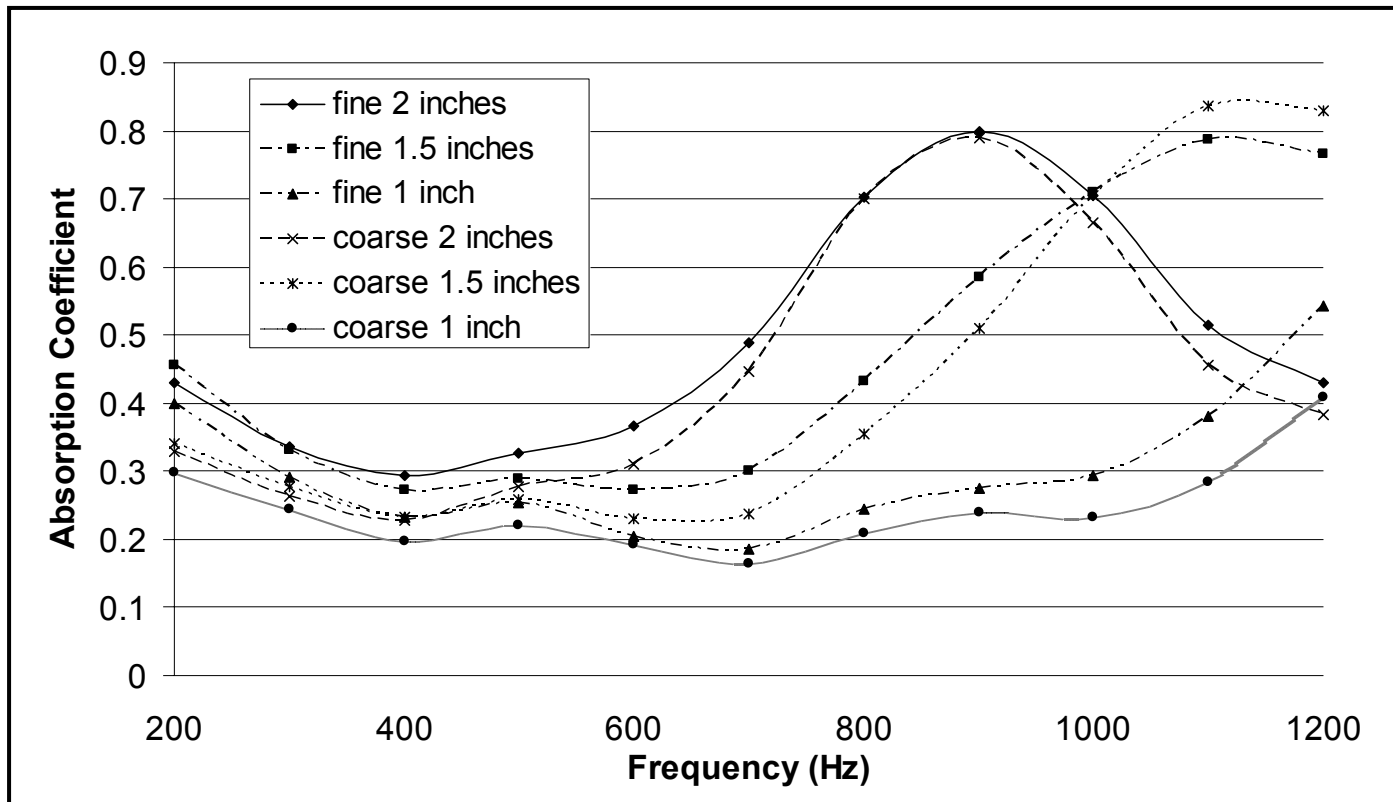


Figure 6.25 Comparison of sound absorption coefficients of OGFC slabs measured by the 6-inch tube



Figure 6.26. Experimental setup for in situ measurements of sound absorption coefficient of slabs

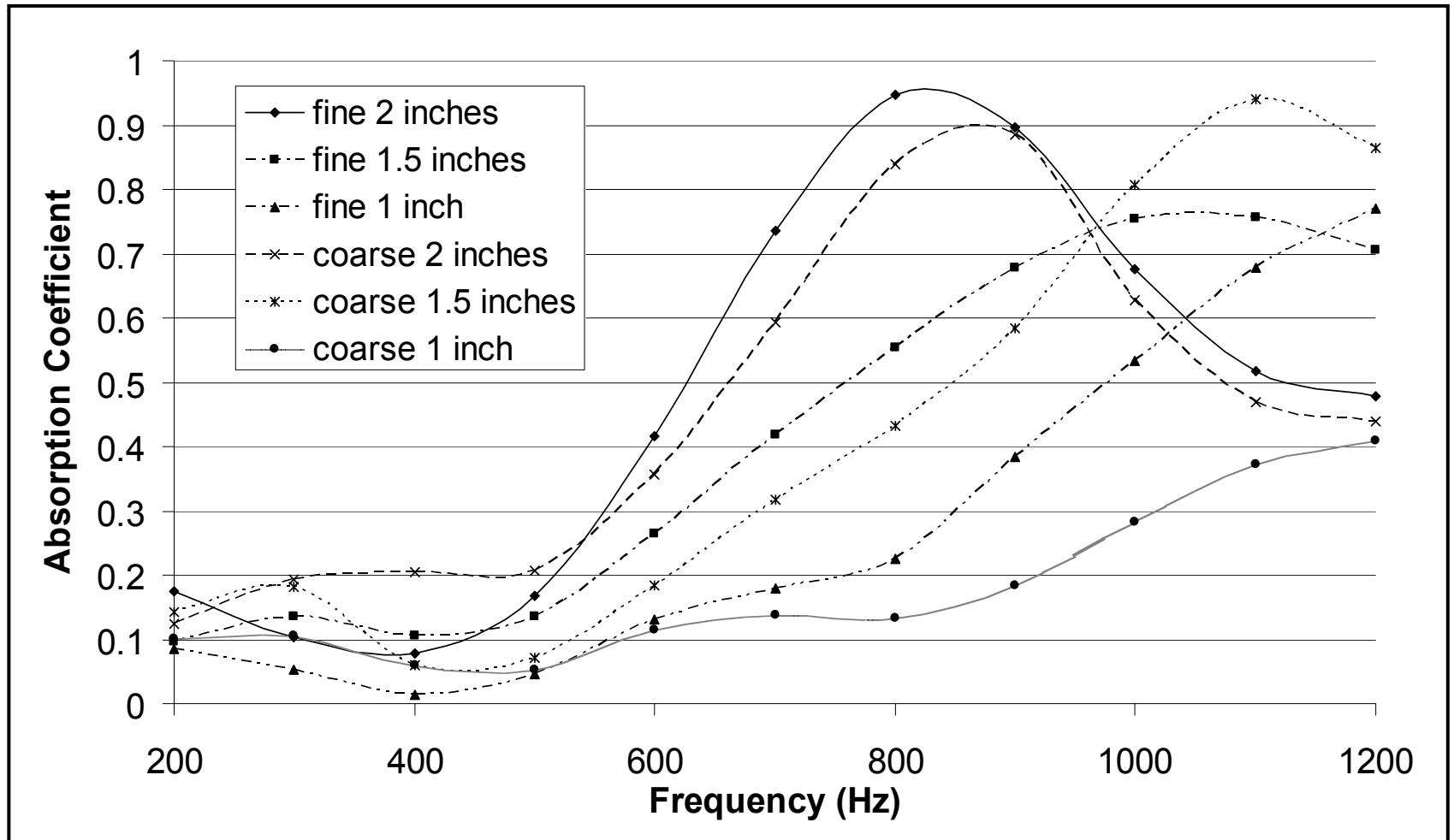


Figure 6.27. Comparison of sound absorption coefficients of OGFC cores measured in 6-inch tube

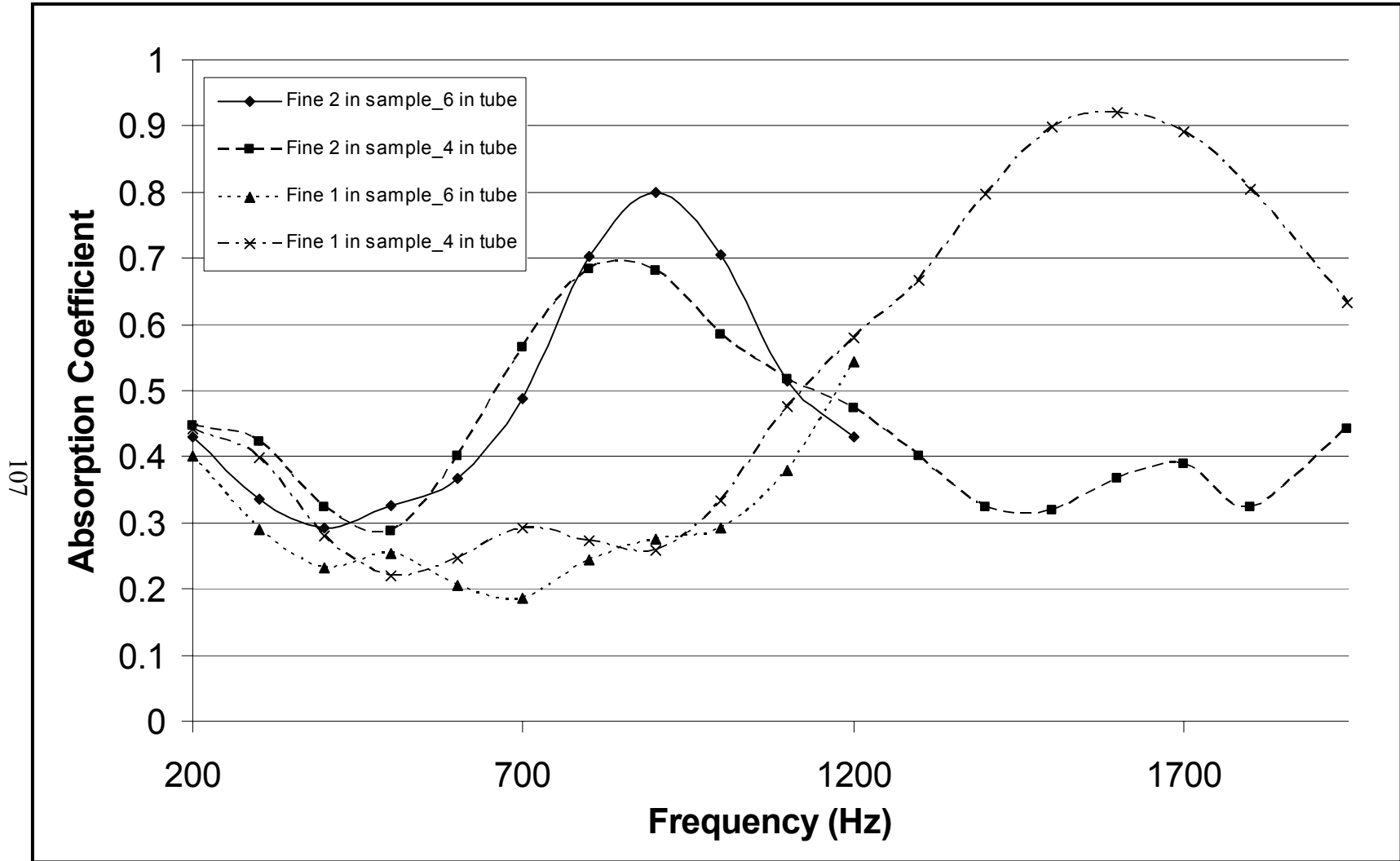


Figure 6.28. Comparison of sound absorption coefficients of OGFC slabs measured by 6-inch and 4-inch tubes

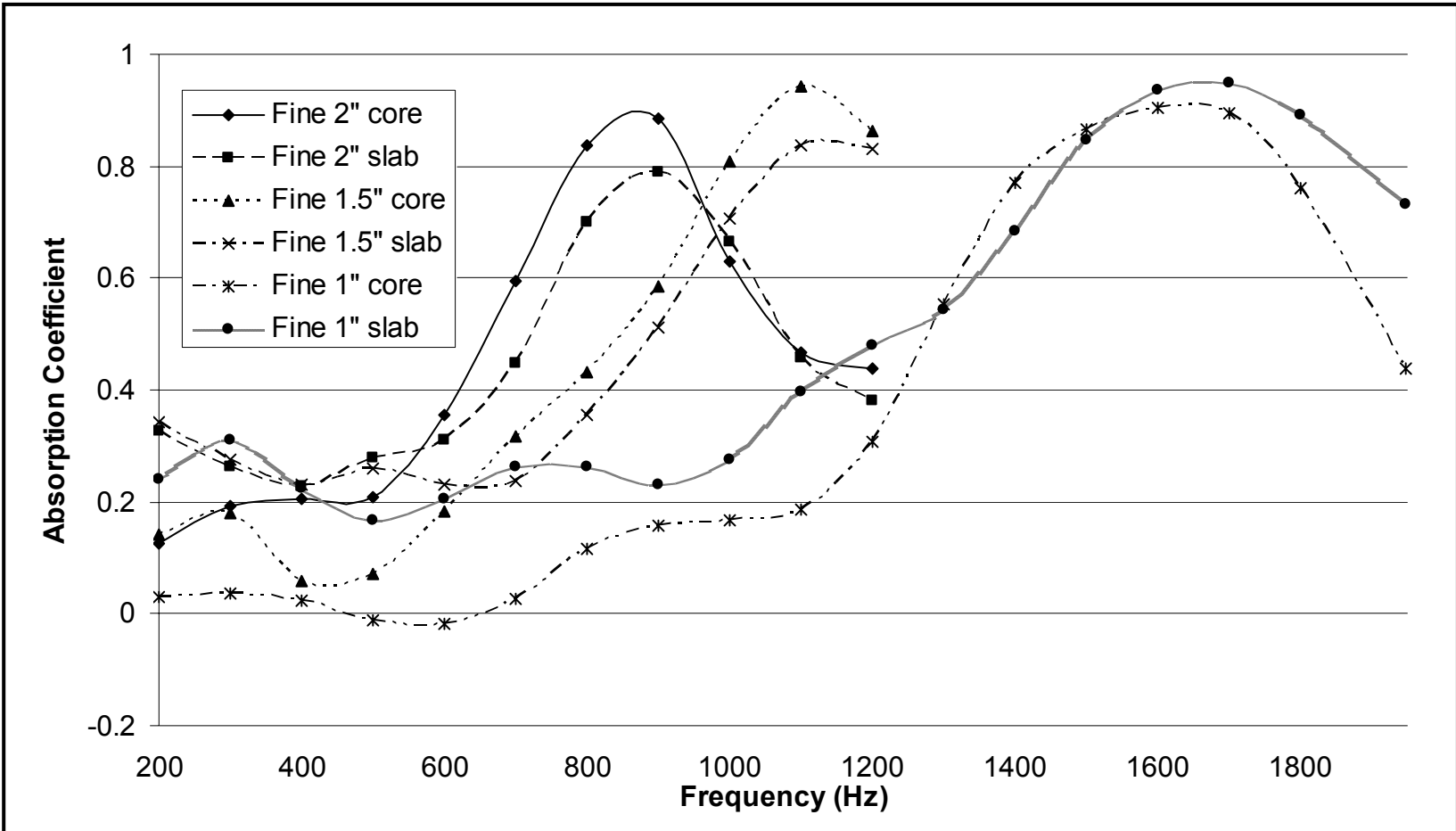


Figure 6.29. Comparison of the sound absorption coefficient of OGFC aggregated fine slabs and cores

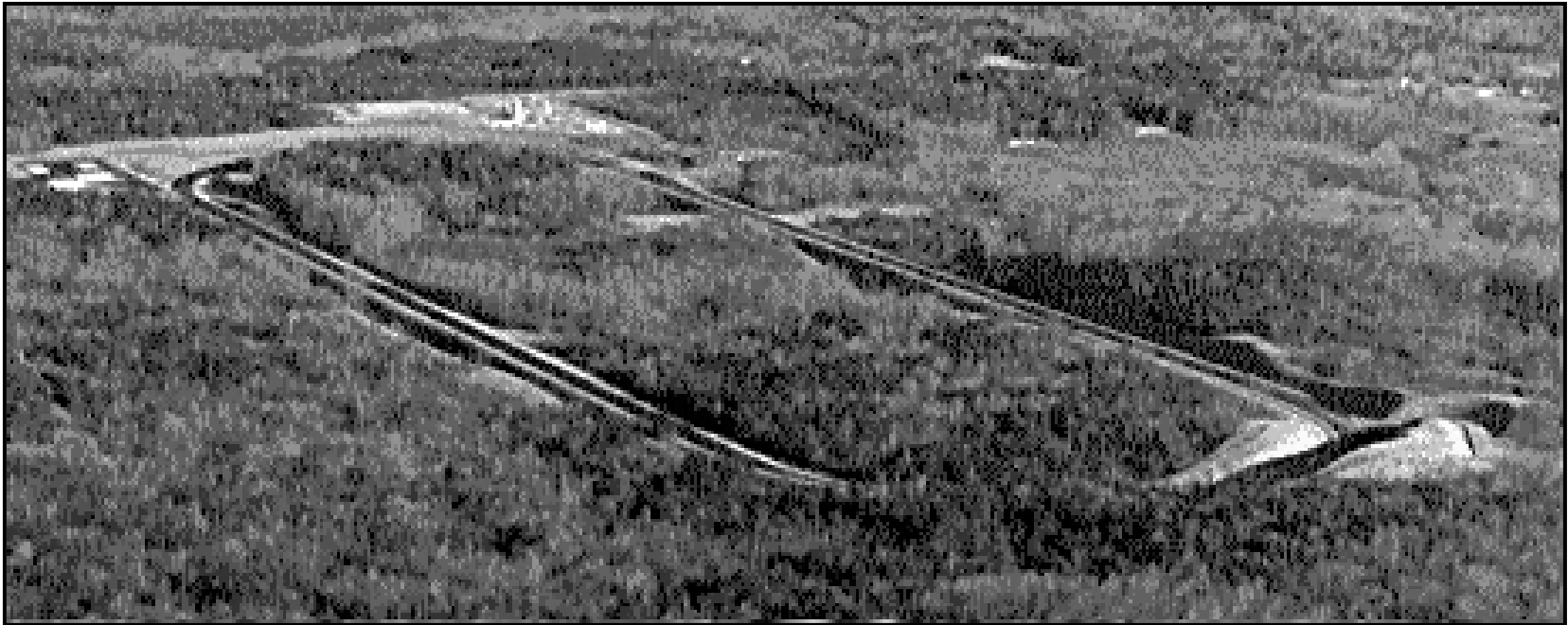


Figure 6.30. NCAT test track



Figure 6.31. NCAT tire noise measurement trailer set-up

CHAPTER 7

CONCLUSIONS

This chapter discusses various conclusions made about the results obtained using the impedance tube method. Both 4-inch and 6-inch diameter impedance tubes were constructed at the Auburn University workshop in conformance with to the ISO standard. The accuracy of measurements made with the impedance tubes was checked using known sound absorbing materials like fiberglass and a metal surface. The results agree very well with known theoretical values thus validating the construction of the impedance tube. The measurements were also taken with open and closed ends for both 4-inch and 6-inch diameter impedance tubes. The sound absorption coefficient of different road samples was measured using this impedance tube. Samples for the measurement were provided by National Center for Asphalt Technology (NCAT). Both dense and porous road surfaces were used for making the measurements. Measurements were made using both 4- and 6-inch core samples with 4-inch and 6-inch diameter impedance tubes. Measurements were repeated with the impedance tube mounted vertically directly on pavement slab surfaces.

As discussed in Chapter 4, the absorption coefficient of large surface area samples can be measured using a 6-inch diameter impedance tube, however, only up to a frequency of 1250 Hz. At frequencies above these limits, cross modes develop and the incident and reflected waves in the tube are not simply plane waves alone, so the tube can

no longer be used to measure the normal incidence sound absorption coefficient of the road surface material. Similarly, a lower cut-off frequency of 240 Hz has to be maintained for the 6-inch diameter tube. If sound waves with a frequency below the limiting value enter the tube as non-plane waves, they will become plane waves after traveling a short distance. For this reason, no measurements should be made closer than one tube diameter to the source end of the tube.

The upper and lower cut-off frequencies for the 4-inch diameter tube have to be maintained as 230 Hz and 2000 Hz respectively. Since the surface area of the core samples are less than half that of the 6-inch cores, the sound absorption coefficients of more core samples were measured to obtain confidence in the results obtained with the 4-inch diameter impedance tube.

Measurements were made using the two different diameter impedance tubes mounted vertically on slabs made from the same pavement types. There were some slight differences in the first peak frequency and magnitude of the peak absorption coefficients determined using cores in the two different diameter tubes than when the tubes were mounted directly in situ on the pavement slab surfaces. The boundary conditions possessed by the samples during the tests are different and this is thought to be a cause for the variation in the results.

It can be concluded that both 4-inch and 6-inch impedance tubes can be used to take measurements using the core samples and also on the slab. These measurement results obtained were comparable for both core and slab samples and also for 4-inch and 6-inch samples.

The peak absorption coefficient measured of the fine and coarse mix aggregate porous surfaces suggests that the first peak frequency and peak absorption coefficient magnitude is only slightly different for the two types of surface. Since the fine mix aggregate porous surface is smoother, it is a better choice for a road surface since it should result in less tire tread impact noise and thus lower overall tire noise should be produced than the coarse aggregate surface. The peak sound absorption coefficient of the road surface sample is related to the road surface thickness. A porous surface of between 1.5 and 2.0 inches thick is recommended for the type of porous surface examined, if a peak absorption frequency of between about 900 to 1000 Hz is desired, to be most effective at reducing interstate highway noise of automobiles. It can also be concluded that the results obtained using the 6-inch tube are more reliable since the road surface sample area that is tested with the 6-inch tube is greater than the sample area tested with the 4-inch tube. The experimental errors should be smaller with the 6-inch tube than the 4-inch tube.

It has been established that the noise benefits provided by porous surfaces are partly dependent upon the complex interference that occurs between sound waves which propagate directly from the vehicle source to the receiver, and the waves which are reflected from the road surface. In addition porous surfaces should also reduce the noise generated by air pumping as the provision of air paths in the surface layer should help to dissipate the air trapped in the tire tread grooves. In general, porous road surfaces have a greater effect in controlling noise from sources, which are located close to the ground than sources, which are more elevated above the road surface. Porous road surfaces therefore offer potentially greater benefits in terms of controlling tire noise than engine noise.

By considering the influence of the surface design on both the propagation and generation of noise together with the influence of other performance requirements, which also affect the design of the road surface, design guidelines for the specification of feasible low noise road surfaces can be determined.

In general factors such as tire type, road surface type, speed, tire inflation etc. influence the overall noise produced by automobiles.

The use of the “statistical pass by” and “close proximity” methods, together with the (“impedance tube”) experimental tests explained before and other methods under development will help to accelerate the introduction of progressively quieter surfaces in different countries. These assessment procedures could provide the authorities with a range of tools to encourage industry to develop complementary designs of tires and road surfaces that will substantially reduce the problem of tire/road noise. Reduction of tire/road noise appears to be one of the most interesting and important environmental challenges of the coming decades.

NOMENCLATURE

- $h_n(t)$ Background noise response
- d_m Distance from the microphone to the reflecting plane (m)
- d_s Distance from the sound source to the reflecting plane (m)
- K_r Geometrical spreading factor accounting for the path length difference between the direct and reflected paths
- $h_i(t)$ Impulse response of the direct path
- $h_r(t)$ Impulse response of the reflected path
- j Parasitic reflections
- $r_p(t)$ Reflection factor of the surface under test
- T_{60} Reverberation time
- c Speed of sound in air
- L_{tr} Tire/road sound level
- $H_i(f)$ Transfer function of the direct path
- $H_r(f)$ Transfer function of the reflected path
- T_w Width of the temporal window used to isolate the sound pressure wave reflected by the surface under test (s)

θ	Phase angle
v	Vehicle speed in km/h
*	Convolution sign
A & B are speed coefficients (constants)	
c	Speed of sound
CPX	Close proximity method
d	The thickness of the porous layer
f	Operating frequency hertz.
f_l	Lower working frequency of the tube, hertz
f_u	Upper working frequency of the tube, hertz
H_{12}	Transfer function
$H_i(f)$	Transfer function of the direct path
$H_r(f)$	Transfer function of the reflected path
K	Constant, 0.586
L	Length of the impedance tube
L	Sound pressure level (SPL) in dB.
L_{veh}	Vehicle sound pressure level,
p_i	Incident wave
p_R	Reflected wave
q	The tortuosity
$Q_w(f)$ Sound power reflection factor from which the sound absorption coefficient can be calculated as discussed below, apart from a factor K , due to geometrical spreading.	
R	Airflow resistance per unit length

R	Reflection coefficient
S	Cross sectional area of the impedance tube
SPB	Statistical pass-by method
SPBI	Statistical pass-by index
SWR	Standing Wave Ratio
V_a	Air voids often just called “air voids” or “porosity”
Z_{mL}	Mechanical impedance
Z_n	Normal surface impedance
α	Absorption coefficient
Ω	Residual air voids content.

REFERENCES

1. Ulf Sandberg, *Tire/road noise myths and realities*, Plenary paper published in the proceedings of The 2001 International Congress and Exhibition on Noise Control Engineering. The Hague, The Netherlands, 2001 August 27-30
2. PM Nelson, *Designing porous road surfaces to reduce traffic noise*. 2001.
3. Ulf Sandberg, Jerzy A Ejsmont, *Development of Three Methods for Measurement of Tire/Road Noise Emission: Coast-by Trailer and Laboratory Drum*, Noise Control Engineering Journal, 2000, Volume 27.
4. Chung J. Y., Blaser D.A. – *Transfer function method of measuring in-duct acoustics properties. Part I: Theory* – J.Acoust.Soc.Am. 68(3), 1980.
5. Chung J. Y., Blaser D.A. – *Transfer function method of measuring in-duct acoustics properties. Part II: Theory* – J.Acoust.Soc.Am. 68(3), 1980.
6. Sandberg, U and Ejsmont, J. A., *Tyre/Road Noise Reference Book*, Informex, Sweden, 2002.
7. Sandberg, U. *A Road Surface for Reduction of Tire Noise Emission*. Proc. Inter-noise 79, Warsaw, Poland, pp. 517-520, 1979.
8. Sandberg, U and Descournet, G. *Road Surface Influence on Tire/Road Noise – Part I*, and Descournet, G. and Sandberg, U. *Road Surface Influence on Tire/Road Noise – Part II*, Proc. Inter-noise 80, Miami, pp 259-272.

9. Seybert, A. F., and Ross, D. F., *Experimental Determination of Acoustic Properties Using a Two-Microphone Random-Excitation Technique*, J. Acoust. Soc. Am., Vol. 61, No. 5, pp. 1362-1370, 1977.
10. *Work Plan for Quiet HMA Pavements*, Douglas Hanson, Robert Bernhard, October 2002.
11. von Meier, A., *Acoustically Porous Road Surfaces, Recent Experiences and New Developments*, Proc. Inter-noise 88, Avignon, France, 1988.
12. *Measurement of the Acoustical and Mechanical Properties of Porous Road Surfaces and Tire/Road Noise*, Malcolm J. Crocker, Zhuang Li, Ravi Karjatkar and Krishna S. Vissamraju. 2003.
13. von Meier, A., van Blockland, G. J., Heerkens, J. C. P., *Noise of Optimized Road Surfaces and Further Improvements by Tyre Choice*, Proc. INTROC 90, Gothenburg, Sweden, 1990.
14. *A novel technique for measuring the reflection coefficient of sound absorbing materials*, H-E de Bree, F.J.M van der Eerden, J.W. van Honschoten.
15. ISO 10534-1:1998, *Acoustics--Determination of sound absorption coefficient and impedance in impedance tubes--Part 1: Method using standing wave ratio*.
16. ISO 10534-2:1998, *Acoustics--Determination of sound absorption coefficient and impedance in impedance tubes--Part 2: Transfer-function method*.
17. First ISO/CD 13472-1:2000, *Acoustics--Procedure for measuring sound absorption properties of road surfaces in situ--Part 1*
18. ASTM E1050:1998, *Standard test method for impedance and absorption of*

- acoustical materials using a tube, two microphones, and a digital frequency analysis system.*
19. ASTM C384, *Test method for impedance and absorption of acoustical materials by the impedance tube method.*
 20. Hamet, J-F., Deffayet, C. and Palla, M-A., Air Pumping Phenomena in Road Cavities, *Proc. Int. Tire/Road Noise Conf.*, Gothenburg, STU information no. 794-1990, NUTEK, Stockholm, 1990.
 21. ISO 11819-2:2000, Acoustics –Measurement of the influence of road surfaces on traffic noise – Part 2: The close proximity method.
 22. Tire/Pavement Noise Study for Michigan Department of Transportation, National center for Asphalt Technology 2002.
 23. ISO 13472-1:2001, Acoustics—*Measurement of sound absorption properties of road surfaces in situ* – Part 1 Extended surface method.
 24. ISO 11819-1:1997, Acoustics—*Measurement of the influence of road surfaces on traffic noise* – Part 1 Statistical Pass-By method.
 25. Haines, James, Standing wave and two-microphone impedance tube round-robin test program, *ASTM Research Report* No. RR: E33-1006, 1989.
 26. W.T. Chu – “Impedance Tube Measurements – A comparative study of current practices” – *Noise Control Engineering Journal*, Vol. 37, n. 1, July-August 1991, pagg. 37-44.
 27. London, A., “The Determination of Reverberant Sound Absorption Coefficients from Acoustic Impedance Measurement,” *Journal of Acoustical Society of America*, Vol 22(2), March 1950, pp. 263-269.

28. Mechel, F.P., "Design Charts for Sound Absorber Layers," *Journal of Acoustical Society of America*, Vol 83(3), March 1988, pp. 1002-1013.
29. Fahy, F.J. *Sound Intensity*, E&FN SPON, London (1995).
30. Harris, C.M., editor, "Shock and Vibration Handbook," *McGraw-Hill*, Third Edition, 1988, Chapter 21, pp. 4-8.
31. Rayleigh, J.W.S., *The Theory of Sound*," *Dover Publications, Inc.*, New York, NY, Vol 2,1896, pp.161.
32. "Condenser Microphones Data Handbook," *Bruel and Kjaer*, Revision September 1982, pp. 56.